Functionalized Molecular Diversity by Gold-Catalyzed Activation of Alkynes

Presented by:

Zuozuo Wu

From People's Republic of China

November 2022

A dissertation submitted to the

Combined Faculty of Mathematics, Engineering and Natural Sciences

Heidelberg University, Germany

for the degree of

Doctor of Natural Sciences (Dr. rer. nat.)

Dissertation

Submitted to the

Combined Faculty of Mathematics, Engineering and Natural Sciences

Heidelberg University, Germany

For the degree of

Doctor of Natural Sciences (Dr. rer. nat.)

Presented by

Zuozuo Wu

Oral examination: December 14th, 2022

Functionalized Molecular Diversity by Gold-Catalyzed Activation of Alkynes

Oral examination: December 14th, 2022

Gutachter: Prof. Dr. A. Stephen K. Hashmi

Prof. Dr. Milan Kivala

GESAMTFAKULTÄT FÜR MATHEMATIK, INGENIEUR UND NATURWISSENSCHAFTEN

Eidesstattliche Versicherung gemäß § 8 der Promotionsordnung für die Gesamtfakultät für Mathematik, Ingenieur- und Naturwissenschaften der Universität Heidelberg

1. Bei der eingereichten Dissertation zu dem Thema
Functionalized Molecular Diversity by Gold-Catalyzed Activation of Alkynes
handelt es sich um meine eigenständig erbrachte Leistung.
2. Ich habe nur die angegebenen Quellen und Hilfsmittel benutzt und mich keiner unzulässigen Hilfe Dritter bedient. Insbesondere habe ich wörtlich oder sinngemäß aus anderen Werken übernommene Inhalte als solche kenntlich gemacht.
3. Die Arbeit oder Teile davon habe ich bislang nicht[1)] an einer Hochschule des In- oder Auslands als Bestandteil einer Prüfungs-oder Qualifikationsleistung vorgelegt.
Titel der Arbeit:

_____

_____

Hochschule und Jahr:_____

Art der Prüfungs-oder Qualifikationsleistung:_____

4. Die Richtigkeit der vorstehenden Erklärungen bestätige ich.
5. Die Bedeutung der eidesstattlichen Versicherung und die strafrechtlichen Folgen einerunrichtigen oder unvollständigen eidesstattlichen Versicherung sind mir bekannt. Ich versichere an Eides statt, dass ich nach bestem Wissen die reine Wahrheit erklärtundnichts verschwiegen habe.

Heidelberg, 17.11.2022 ZuoZuoWu

Ort und Datum Unterschrift

1) Nicht Zutreffendes streichen. Bei Bejahung sind anzugeben: der Titel der andernorts vorgelegten Arbeit, die Hochschule, das Jahr der Vorlage und die Art der Prüfungs- oder Qualifikationsleistung.

Acknowledgements

PhD, ‘Permanent Head Damage’. Hahaha it’s a joke, but for sure it’s not easy to finish the PhD study, especially for me. I was not an organic chemistry student before. At the beginning, I even can’t understand everything, and I need to learn everything. It’s horrible because I am a competitive girl, but I have to admit that I am ordinary, ordinary like everyone else. But thanks god, I done all finally after three years fighting, applaud for myself. Heidelberg is a magic city, beautiful scenery, friendly people and strong academic, all are attractive and unforgettable. In my deep heart, I am so proud that now I am an alumnus of Heidelberg University. The days of chasing my academic dreams in Heidelberg University always make me feel empowered.

Thousands thanks to the China Scholarship Council (CSC). Without the generous financial support and care, these researches can’t be done.

Prof. Dr. A. Stephen K. Hashmi is the best supervisor, I want to express my greatest sincere appreciation to him. His enthusiasm for scientific research, rigorous scientific research attitude and meticulous personality charm deeply attracted me. During the whole study process, Prof. Hashmi teach me a lot and support me always. In the daily life, he encourages me to enjoy the days in Germany and live happily. It is with his big help and support, study and life in Heidelberg are so smooth and happy.

Thanks so much to Prof. Dr. Milan Kilava for being my second Gutachter.

I really appreciate Dr. Matthias, he is very humble and smart, he helped me a lot with experiments and manuscripts, as well as doctoral thesis. I always get inspiring suggestions from him; my PhD study is inseparable from his kindly help.

Many thanks to Frau Petra Krämer for her generous help in numerous IR tests, data analysis and catalyst supply; Great thanks to Frau Christiane Eckert for her assistance

and management, she is independent and brave, I learned a lot and enjoyed every chat with her. Thanks Frau Ann-Sophie Mack for her generous support in chemical ordering and equipment maintenance.

A lot of thanks to the Institute of Organic Chemistry and all the staff for the analytical and technical help, including HRMS, X-ray single crystal structure, NMR, glass workshop and chemical store. Especially thanks Matthias Hoyer technician for his big help on HRMS.

Much thanks to the previous and present members of Prof. Hashmi's group. All colleagues are friendly, you all make my life here wonderful. Especially thanks to Dr. Xiaojia Si and Dr. Lumin Zhang for the great help at the most difficult beginning. Thanks to Dr. Tao Wang, Dr. Chao Hu and Dr. Tapas Adak for the help on the research projects. Thanks Martin Dietl and Philipp Stein for help me on the experiment part. Thanks to Dr. Jin Xie, Dr. Hongming Jin and Dr. Yangyang Yang for their kindly encourage. Thanks to Dr. Jun Li, Dr Xianhai Tian, Dr. Lina Song, Dr. Sina Witzel, Dr. Chunyu Han, Dr. Vanessa Vethacke, Dr. Shaista Tahir, Robin Heckershoff, Alexandra Mackenroth, Kirsten Emler, Hongwei Shi, Michael Schukin, Yaowen Liu, Huili Zhang, Julian Melder, Justin Kahle, Qiaoying Sun, Jonas Wunsch, Henrik Habeck, Roonak Nikbakht, Ali Keshavarzi, Hadil Al Shurafa, Elena Michel, Rebeka Eshagh-Saatlo, Georg Leistikow, Simon Kohl, Yu Tian for their help.

A lot of thanks to my nice and excellent friends in Germany, it is you all who made me have a such good experience of studying and living abroad.

Last but not least, I am so grateful that my father Mr. Longbin Zhang, my mother Mrs. Xiaoqin Wu, my father-in-law Mr. JianSheng Zhou, my mother-in law Mrs. Hejiao Xu and my sweet boyfriend Mr. Nanwei Zhou love me very much and give me the most unconditional support in every aspect.

Contents

Publications

[1] **Z. Wu**, T. Adsk, M. C. Dietl, T. Wang, C. Hu, H. Shi, P. Krämer, M. Rudolph, F. Rominger, A. S. K. Hashmi. "Synthesis of α-Ketoamide via Gold(I) Carbene Intermediates" *Org. Lett.* **2022**, *24* (24), 4349-4353.

[2] **Z. Wu**, M. C. Dietl, P. M. Stein, T. Wang, M. Rudolph, A. S. K. Hashmi. " Gold-Catalyzed Hydroamination of Terminal Alkynes as One-Pot Access to Oximes", submitted.

[3] X. Si, L. Zhang, **Z. Wu**, M. Rudolph, A. M. Asiri, A. S. K. Hashmi. "Visible Light-Induced α-C(sp^3)-H Acetalization of Saturated Heterocycles Catalyzed by a Dimeric Gold Complex" *Org. Lett.* **2020**, *22* (15), 5844-5849.

Abbreviations

Ar	Aryl
Bu	Butyl
calcd.	Calculated
Cy	Cyclohexyl
DCM	Dichloromethane
DCE	1,2-Dichloroethane
DCB	1,2-Dichlorobenzene
PhBr	Bromobenzene
PhMe	Toluene
EA	Ethyl acetate
EI	Electron ionization
eq.	Equivalent
ESI	Electrospray Ionization
Et	Ethyl
GC	Gas chromatography
h	Hour
Hex	Hexyl
HRMS	High resolution mass spectrometry
Hz	Herz
IR	Infrared
mp	Melting point
m/z	mass per charge
Me	methyl
MHz	Megahertz
min	minute
Ms	Mesyl
TMS	Tetramethylsilane

MS	Mass spectrometry
NBS	*N*-bromo succinimide
NMR	Nuclear magnetic resonance
PE	Petroleum ether
Ph	Phenyl
Pr	Propyl
rt	room temperature
R_f	Ratio of fronts
t	*tert*
o	*ortho*
m	*meta*
p	*para*
XPhos	2-Dicyclohexylphosphino-2',4',6'-triisopropyl-1,1'-biphenyl
DMAP	4-Dimethylaminopyridine
JohnPhos	2-Di-*tert*-butylphosphino biphenyl
TLC	Thin layer chromatography
HOSA	Hydroxylamine-O-sulfonic acid
Dppm	Bis(diphenylphosphino)methan
OTf	Trifluoromethanesulfonyl
Ts	Toluenesulfonyl

Abstract

In Chapter 2, a gold-catalyzed reaction of a bromoalkyne with anthranils to synthesis α-ketoamides is covered. In this reaction, two equivalents nitrene are used to functionalize a C-C triple bond by gold catalysis. Subsequently one equivalent nitrene remains in the amide function of the desired product, while the other equivalent of nitrene is eliminated during the hydrolysis process as an amine. This particular hydrolysis of the intermediate α-iminoimidoyl halides opens access to α-ketoamides for a wide range of haloalkynes.

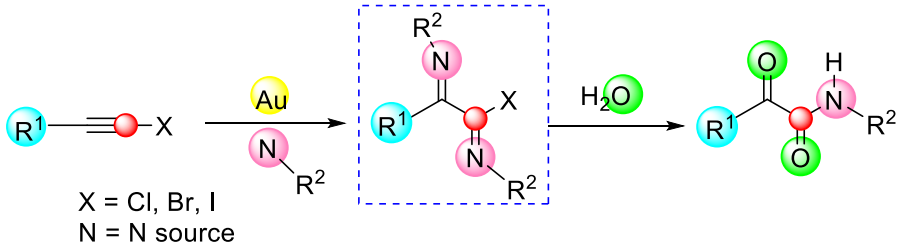

In Chapter 3, a one-step gold-catalyzed hydroamination of alkynes with hydroxylamine-O-sulfonic acid (HOSA) is reported. In this reaction, the limits that traditional synthesis of oximes is highly dependent on carbonyl compounds, is overcome, which expands the diversity of accessible oximes. Green chemistry metrics for this facile reaction are also calculated, this process shows 100% carbon efficiency.

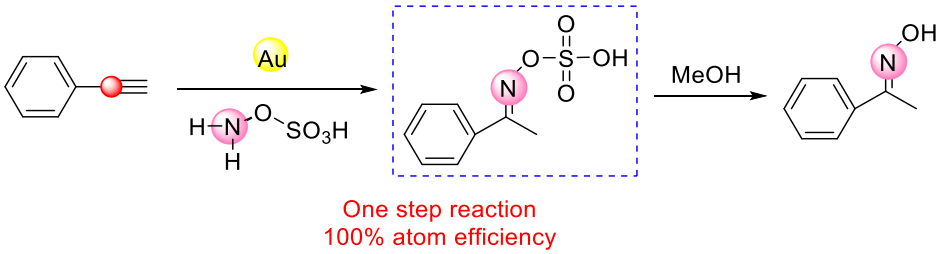

Kurzzusammenfassung

In Kapitel 2 wird eine goldkatalysierte Reaktion eines Bromalkins mit Anthranilen zur Synthese von α-Ketoamiden behandelt. Bei dieser Reaktion werden durch Goldkatalyse zwei Äquivalente Nitren an eine funktionalisierte C-C-Dreifachbindung angelagert und ein Äquivalent Nitren verbleibt in der Amidgruppe des Produktes, das andere Äquivalent Nitren wird während des Hydrolyseprozesses als Amin abgespalten wird. Diese spezielle Hydrolyse der intermediären α-Iminoimidoylhalogenide führt für eine breite Palette von Halogenalkinen zu α-Ketoamide.

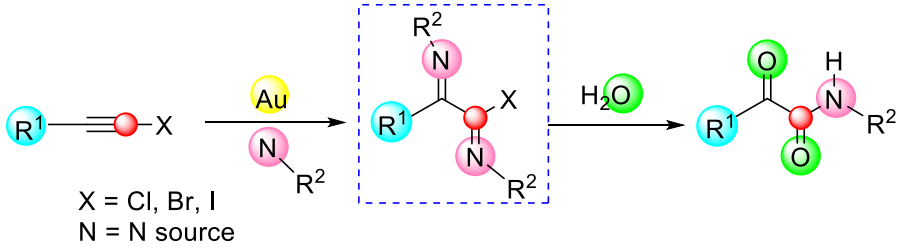

In Kapitel 3 wird über eine goldkatalysierte Eintopf-Hydroaminierung von Alkinen mit Hydroxylamin-O-sulfonsäure (HOSA) berichtet. Bei dieser Reaktion wird die Einschränkung überwunden, dass die traditionelle Synthese von Oximen stark von Carbonylverbindungen abhängt, und die Diversität der zugänglichen Oxime erweitern. Metrische Parameter der grünen Chemie wurden berechnet, die Reaktion weist einen 100% Kohlenstoffeffizienz auf.

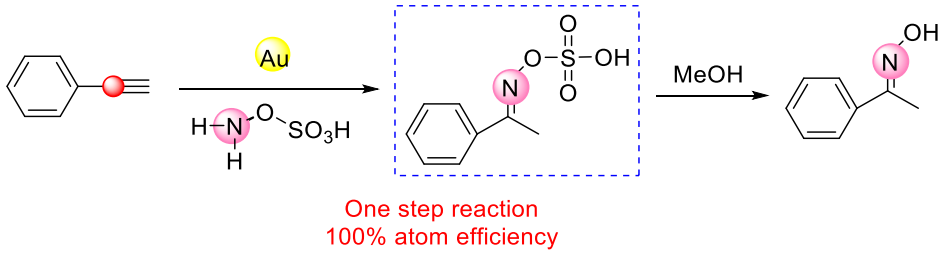

Chapter 1. General Introduction

1.1 Gold chemistry

In average one million tons of earth only contain ten pounds of gold. This scarcity, as well as its beauty and chemical properties account for its high value during the whole history of mankind. Initially, gold was used extensively in coinage and jewelry, however today the applications of gold are vast.[1] Gold has interesting chemical properties, it is a noblemetal. Fascinating in its complexity for academic chemists, gold has potential applications in materials science, nanotechnology, electronics, pharmaceutical chemistry and catalysis.[2]

1.2 Gold catalysis

The catalytic effect of gold can be divided into two parts, namely heterogeneous and homogeneous gold catalysis. Even though gold has an excellent coordination and organometallic chemistry, it was widely considered to be catalytically inactive for a long time. [3] The first significant developments of gold catalysts are known since 1965 when the German company Knapsack produced vinyl acetate through the oxidative acetoxylation of ethylene.[4] Until 1973, when Bond et al. reported the hydrogenation of olefins over supported gold catalysts, gold was discovered to be superior to other catalysts.[5] Later, several heterogeneous gold-catalyzed reactions were reported.[6] When Ito et al. reported an unknown catalytic asymmetric aldol reaction by a gold complex, a creative start in homogeneous asymmetric catalysis was established.[7] It begin to blossom until the work of Teles and specifically Hashmi in 1998-2000 unveiled the potential of the homogeneous gold catalysis.[5, 8] Since 2001 much work was devoted to gold catalysis and a boom established till nowadays.

1.2.1 Heterogenous gold catalysis

Heterogeneous gold catalysis refers to the catalysis of chemical reactions by gold, typically supported on metal oxide substrates. Heterogeneous gold catalysis has a wide range in application such as carbon monoxide (CO) oxidation, water gas shift, epoxidations and selective hydrogenations.[9] However, this chapter is focused on homogeneous gold catalysis, so the details about heterogeneous gold catalysis will not be discussed here.

1.2.2 Homogeneous gold catalysis

Homogeneous gold catalysis includes all chemical reactions in which the substrate(s) and the gold catalyst are in the same state.[5] Homogeneous gold catalysts offer several important advantages over their heterogeneous counterparts.[10,11] Out of the different oxidation states possible for gold, in the presence of organic substrates, gold(0), gold(I), and gold(III) are possible. In homogeneous gold catalysis, the common oxidation states of gold are gold(I) and less common gold(III). Attributed to the energetically lower LUMO and poor back-donation of the gold species, these gold catalysts are regarded as the most powerful catalysts for the electrophilic activation of unsaturated carbon-carbon multiple bonds (alkynes, allenes, alkenes) towards a variety of nucleophiles.[12] It is generally accepted that most gold-catalyzed reactions go through three major stages (Scheme 1.1).[13] In stage 1, a nucleophile attacks an $[L\text{-}Au]^+$-activated alkyne (or alkene) **1** to form a *trans*-alkenyl gold complex intermediate **2** (or an alkyl gold complex in the case of alkenes). In stage 2, the resulting vinyl complex **3** reacts with an electrophile (E^+), usually a proton, to yield the final product **4** via proto deauration, which also regenerates the cationic gold species. Additionally, like with every other catalyst, in gold-catalyzed reactions a decay or deactivation of the catalyst takes place (stage 3).[14] In some gold-catalyzed reactions, the formation of off-cycle gold species such as *gem*-diaurated vinyl species was observed.[15]

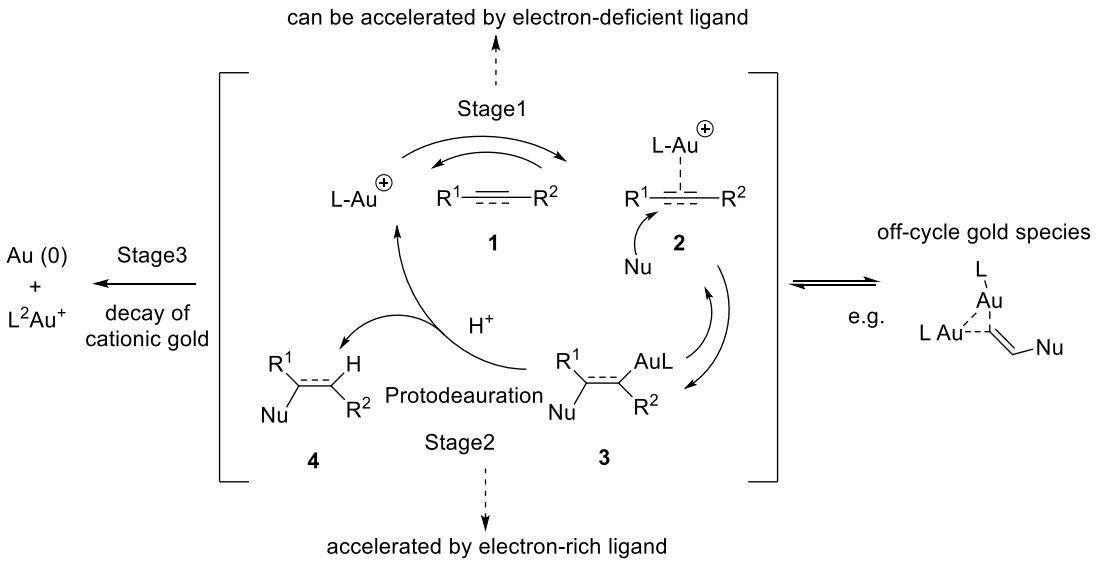

Scheme 1.1 Typical catalytic cycle of gold catalysis

It is obvious that the ligands make an important contribution in the tuning of reactivity of homogeneous gold catalysts, the common ligands are shown in Scheme 1.2. There has also been progress in the design of ligands for gold catalysis.[16]

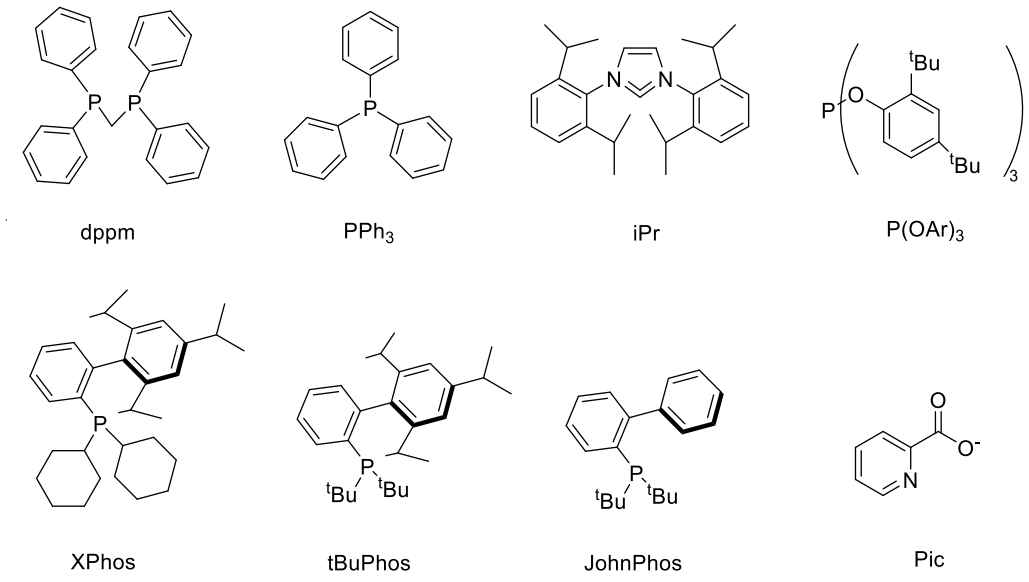

Scheme 1.2 Common ligands used in gold catalysis

Besides the ligands, counter anions also play an indispensable role for homogeneous gold catalysts. Commonly used counter anions can be divided into halides, oxygen-based, nitrogen-based, carbon-based, boron-based, and other fluorinated counterions (Scheme 1.3).[17] Due to the relatively high stability and acceptable price, OTf^-, SbF_6^-,

NTf_2^- are the most commonly used counter anions in homogeneous gold catalysis.[17,18]

Halides	B-based	C-based	N-based	O-based	Other fluorinated
Cl^-	$BArF_4^-$	CN^-	$N(SO_2Ph)_2^-$	OTs^-	SbF_6^-
Br^-	BF_4^-	$HCTf_2^-$	NTf_2^-	OMs^-	PF_6^-
I^-	$B(C_6F_5)_4^-$	CTf_3^-		OTf^-	
	$[Me_3NB_{12}Cl_{11}]^-$	$TsC(CN)_2^-$		TFA^-	
				ClO_4^-	
				chiral Phosphate	

Scheme 1.3 Common counter anions in gold catalysis

1.3 Gold-catalyzed organic reactions

Homogeneous gold-catalyzed reactions have been widely recognized as a vital tool in the field of organic synthesis (Scheme 1.4).[11] Homogeneous gold catalysis is valuable in constructing complex molecules.

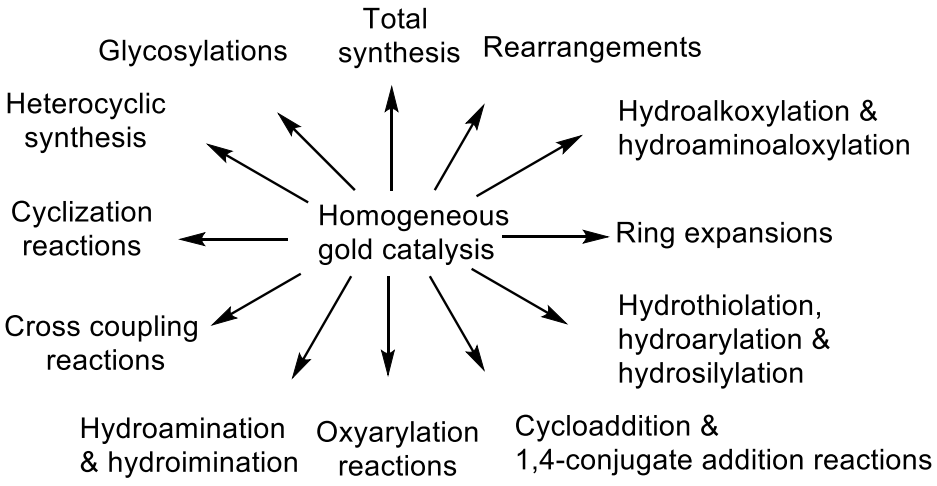

Scheme 1.4 Homogeneous gold catalysis in organic transformations

1.3.1 Gold-catalyzed transformation of alkynes

By far, the most common reactivity pattern in gold-catalyzed organic reactions is the

gold-catalyzed activation of unsaturated C-C multiple bonds. C-C multiple bonds of alkynes, allenes, or olefins coordinate to gold complexes, this very efficiently activates them for the attack of a nucleophile. Scheme 1.5 show the general example of a nucleophilic addition to a C-C multiple bonds, the gold catalyst interacts with the π-system of the substrate to construct the intermediate first, and then the nucleophile attacks.[5b] In this thesis, we mainly focus on alkyne hydro-functionalization reactions.

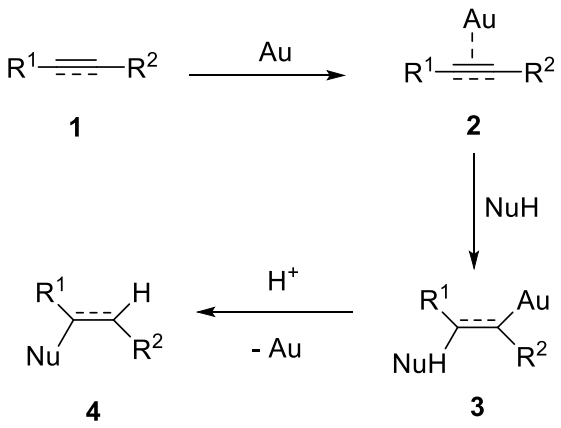

Scheme 1.5 General procedure of a nucleophilic addition to a C-C multiple bonds

Alkyne Hydration: Hydration is the simplest and one of the most intensively studied alkyne hydro-functionalization reactions.[19a] Alkynes can be hydrated by two different methods. The direct addition of water with catalysts yields the Markovnikov product. In contrast, the indirect hydration by the reaction sequence of hydroboration, oxidation and hydrolysis results in the anti-Markovnikov product. The gold-catalyzed reaction generally exhibits Markovnikov regioselectivity in the case of terminal alkynes, whereas with internal triple bonds the regioselectivity is generally poor, unless a directing group is present in the substrate (Scheme 1.6).[19b] The enol product readily tautomerizes to the ketone, and consequently the overall reaction converts alkynes into ketones, and in particular terminal alkynes into methyl ketones.

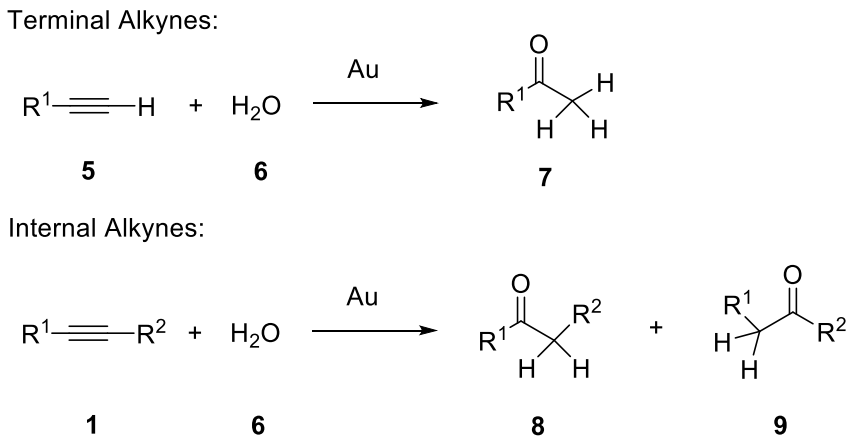

Scheme 1.6 Gold-catalyzed alkynes hydration

Alkyne Hydroalkoxylation: In general, addition to terminal alkynes occurs at the internal carbon to give the corresponding ketal **11** or enol ether **12** products (Scheme 1.7). In contrast, internal alkynes can potentially furnish two possible enol ether products. Depending on the position of the alkyne being attacked by the nucleophile, **13** and **14**, in addition to the corresponding ketals **15** and **16**, could all be formed. There are several considerations for determining the selectivity of these reactions including steric, electronics, and the identity of the nucleophile.[20]

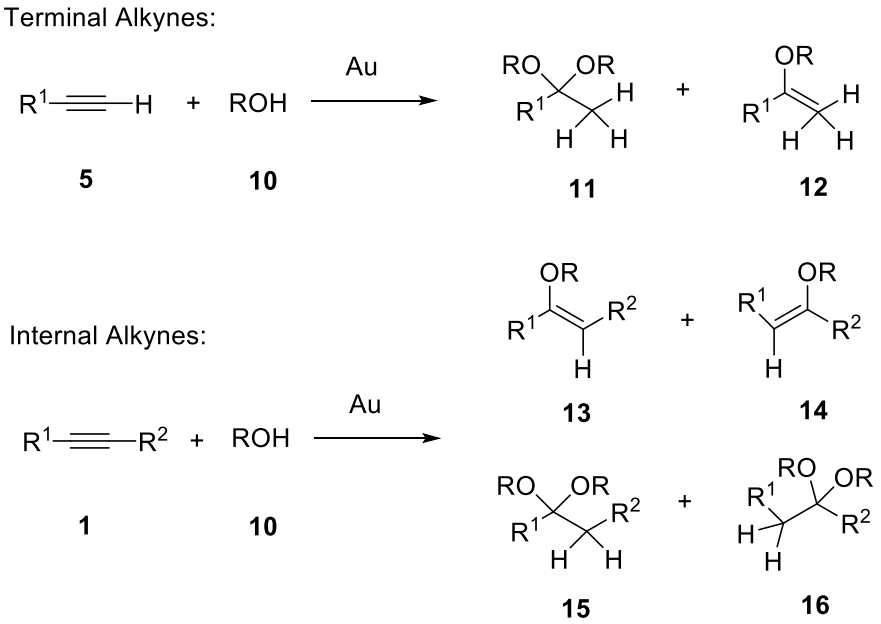

Scheme 1.7 Gold-catalyzed hydroalkoxylation of alkynes

Alkyne Hydroamination: Alkyne hydroamination is defined as the addition of the

nitrogen atom and a hydrogen atom of a primary or secondary amine onto the carbon-carbon triple bond which is an effective method for the construction of C-N bonds in N-heterocycles synthesis. Alkyne hydroamination is a much broader reaction class compared to alkyne hydration and alkyne hydroalkoxylations, since there is a plethora of molecules containing a nucleophilic N-H function that can be used as reactants.[21]

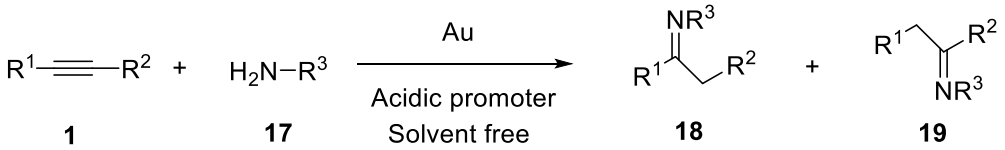

Scheme 1.8 Gold-catalyzed alkyne hydroamination

The Beauchemin group has established a versatile chemistry of Cope-type hydroamination via a concerted 5-membered cyclic transition state for the direct amination using hydroxylamine and hydrazine derivatives (Scheme 1.9a).[22] In 2013, Bao et al. reported the synthesis of 3,5-disubstituted pyrazoles via the nucleophilic attack of hydrazine onto 1,3-dialkynes through an allene intermediate, which further undergoes electrophilic cyclization to create a new C-N bond. The theoretical aspects of the mechanism of Cope-type hydroamination have been investigated by Tang et al. in 2014 (Scheme 1.9b).[23]

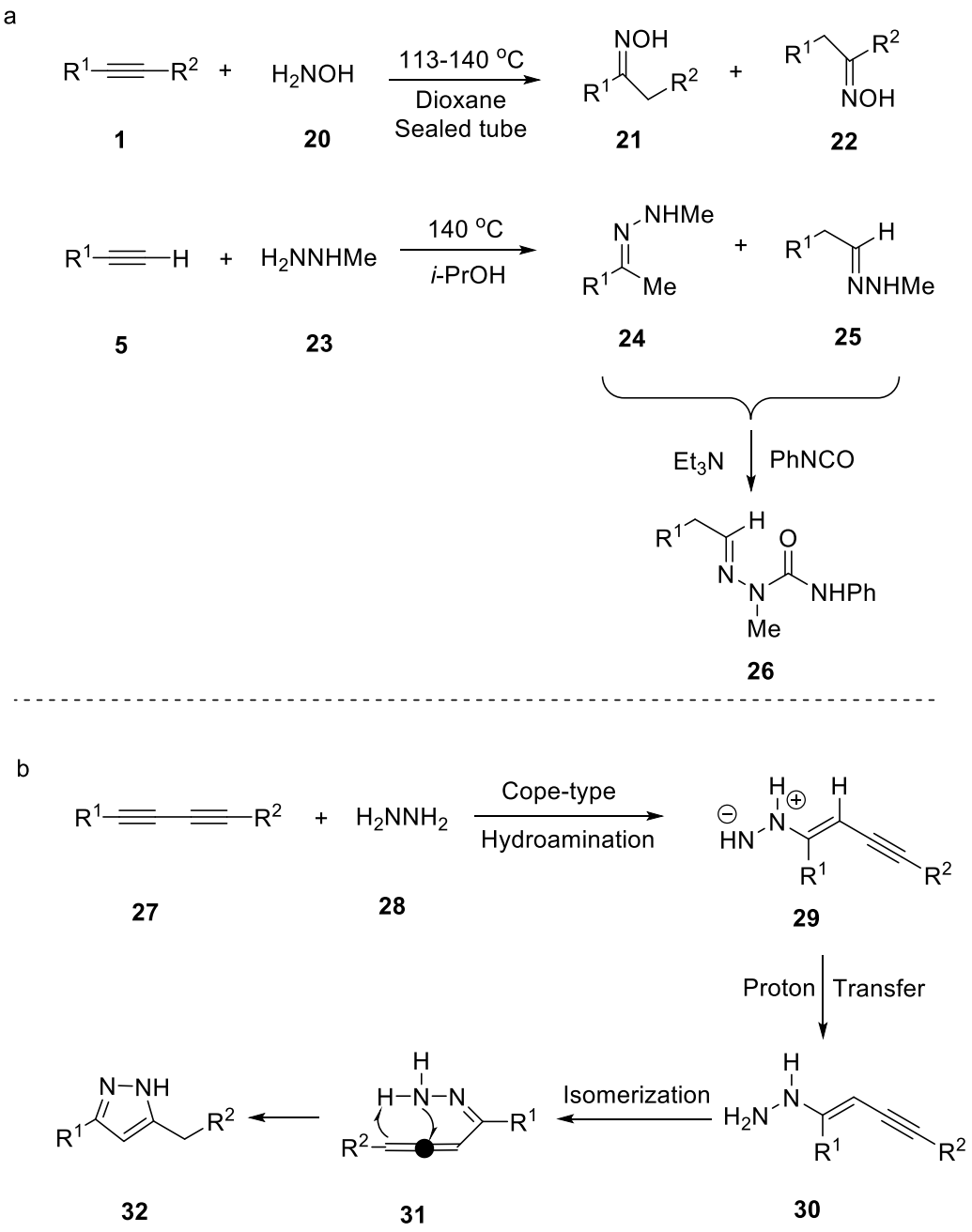

Scheme 1.9 Cope-type hydroamination of alkynes

1.3.2 Gold carbene intermediates in gold-catalyzed reaction

In many gold-catalyzed alkyne transformations, gold carbenes have been proposed as the key intermediates for constructing diverse complex and useful building blocks after initial reports by the Hashmi group.[24] Among these gold carbene species, α-imino gold carbenes have received considerable attention. The development involving α-imino

gold carbene intermediates to facilitate the synthesis of challenging heterocycles is an ongoing endeavor.[25] Gold carbene intermediates can be exploited for the rapid synthesis or late-stage modification of biologically important compounds. General route to vinyl gold intermediates and unfunctionalized gold carbene intermediates are listed in Scheme 10.[26]

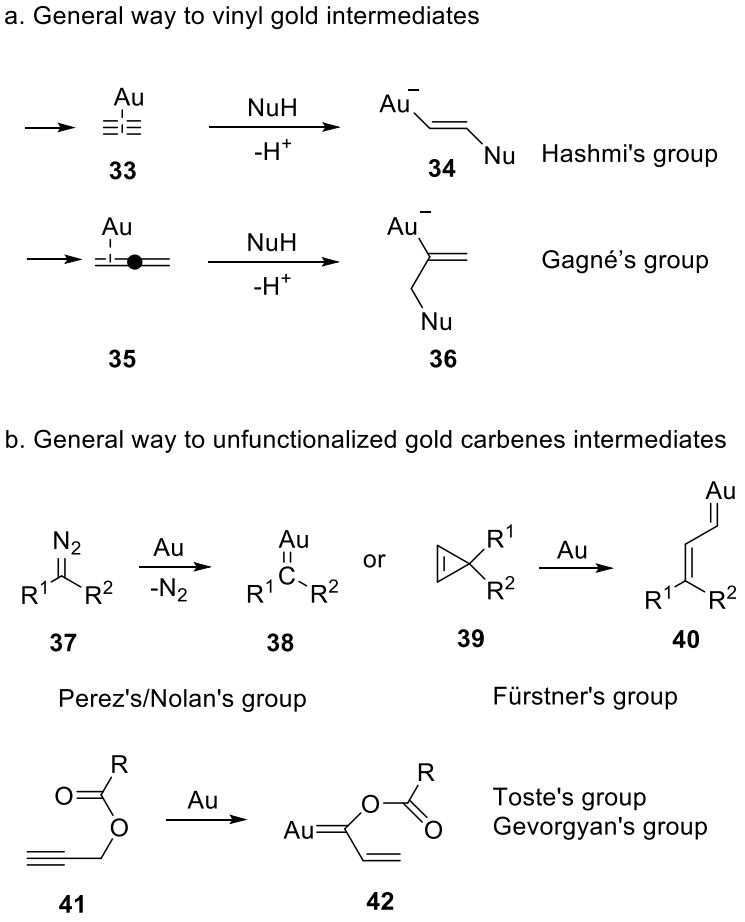

Scheme 1.10 General way to vinyl gold intermediates and unfunctionalized gold carbene intermediates

1.4 Greener and sustainable trends in organic chemistry

The diverse field of chemistry requires various greener pathways in our quest toward attaining sustainability. Continual developments in green organic synthesis and transformation have established since the last 30 years.[27] Green organic chemistry towards future chemical processes and products by inventing novel reactions that can

maximize the desired products and at the same time minimize the by-products, constructing new synthetic scheme and apparat that can simplify operations in chemical productions, and seeking greener solvents that are inherently environmentally and ecologically benign.[28]

1.4.1 Green chemistry principle

The aim of green chemistry is to reduce chemistry-related impact on human health and virtually eliminate contamination of the environment through dedicated, sustainable prevention programs. Green chemistry searches for alternative, environmentally friendly reaction media and at the same time strives to increase reaction rates and lower reaction temperatures. The 12 Principles of Green Chemistry[29,30] are as following:

(1) Prevention: It is better to prevent waste than to treat or clean up waste after it has been created. (2) Atom Economy: Synthetic methods should be designed to maximize the incorporation of all materials used in the process into the final product. (3) Less Hazardous Chemical Syntheses: Wherever practicable, synthetic methods should be designed to use and generate substances that possess little or no toxicity to human health and the environment. (4) Designing Safer Chemicals: Chemical products should be designed to affect their desired function while minimizing their toxicity. (5) Safer Solvents and Auxiliaries: The use of auxiliary substances (e.g., solvents, separation agents, etc.) should be made unnecessary wherever possible and innocuous when used. (6) Design for Energy Efficiency: Energy requirements of chemical processes should be recognized for their environmental and economic impacts and should be minimized. If possible, synthetic methods should be conducted at ambient temperature and pressure. (7) Use of Renewable Feedstocks: A raw material or feedstock should be renewable rather than depleting whenever technically and economically practicable. (8) Reduce Derivatives: Unnecessary derivatization (use of blocking groups, protection/ deprotection, temporary modification of physical/chemical processes) should be minimized or avoided if it possible, because such steps require additional reagents and can generate waste. (9) Catalysis: Catalytic reagents (as selective as possible) are

superior to stoichiometric reagents. (10) Design for Degradation: Chemical products should be designed so that at the end of their function they break down into innocuous degradation products and do not persist in the environment. (11) Real-time Analysis for Pollution Prevention: Analytical methodologies need to be further developed to allow for real-time, in-process monitoring and control prior to the formation of hazardous substances. (12) Inherently Safer Chemistry for Accident Prevention: Substances and the form of a substance used in a chemical process should be chosen to minimize the potential for chemical accidents, including releases, explosions, and fires.

Green chemistry metrics describe aspects of a chemical process relating to the principles of green chemistry. The metrics serve to quantify the efficiency or environmental performance of chemical processes and allow changes in performance to be measured.[31] Atom economy was designed as a framework by which organic chemists would pursue "greener" chemistry. The atom economy number is how much of the reactants remain in the final product.[32] The atom economy is calculated by:

$$\text{Atom economy (\%)} = \frac{\text{Molecular mass of desired product}}{\text{Molecular mass of all reactants}} \times 100\% \qquad \text{Equation (1)}$$

Carbon economy is how much carbon ends up in the useful product compared to how much carbon was used to create the product.[32] The atom economy is calculated by:

$$\text{Carbon economy (\%)} = \frac{\text{Number of carbon in desired product}}{\text{Number of carbon in reactants}} \times 100\% \qquad \text{Equation (2)}$$

The E-factor of a chemical process is the ratio of the mass of waste per mass of product.[33] E-factor is calculated by:

$$\text{E-factor} = \frac{\text{Mass of total waste}}{\text{Mass of product}} \qquad \text{Equation (3)}$$

The reaction mass efficiency is the percentage of actual mass of desire product to the

mass of all reactants used. It considers both atom economy and chemical yield.[34] The reaction mass efficiency is calculated by:

$$\text{Reaction mass efficiency } (\%) = \frac{\text{Mass of desired product}}{\text{Mass of all reactants}} \text{ x } 100\% \quad \text{Equation (4)}$$

1.4.2 Interdisciplinary of organic chemistry

In addition to green chemistry, the development of organic chemistry should also consider interdisciplinary collaboration and communication. We live in an interconnected world, and the sciences aren't confined to neat boxes either. Chemistry contributes to all the other science disciplines and is interdisciplinary by nature.[35,36] Only by keeping greener and sustainable key points in mind, chemistry can truly be better sustainable and contribute to humanity.

1.5 Research objectives

This doctoral thesis focuses on gold-catalyzed alkyne hydro-functionalization reactions. (1) Exploring a facile route to synthesis α-ketoamide by gold-catalyzed two-fold reaction of anthranil and bromoalkyne. (2) Developing a one-pot gold-catalyzed hydroamination of terminal alkyne with hydroxylamine-O-sulfonic acid (HOSA) delivering oximes.

1.6 References

[1] a) Schmidbaur, H., (ed), Gold: Progress in Chemistry, Biochemistry and Technology. John Wiley & Sons: New York, **1999**. b) Hashmi, A. S. K., Introduction: Gold Chemistry, *Chem. Rev.* **2021**, *121* (14), 8309-8310.

[2] a) Pappas, S., Gold: Facts, History and Uses of the Most Malleable Chemical Element. **2022**. b) Schmidbaur, H., Gold Chemistry is Different. *Interdiscip. Sci. Rev.* **1992**, *17* (3), 213-220.

[3] a) Armer, B.; Schmidbaur, H., Organogold Chemistry. *Angew. Chem. Int. Ed.* **1970**, *82* (3), 120-133. b) Schmidbaur, H., Is Gold Chemistry a Topical Field of Study? *Angew. Chem. Int. Ed.* **1976**, *15* (12), 830-843. c) Schmidbaur, H., Gold-Chemie: ein Eldorado. *Naturwiss. Rundsch*. **1995**, *48* (12), 443-451.

[4] Sennewald, K.; Vogt, W.; Glaser, H., Process for the Preparation of Vinyl Acetate. Patent DE1244766B. **1967**.

[5] a) Bond, G. C., The Catalytic Properties of Gold. *Gold Bulletin.* **1972**, *5* (4), 11-13. b) Hashmi, A. S. K., Homogeneous Catalysis by Gold. *Gold Bulletin.* **2004**, *37* (1), 51-65. c) Bond, G. C.; Sermon, P. A.; Webb, G.; Buchanan, D. A.; Wells, P. B., Hydrogenation over Supported Gold Catalysts. *J. Chem. Soc. Chem. Commun.* **1973**, *13*, 444-445.

[6] a) Masatake, H.; Tetsuhiko, K.; Hiroshi, S.; Nobumasa, Y., Novel Gold Catalysts for the Oxidation of Carbon Monoxide at a Temperature far Below 0 °C. *Chem. Lett.* **1987**, *16* (2), 405-408. b) Hutchings, G. J., Vapor Phase Hydrochlorination of Acetylene: Correlation of Catalytic Activity of Supported Metal Chloride Catalysts. *J. Catal.* **1985**, *96* (1), 292-295. c) Hashmi, A. S. K.; Hutchings, G. J., Gold Catalysis. *Angew. Chem., Int. Ed.* **2006**, *45* (47), 7896-7936.

[7] Ito, Y.; Sawamura, M.; Hayashi, T., Catalytic Asymmetric Aldol Reaction: Reaction of Aldehydes with Isocyanoacetate Catalyzed by a Chiral Ferrocenylphosphine-Gold (I) Complex. *J. Am. Chem. Soc.* **1986**, *108* (20), 6405-6406.

[8] a) Teles, J. H.; Brode, S.; Chabanas, M., Cationic Gold(I) Complexes: Highly Efficient Catalysts for the Addition of Alcohols to Alkynes. *Angew. Chem., Int. Ed.* **1998**, *37* (10), 1415-1418. b) Prati, L.; Rossi, M., Gold on Carbon as A New Catalyst for Selective Liquid Phase Oxidation of Diols. *J. Catal.* **1998**, *176* (2), 552-560.

[9] Takei, T.; Akita, T.; Nakamura, I.; Fujitani, T.; Okumura, M.; Okazaki, K.; Huang, J. H.; Ishida, T.; Haruta, M., Heterogeneous Catalysis by Gold. *Adv. Catal.* vol. **2012**, *55* (1), 1-124.

[10] Cole-Hamilton, D.J., Homogeneous Catalysis--New Approaches to Catalyst Separation, Recovery, and Recycling. *Science*. **2003**, *299* (5613), 1702-1706.

[11] a) Fürstner, A.; Davies, P. W., Catalytic Carbophilic Activation: Catalysis by Platinum and Gold π Acids. *Angew. Chem., Int. Ed.* **2007**, *46* (19), 3410-3449. b) Arcadi, A., Alternative Synthetic Methods through New Developments in Catalysis by Gold. *Chem. Rev.* **2008**, *108* (8), 3266-3325. c) Corma, A.; Leyva-Pérez, A. ; Sabater, M. J., Gold-Catalyzed Carbon-Heteroatom Bond-Forming Reactions. *Chem. Rev.* **2011**, *111* (3), 1657-1712. d) Shahzad, S. A.; Sajid, M. A.; Khan, Z. A.; Canseco-Gonzalez, D., Gold Catalysis in Organic Transformations: A review. *Synth. Commun.* **2017**, *47* (8), 735-755.

[12] Gorin, D. J.; Toste, F. D., Relativistic Effects in Homogeneous Gold Catalysis. *Nature*. **2007**, *446* (7134), 395-403.

[13] Malhotra, D.; Hammond, G. B.; Xu, B., Ligand Design in Gold Catalysis and Chemistry of Gold-Oxonium Intermediates. Homogeneous Gold Catalysis. **2015**, 1-23.

[14] Kumar, M.; Jasinski, J.; Hammond, G. B.; Xu, B., Alkyne/Alkene/Allene-Induced Disproportionation of Cationic Gold (I) Catalyst. Chem. A. Eur. J, **2014**, *20* (11), 3113-3119.

[15] Brown, T. J.; Weber, D.; Gagne´, M. R.; Widenhoefer, R. A., Mechanistic Analysis of Gold(I)-Catalyzed Intramolecular Allene Hydroalkoxylation Reveals an Off-Cycle Bis(gold) Vinyl Species and Reversible C-O Bond Formation. *J. Am. Chem. Soc*. **2012**, *134* (22), 9134-9137.

[16] Wang, Y. M.; Lackner, A. D.; Toste, F. D., Development of Catalysts and Ligands for Enantioselective Gold Catalysis. *Acc. Chem. Res.* **2014**, *47* (3), 889-901.

[17] a) Zeng, X.; Liu, S.; Xu, B., Stable Yet Reactive Cationic Gold Catalysts with Carbon Based Counterions. *RSC Adv*. **2016**, *6* (81), 77830-77833. b) Lu, Z. C.; Li, T. T.; Mudshinge, S. R.; Xu, B.; Hammond, G. B., Opmization of Catalysts and Conditions in Gold(I) Catalysis-Counterion and Additive Effects, *Chem. Rev.* **2021**, *121* (14), 8452-8477.

[18] a) Nieto-Oberhuber, C.; López, S.; Munoz, M. P.; Cárdenas, D. J.; Buñuel, E.; Nevado, C.; Echavarren, A. M., Divergent Mechanisms for the Skeletal Rearrangement and [2+2] Cycloaddition of Enynes Catalyzed by Gold. *Angew. Chem., Int. Ed.* **2005**,

117 (38), 6302-6304. b) Nieto-Oberhuber, C.; Muñoz, M.P.; López, S.; Jiménez-Núñez, E.; Nevado, C.; Herrero-Gómez, E.; Raducan, M.; Echavarren, A. M., Gold(I)-Catalyzed Cyclizations of 1,6-Enynes: Alkoxycyclizations and exo/endo Skeletal Rearrangements. *Chem. -Eur. J.* **2006**, 12 (6), 1677-1693.

[19] a) Hintermann, L.; Labonne, A., Catalytic Hydration of Alkynes and Its Application in Synthesis. *Synthesis*. **2007**, *08* (2007), 1121-1150. b) Goodwin, J. A.; Aponick, A., Regioselectivity in the Au-Catalyzed Hydration and Hydroalkoxylation of Alkynes. *Chem. Commun*. **2015**, *51* (42), 8730-8741.

[20] a) Alonso, F.; Beletskaya, I. P.; Yus, M., Transition-Metal-Catalyzed Addition of Heteroatom-Hydrogen Bonds to Alkynes. *Chem. Rev.* **2004**, *104* (6), 3079-3160. b) Huguet, N.; Echavarren, A. M., Gold-Catalyzed O-H Bond Addition to Unsaturated Organic Molecules. Hydrofunctionalization. Springer, Berlin, Heidelberg. **2011**, 291-324. c) Obradors, C.; Echavarren, A. M.; Intriguing Mechanistic Labyrinths in Gold(I) Catalysis. *Chem. Commun*. **2013**, *50* (1), 16-28. d) Wang, D.; Cai, R.; Sharma, S.; Jirak, J.; Thummanapelli, S. K.; Akhmedov, N. G.; Zhang, H.; Liu, X.; Petersen, J. L.; Shi, X., "Silver effect" in Gold(I) Catalysis: an Overlooked Important Factor. *J. Am. Chem. Soc*. **2012**, *134* (21), 9012-9019. e) Biasiolo, L.; Trinchillo, M.; Belanzoni, P.; Belpassi, L.; Busico, V.; Ciancaleoni, G.; D'Amora, A.; Macchioni, A.; Tarantelli, F.; Zuccaccia, D., Unexpected Anion Effect in the Alkoxylation of Alkynes Catalyzed by N-Heterocyclic Carbene (NHC) Cationic Gold Complexes. *Chem. -Eur. J.* **2014**, *20* (45), 14594-14598. f) Zhdanko, A.; Maier, M. E., Explanation of Counterion Effects in Gold (I)-Catalyzed Hydroalkoxylation of Alkynes. *ACS Catal.* **2014**, *4* (8), 2770-2775.

[21] a) Huang, L.; Arndt, M.; Gooßen, K.; Heydt, H.; Gooßen, L. J., Late Transition Metal-Catalyzed Hydroamination and Hydroamidation. *Chem. Rev.* **2015**, *115* (7), 2596-2697. b) Tashrifi, Z.; Mohammadi Khanaposhtani, M.; Biglar, M.; Larijani, B.; Mahdavi, M., Recent Advances in Alkyne Hydroamination as a Powerful Tool for the Construction of C-N Bonds. *Asian J. Org. Chem*. **2020**, 9 (7), 969-991.

[22] a) Moran, J.; Gorelsky, S. I.; Dimitrijevic, E.; Lebrun, M. E.; Bedard, A. C.; Seguin, C.; Beauchemin, A. M., Intermolecular Cope-Type Hydroamination of Alkenes and

Alkynes using Hydroxylamines. *J. Am. Chem. Soc.* **2008**, *130* (52), 17893-17906. b) Beauchemin, A. M.; Moran, J.; Lebrun, M.; Seguin, C.; Dimitrijevic, E.; Zhang, L.; Gorelsky,S. I., Intermolecular Cope-Type Hydroamination of Alkenes and Alkynes. *Angew. Chem., Int. Ed.* **2008**, *47* (8), 1410-1413. c) Cebrowski, P. H.; Roveda, J. G.; Moran, J.; Gorelsky, S. I.; Beauchemin, A. M., Intermolecular Cope-Type Hydroamination of Alkynes using Hydrazines. *Chem. Commun.* **2008**, *10* (4), 492-493.

[23] a) Wang, L.; Yu, X.; Feng, X.; Bao, M., Synthesis of 3,5-Disubstituted Pyrazoles via Cope-Type Hydroamination of 1,3-Dialkynes. *J. Org. Chem.* **2013**, *78* (4), 1693-1698. b) Wang, Y.; Wei, D.; Zhang, W.; Wang, Y.; Zhu, Y.; Jia, Y.; Tang, M., A Theoretical Study on the Mechanisms of the Reactions Between 1,3-Dialkynes and Ammonia Derivatives for the Formation of Five-Membered N-Heterocycles. *Org. Biomol. Chem.* **2014**, *12* (38), 7503-7514.

[24] a) Hashmi, A. S. K.; Schwarz, L.; Choi, J. H.; Frost, T. M., A New Gold-Catalyzed C-C Bond Formation. *Angew. Chem., Int. Ed.* 2000, 39(13), 2285-2288. b) Hashmi, A. S. K.; Frost, T. M.; Bats, J. W., Highly Selective Gold-Catalyzed Arene Synthesis. *J. Am. Chem. Soc.* **2000**, *122* (46), 11553-11554.

[25] Davies, P.; Garzon Sanz, M., Nucleophilic Nitrenoids through -Acid Catalysis. *Asian. J. Org. Chem.* **2015**, *4* (8), 694-708.

[26] a) Fructos, M. R.; Belderrain, T. R.; de Frémont, P.; Scott, N. M.; Nolan, S. P.; Díaz-Requejo, M. M.; Pérez, P. J., A Gold Catalyst for Carbene-Transfer Reactions from Ethyl Diazoacetate. *Angew. Chem., Int. Ed.* **2005**, *117* (33), 5418-5422. b). Fürstner, A.; Morency, L., On the Nature of the Reactive Intermediates in Gold-Catalyzed Cycloisomerization Reactions. *Angew. Chem., Int. Ed.* **2008**, *47* (27), 5030-5033. c) Johansson, M. J.; Gorin, D. J.; Staben, S. T.; Toste, F. D., Gold(I)-Catalyzed Stereoselective Olefin Cyclopropanation. *J. Am. Chem. Soc.* **2005**, *127* (51), 18002-18003. d) Xia, Y.; Dudnik, A. S.; Gevorgyan, V.; Li, Y., Mechanistic Insights into the Gold-Catalyzed Cycloisomerization of Bromoallenyl Ketones: Ligand-Controlled Regioselectivity. *J. Am. Chem. Soc.* **2008**, *130* (22), 6940-6941. e) Nunes dos Santos Comprido, L.; Klein, J. E.; Knizia, G.; Kastner, J.; Hashmi, A. S. K., The Stabilizing

Effects in Gold Carbene Complexes. *Angew. Chem., Int. Ed.* **2015**, *54* (35), 10336-10340. f) Fürstner, A.; Hannen, P.; Carene Terpenoids by Gold-Catalyzed Cycloisomerization Reactions. *Chem. Commun.* **2004**, 22, 2546-2547. g) Fürstner, A.; Hannen, P., Platinum- and Gold-Catalyzed Rearrangement Reactions of Propargyl Acetates: Total Syntheses of (-)-α-Cubebene,(-)-Cubebol, Sesquicarene and Related Terpenes. *Eur. J. Chem.* **2006**, *12* (11), 3006-3019. h) Wang, Y.; Zheng, Z.; Zhang, L., Intramolecular Insertions into Unactivated C(sp^3)-H Bonds by Oxidatively Generated β-Diketone-α-Gold Carbenes: Synthesis of Cyclopentanones. *J. Am. Chem. Soc.* **2015**, *137* (16), 5316-5319. i) Li, J.; Ji, K.; Zheng, R.; Nelson, J.; Zhang, L., Expanding the Horizon of Intermolecular Trapping of In-situ Generated α-oxo Gold Carbenes: Efficient Oxidative Union of Allylic Sulfides and Terminal Alkynes via C-C Bond Formation. *Chem. Commun.* **2014**, *50* (31), 4130-4133. j) Shu, C.; Li, L.; Xiao, X.; Yu, Y.; Ping, Y.; Zhou, J.; Ye, L., Flexible and Practical Synthesis of 3-Oxyindoles through Gold-Catalyzed Intermolecular Oxidation of o-Ethynylanilines. *Chem. Commun.* **2014**, *50* (63), 8689-8692.

[27] Varma, R. S., Greener and Sustainable Trends in Synthesis of Organics and Nanomaterials. *ACS Sustainable Chem. Eng.* **2016**, *4* (11), 5866-5878.

[28] Li, C. J.; Trost, B. M., Green Chemistry for Chemical Synthesis, *PNAS*. **2008**, *105* (36), 13197-13202.

[29] Kharissova, O. V.; Kharisov, B. I.; Oliva González, C. M.; Méndez, Y. P.; López, I., Greener synthesis of chemical compounds and materials. *R. Soc. Open Sci.* **2019**, *6* (11), 191378.

[30] Anastas, P.; Eghbali, N., Green Chemistry: Principles and Practice. *Chem. Soc. Rev.* **2010**, *39* (1), 301-312.

[31] a) Trost, B.M., The Atom Economy-A Search for Synthetic Efficiency. *Science*, **1991**, *254* (5037), 1471-1477. b) Tobiszewski, M.; Marć, M.; Gałuszka, A.; Namieśnik, J., Green Chemistry Metrics with Special Reference to Green Analytical Chemistry. *Molecules*, **2015**, *20* (6), 10928-10946. c) Outili, N.; Kerras, H.; Nekkab, C.; Merouani, R. ; Meniai, A. H., Biodiesel Production Optimization from Waste Cooking Oil Using

Green Chemistry Metrics. *Renew. Energy*. **2020**, 145, 2575-2586. d) Selva, M.; Perosa, A., Green Chemistry Metrics: A Comparative Evaluation of Dimethyl Carbonate, Methyl Iodide, Dimethyl Sulfate and Methanol as Methylating Agents. *Green Chem.* **2008**, *10* (4),457-464.

[32] a) Trost, B.M., Atom Economy - A Challenge for Organic Synthesis: Homogeneous Catalysis Leads the Way. *Angew. Chem., Int. Ed.* **1995**, *34* (3), 259-281.

[33] Sheldon, R. A., The E Factor: Fifteen Years on. *Green Chem*. **2007**, *9* (12), 1273-1283. b) Trost, B.M., On Inventing Reactions for Atom Economy. *Acc. Chem. Res.* **2002**, *35* (9), 695-705. c) Freund, R.; Lächelt, U.; Gruber, T.; Rühle, B.; Wuttke, S., Multifunctional Efficiency: Extending the Concept of Atom Economy to Functional Nanomaterials. *ACS nano*, **2018**, *12* (3), 2094-2105.

[34] a) Dicks, A. P.; Hent, A., Atom economy and reaction mass efficiency. Green Chemistry Metrics, Springer, Cham. **2015**, 17-44. b) Sheldon, R. A., Fundamentals of Green Chemistry: Efficiency in Reaction Design. *Chem. Soc. Rev.* **2012**, *41* (4), 1437-1451. c) Eissen, M.; Lenoir, D., Mass Efficiency of Alkene Syntheses with Tri-and Tetrasubstituted Double Bonds. *ACS Sustain. Chem. Eng.* **2017**, *5* (11), 10459-10473.

[35] Cann, M. C.; Dickneider, T. A., Infusing the Chemistry Curriculum with Green Chemistry using Real-World Examples, Web Modules, and Atom Economy in Organic Chemistry Courses. *J. Chem. Educ.* **2004**, *81* (7), 977.

[36] Küpper, F. C., Feiters, M. C.; Olofsson, B.; Kaiho, T.; Yanagida, S.; Zimmermann, M. B.; Carpenter, L. J.; Luther III, G. W.; Lu, Z.; Jonsson, M.; Kloo, L., Commemorating Two Centuries of Iodine Research: An Interdisciplinary Overview of Current Research. *Angew. Chem., Int. Ed.* **2011**, *50* (49), 11598-11620.

Chapter 2. Facile Synthesis of α-Ketoamides via Gold(I) Carbene Intermediates

2.1 Introduction

α-Ketoamide is an important motif in a broad spectrum of drugs, including anti-inflammatory, anti-HIV, anti-tumor and even inhibitors of coronavirus. As the key components of biomedicines, the development of synthetic methods for *α*-ketoamide has increased considerably in recent years.[1-4] Biologically active of α-ketoamides are shown Scheme 2.1.

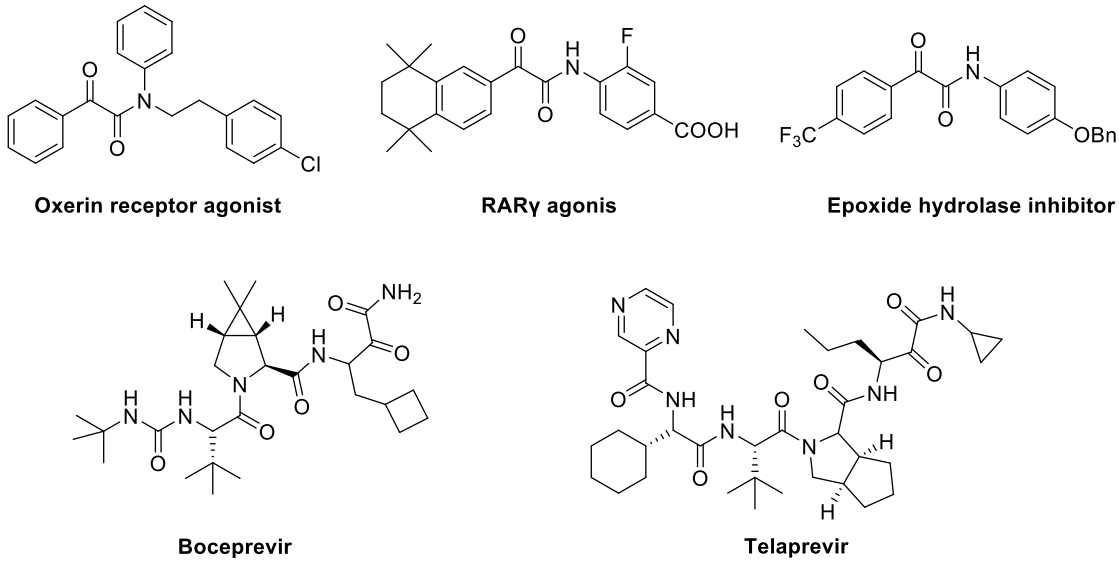

Scheme 2.1 Biological activity of α-ketoamides

Among the most common approaches to form the α-ketoamide molecule are amidations of α-keto acids,[5, 6] oxidation of α-aminoamides,[7] α-cyanamides[8] and α-hydroxyamides,[9] the process of isocyanides with aromatic acyl chlorides or anhydrides followed by hydrolysis of α-ketoimidoyl chloride,[10] transition metal-catalyzed carbonylative amination of aryl halides,[11-13] and the activation by bimolecular oxygen.[14-17] Although there have been many attempts to synthesize α-ketoamides, the development of facile reaction routes is still an challenging. Especially,

the adding of functional groups as synthetic materials for further reactions is still a daunting task. The use of anthranil to introduce useful formyl groups for synthesis process is a good option, anthranil has a relatively weak N-O bond that releases its masked formyl subunit upon cleavage. But normally, it's hard to adding formyl group and the compatibility of functional group remains a challenge. In 2016, Hashmi and co-workers, for the first time, explored the possibility of anthranils as a new nitrene transfer reagent.[18a] They developed a formal [3+2] annulation of anthranils and alkynes, furnishing unprotected 7-acylindoles (Scheme 2.2a). Importantly, this reaction tolerates not only activated alkynes, such as ynamides and alkynyl aryl ethers, but also non-polarized alkynes. The replacement of normal alkynes to propargylic silyl ethers afforded diverse functionalized quinolones instead of the expected indole products.[18b] This reaction process via an α-imino gold carbene intermediate and a subsequent 1,2-H shift, followed by an intramolecular condensation annulation (Scheme 2.2b). In further extensions of these works, they described two more regioselective C−H annulation reactions to access N-doped polycyclic aromatic hydrocarbons[18c] (Scheme 2.2c) and 2-amino quinolone derivatives[18d] (Scheme 2.2d) by using different alkynes. On the basis of this intriguing principle, several methods have been established for the production of α-ketoamides. Zou et.al proposed a copper-catalyzed amidation of α-keto acids with anthranils protected by Ar.[19a] Wu et.al reported that methyl ketones oxidized amidation with anthranils.[19b]

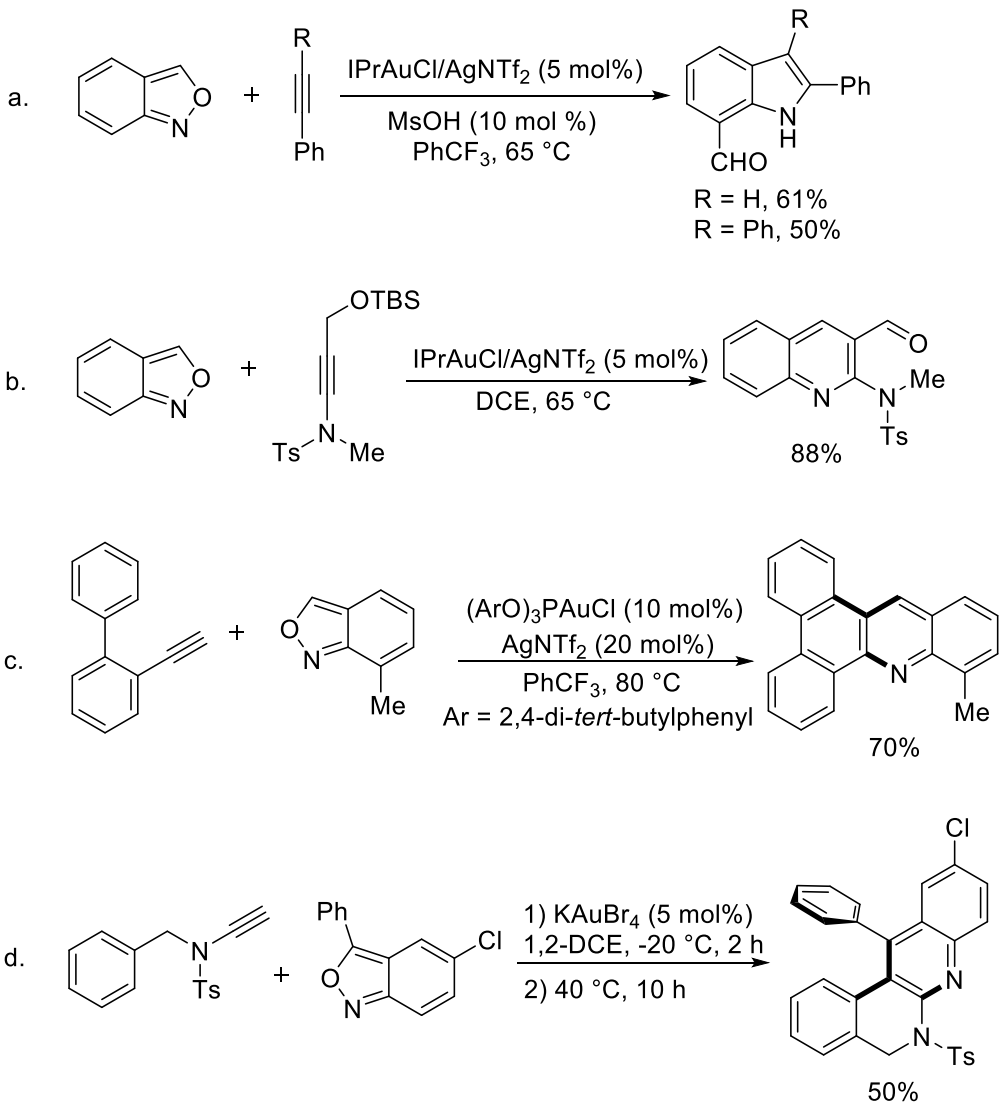

Scheme 2.2 Previous reports of anthranil as nitrene transfer reagent

Our proposed method purposed in the employ of haloalkynes and anthranil to construct α-ketoamides with gold catalyst. However, gold-catalyzed process of anthranils with either normal alkynes or ynamides usually form indole or quinoline derivatives, this is confirmed by our group previous work (Scheme 2.3a).[20-26] We anticipated that the particular electronic properties of haloalkynes combined with the attached heteroatom would allow the synthesis of the α-ketoamides. We hypothesized that two-fold addition of anthranil would from α-iminoimidoyl halide species after formation of an intermediate α-imino carbene, that is subsequently oxidation by a second molecule of anthranil.[27-29] The hydrolysis of the imidhalide brings us to the final target. (Scheme 2.3b)

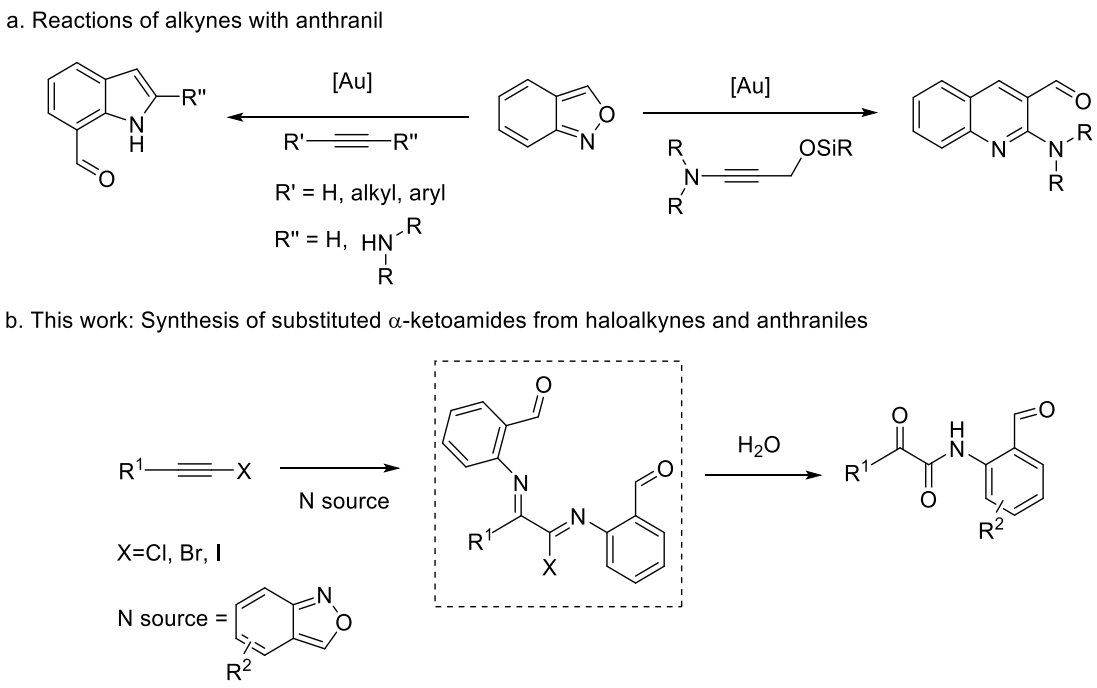

Scheme 2.3 Known reactions of anthranil with alkynes and the reaction developed here

2.2 Result and discussion

2.2.1 Optimization of the reaction conditions

As showed in Table 2.1, our initial attempt was carried with 1.0 equivalent of bromoalkyne (**1a**), 2.0 equivalent of anthranil (**2a**), 5 mol% equivalent of $IPrAuNTf_2$ and $IPrAuSbF_6$ in 1,2-dichloroethane (DCE) solvent at 60 °C (entries 1 and 2), the yield of α-ketoamide product (**3a**) is almost same, the change of silver salts as co-catalyst didn't affect the reaction efficiency. Then, we confirmed that an exchange of the ligand form IPr to Buchwald-type phophine ligands (entries 1-8) at the gold complexes led to higher yields (28-48% yields). Obviously, gold catalyst PPh_3AuNTf_2 shown the better performance, with a 48% yield of α-ketoamide. Next, a solvent screening showed that the 1,2-dichlorobenzene (DCB) delivered a better yield (58%, entries 9-12). Finally, 10 mol% MsOH and 2.0 equivalent of water as addition increased the reaction yield to 75% yield (entry 13), 10 mol% TMsOTf with 2.0 equivalent of water as an additive delivered a 58% yield (entry 14). With regard to the temperature effect, we conducted the reaction

at room temperature and at 100 °C (entries 15-16), the yield indicated that in this reaction 60 °C are better. Of course, neither TMsOTf, MsOH, $AgNTf_2$ nor catalyst free were effective to synthesize the desired product (entries 17-20). According to all these results, the scope was explored using PPh_3AuNTf_2 as catalyst, MsOH as addictive, 60 °C in DCB.

Table 2.1 Optimization of the Reaction Conditions

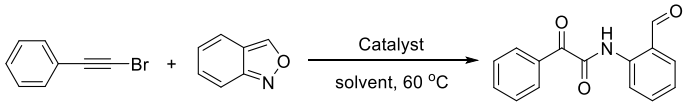

1a **2a** **3a**

Entry	Catalyst	Solvent	Conversion	Yield (%)
1	$IPrAuNTf_2$	DCE	≥98	41
2	$IPrAuSbF_6$	DCE	≥98	40
3	$(ArO)_3PAuNTf_2$	DCE	≥98	37
4	PPh_3AuNTf_2	DCE	≥98	48
5	$DMSAuNTf_2$	DCE	≥98	33
6	$(DMAP)_2AuNTf_2$	DCE	≥98	34
7	$CyJohnphosAuNTf_2$	DCE	≥98	28
8	$XPhosAuNTf_2$	DCE	≥95	43
9	PPh_3AuNTf_2	DCB	≥98	58
10	PPh_3AuNTf_2	PhBr	≥98	25
11	$P\ Ph_3AuNTf_2$	PhMe	≥98	22
12	PPh_3AuNTf_2	DCM	≥98	27
13[a]	**PPh_3AuNTf_2**	**DCB**	**⩾98**	**75**
14[b]	PPh_3AuNTf_2	DCB	≥98	58
15[c]	PPh_3AuNTf_2	DCB	≥98	26
16[d]	PPh_3AuNTf_2	DCB	≥98	39
17	$AgNTf_2$	DCB	30	trace
18	MsOH	DCB	trace	0
19	TMsOTf	DCB	trace	0
20	Catalyst Free	DCB	0	0

Reaction conditions: **1a** (1 equivalent), **2a** (2 equivalent), catalyst (5 mol% equivalent), solvent (1 mL) at 60 °C temperature for 24 h. [a]Used MsOH (10 mol% equivalent) and H_2O (2 equivalent). [b]Used TMsOTf (10 mol% equivalent) and H_2O (2 equivalent).

[c]Reacted at room temperature. [d]Reacted at 100 °C. DCE=1,2-dichloroethane, DCB=1,2-dichlorobenzene.

2.2.2 Substrate scope

After the reaction optimization, we next seek to explore the reaction scope. Numerous bromoalkynes were employed as shown in Scheme 2.4. In our optimized reaction system, we gained product **3a** with an increased yield of 75% with the use of bromoalkyne, by the way, using chloroalkyne or iodoalkyne as starting material we observed 56% or 43% yield. The X-ray structure analysis of product **3a** is shown in Scheme 2.5. The phenyl groups of bromoalkynes substituted by *o*-Cl (product **3b**), *p*-CF_3 (product **3c**), *m*-F/Me (product **3d** & **3e**), *p*-tBu (product **3f**) *p*-OMe (product **3g**) and *p*-Cl (product **3h**) giving the expected α-ketoamide products in yields 48% to 59%. The phenyl group substitution of bromoalkynes **1a** only has a small effect on the effciency of the reaction. Not only electron-withdrawing but also electron-donating substituents of bromoalkyne worked smoothly with anthranil **2a** to deliver the desired products. Alkyl-substituted alkynes from octayne to propyne were used for the synthesis of alkyl α-ketoamide (products **3i**-**3m**), we isolated a yield of 52-61%. Bromoalkynes with a isobutyl (**3n**) or a cyclohexyl group (**3o**) groups also could be converted in 60% and 55% yield. Bromoalkynes bearing of cyclopentyl (product **3p**) and cyclohexyl (product **3q**) groups less the product yields (32-35% yields). Obviously, phenyl-substituted bromoalkynes showed a better result than bromoalkynes with alkyl substituents. Furthermore, anthranils substituted by chloro- and bromo-group were converted (**3r**-**3s**) in yields of 42% and 45%. All above candidates demonstrate that using bromoalkynes and anthranil to construct α-ketoamides have a broad scope.

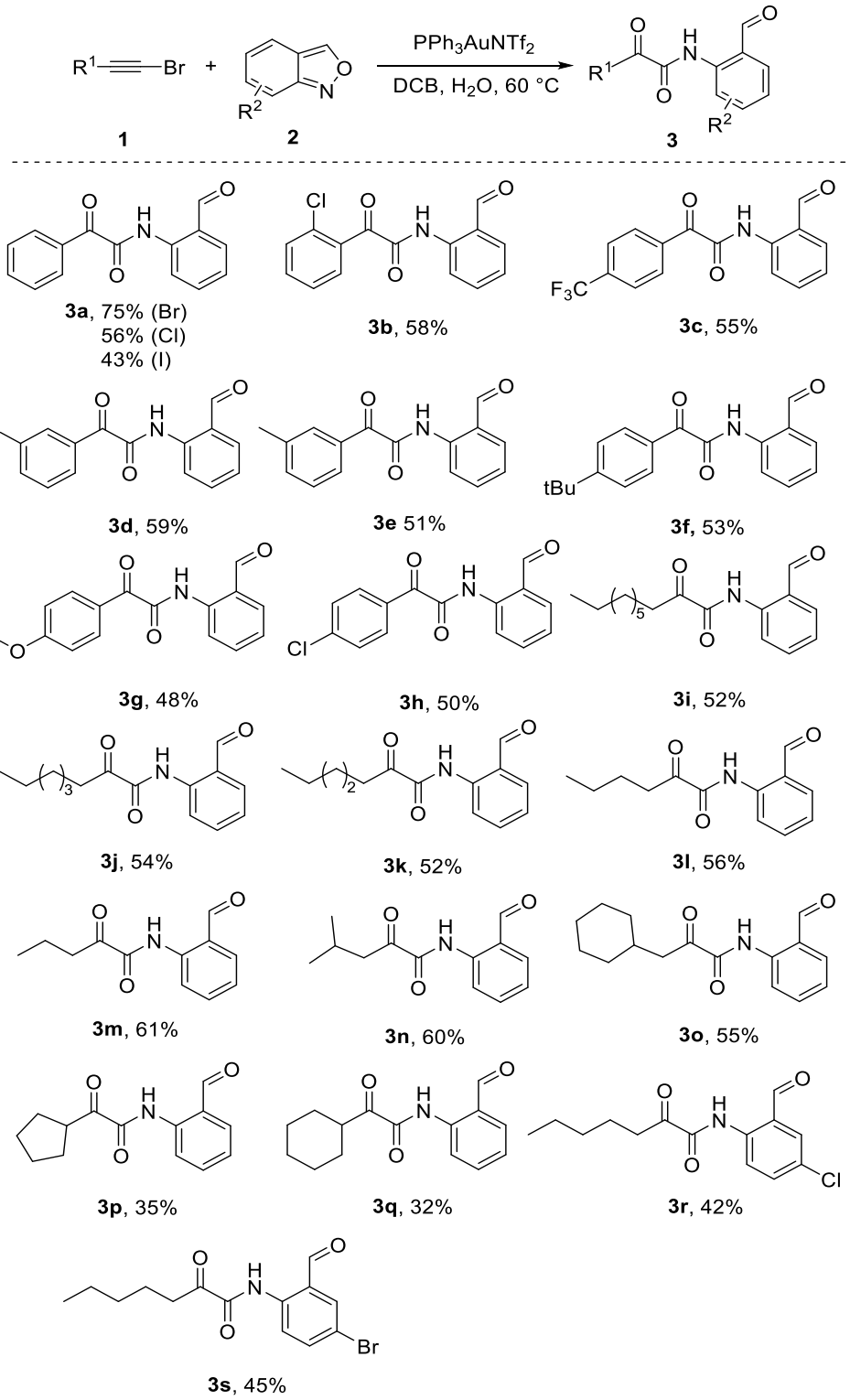

Scheme 2.4 Reaction scope. reaction conditions: **1a** (0.2 mmol), **2a** (0.4 mmol), H_2O (0.4 mmol), PPh_3AuNTf_2 (5 mol%) and MsOH (10 mol%) in DCB (1 mL) at 60 °C temperature for 24 h.

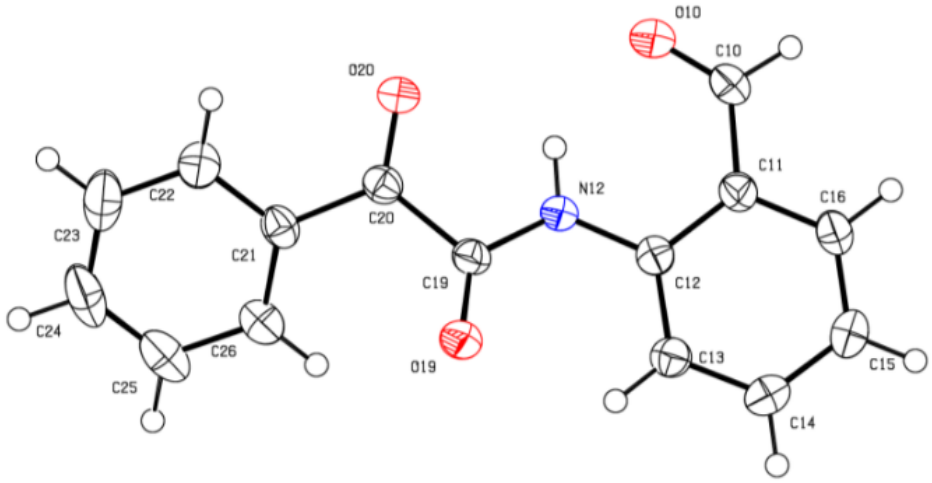

Scheme 2.5 Solid state molecular structure of **3a**

2.2.3 Mechanistic study

After we finished the reaction scope, the reaction mechanism was explored. The first control experiment was the reaction of bromoalkyne **1a** with H_2O (2 equiv) in presence of the catalyst PPh_3AuNTf_2 (Scheme 2.6). We only obtained the product ω-bromoacetophenone **4** (Scheme 2.6a). This indicates the nucleophilic attack of H_2O preferred the carbon closest to phenyl group of the bromoalkyne. So, we surmise that an α-imino gold carbene intermediate is involved, which reacts with anthanil. To further verify the source of oxygen atoms in **3a**, we ran our standard model reaction by adding $H_2{}^{18}O$ under N_2 (Scheme 2.6b). The two-fold ^{18}O labelled product 3a-^{18}O,^{18}O was observed, the HRMS data is given in Scheme 2.7. The result said that the oxygen atoms in **3a** originate from H_2O.

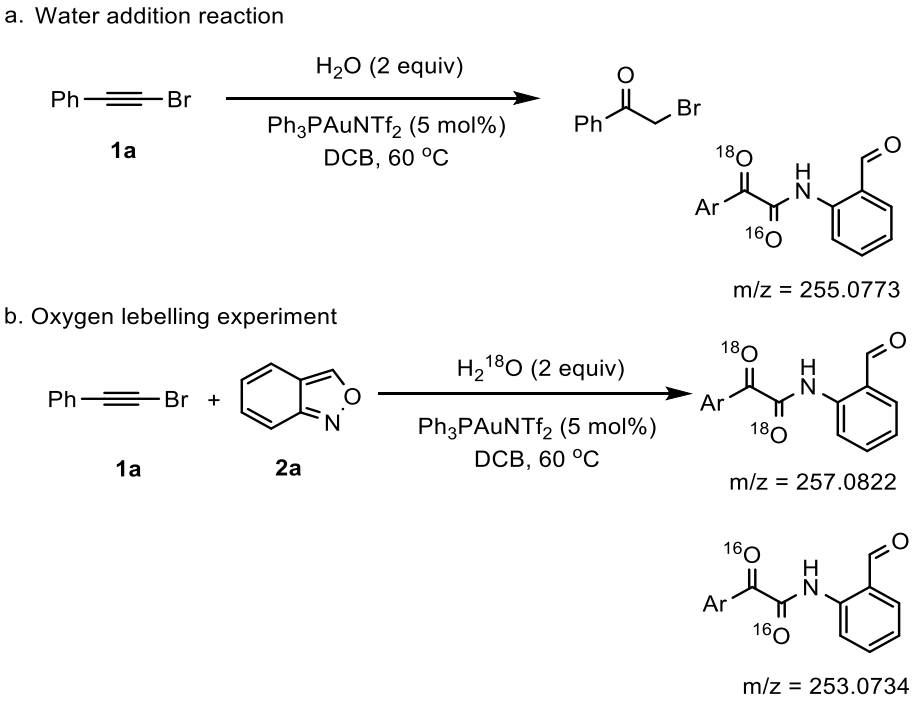

Scheme 2.6 Mechanistic investigation

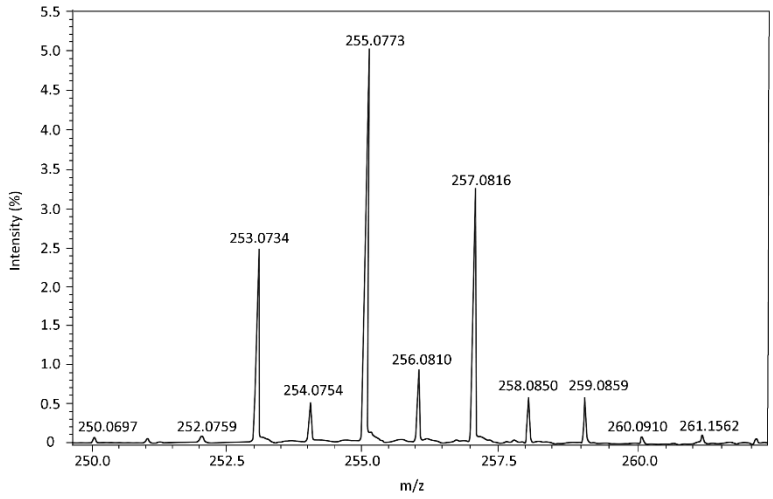

Scheme 2.7 The HRMS spectrum of ^{18}O labelling experiment

According to our mechanistic experiments, here we propose the following reaction mechanism (Scheme 2.8). The Lewis acidity of cationic Au activates the bromoalkyne and let it sufficiently electrophilic, which extremely accelerates the pace of nucleophilic addition of anthranil onto the alkyne. Then the generated Au-carbene intermediate **I** react with anthranil to form intermediate **II**. Then, **II** reacts with H_2O to result intermediate **III** with the elimination of HBr. Then the intermediate **III** is converted to

the amide intermediate **IV**. Finally, the H_2O addition to the intermediate **IV** delivers our desired product **3a** by setting free 2-aminobenzaldehyde.[30]

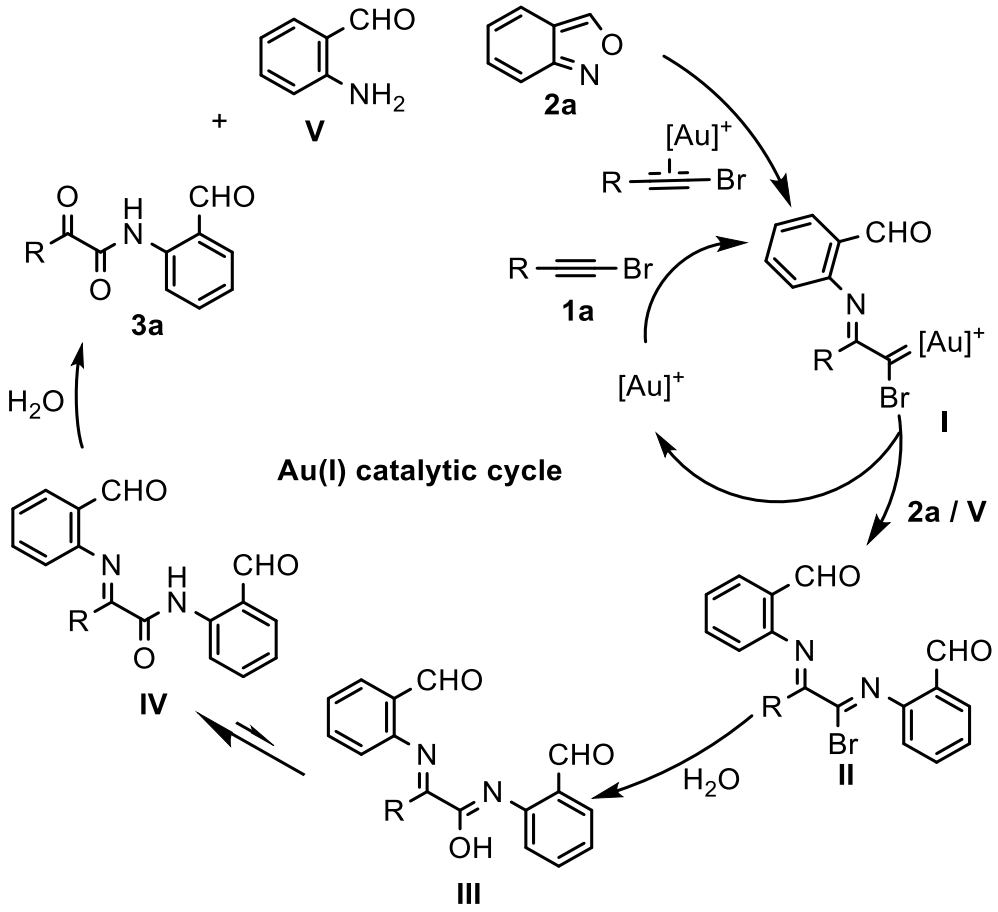

Scheme 2.8 The plausible reaction mechanism

The computational research was conducted ORCA 4.2.11 on the PBE02,3/def2-SVP4 level of theory, for gold also def2-TZVP4 was employed (Scheme 2.9). My colleague Martin C. Dietl conducted that computation. 1,2-Dichlorobenzene was simulated with the conductor-like polarizable continuum model (CPCM).[31,36] To simplify the computational, catalyst PPh_3AuNTf_2 was simplified to PMe_3AuNTf_2. The catalytic process is started by the exchange of ligand between PMe_3AuNTf_2 and substrate **I** to deliver the π-complex **II** tolerate an endergonic reaction route with a free energy of +20.8 kcal/mol (Scheme 6). Then, **II** is attacked by one equivalent of anthranil to obtain the transition state **III** at ΔG = +33.4 kcal/mol, which then leads to **IV** (ΔG = - 0.22 kcal/mol). **IV** breaks the tethered anthranil unit to the corresponding aldehyde **V** at ΔG

= 0.34 kcal/mol. The attack of another equivalent of anthranil proceeds barrier-free to make compound **VI** at ΔG = -38.5 kcal/mol. The catalytic cycle closes with the elimination of the Au catalyst to obtain the diamine **VII** (ΔG = - 51.9 kcal/mol), **VII** subsequently is hydrolyzed to **VIII** (ΔG = - 65.3 kcal/mol). **VIII** tautomerization to form the amide **IX** (ΔG = 77.2 kcal/mol). Final hydrolysis to deliver the α-ketoamide X at ΔG = - 96.0kcal/mol, 2-amino benzaldehyde is leaving.[32-36]

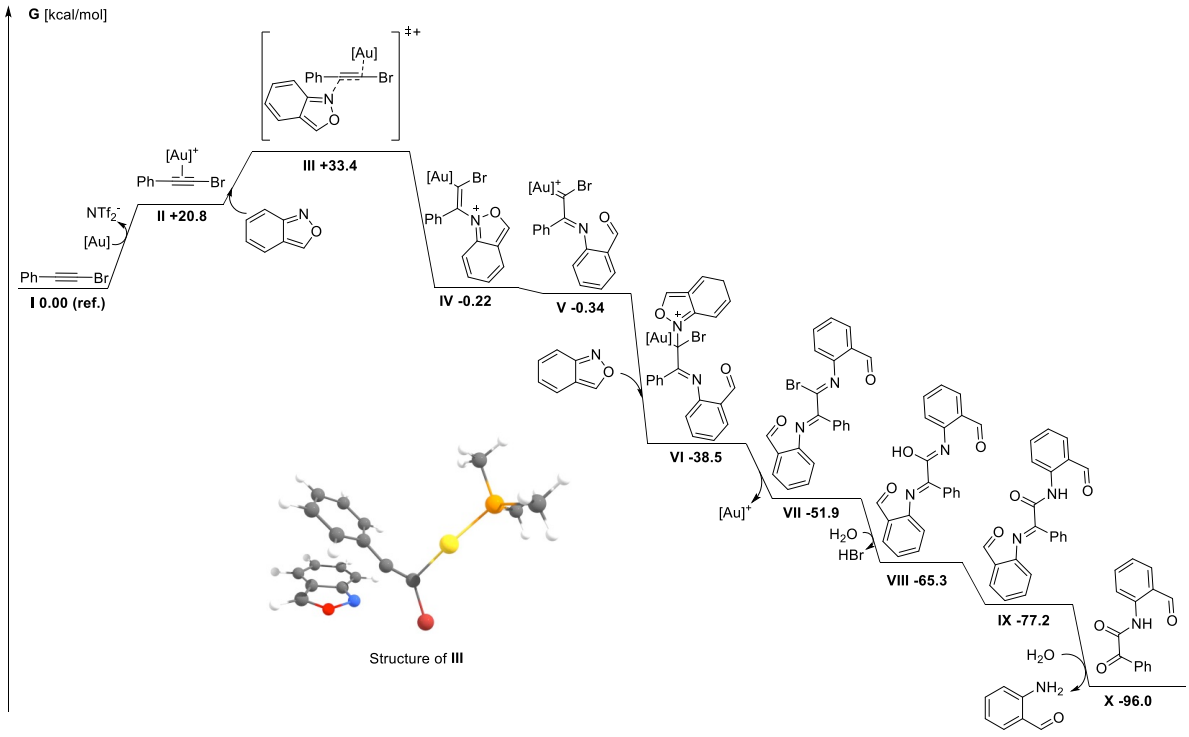

Scheme 2.9 Computational study of the mechanism.

2.2.4 Green chemistry metrics

Generally, modern chemical syntheses process should be based upon green chemistry principles.[37] Thus, we have evaluated the green chemistry metrics for the synthesis of *α*-ketoamide (**3a**) on a preparative scale (Table 2). As given in equation (1) and equation (2), atom economy (AE) is "how much of the reactants remain in the final desired product", reaction mass efficiency (RME) is "the percentage of the mass of the reactants that remain in the product.[14,37] Overall, our green process can enable the synthesis of *α*-ketoamide (**3a**) with an E-factor of 35.7, 57.9% atom economy,43.4%

atom efficiency, -68% carbon efficiency and 42.1% reaction mass efficiency.

$$\text{Atom economy}(\%) = \frac{\text{Molecular mass of desired product}}{\text{Molecular mass of all reactants}} \times 100\% \quad \text{Equation (1)}$$

$$\text{Reaction mass efficiency}\ (\%) = \frac{\text{Mass of desired product}}{\text{Mass of all reactants}} \times 100\% \quad \text{Equation (2)}$$

Table 2.2 Evaluation of green chemistry metrics for the synthesis of *α*-ketoamide

Reactant (1a)	bromoalkyne	0.036g	0.0002 mol	FW 181.03
Reactant (2a)	anthranil	0.047g	0.0004 mol	FW 119.12
Auxiliary	H_2O	0.0072g	0.0004 mol	FW 18.01
Solvent	DCB	1.306g		
Product (3a)	α-Ketoamide	0.038g	0.00015mol	FW 253.26

Product yield= 75%

E-factor= $\frac{0.036+0.047+0.0072+1.306-0.038}{0.038}$ =35.7 Kg waste per Kg product

Atom economy=$\frac{253.26}{437.28}$=57.9%

Atom efficiency=75% x 57.9%/100 = 43.4%

Carbon efficiency=$\frac{15}{8+7+7}$=68%

Reaction mass efficiency=$\frac{0.038}{0.036+0.047+0.0072}$=42.1%

2.3 Conclusions

In summary, we explored a Au-catalyzed process involving a diamine intermediate which subsequently provides the target product by hydrolysis. These experimental results represent a synthetic strategy involving a gold-catalyzed addition of two equivalents of nitrene to a C-C triple bond. One equivalent nitrene remains in the final product, another equivalent nitrene is eliminated as 2-aminobenzaldehyde during the hydrolysis process. A particular mixed N, O functionalization is achieved by this way. This protocol could be valuable and helpful in the field of lead finding in medicinal or pharmaceutical chemistry.

2.4 References

[1] Chiou, A.; Markidis, T.; Constantinou-Kokotou, V.; Verger, R.; Kokotos, G., Synthesis and Study of a Lipophilic α-ketoamide Inhibitor of Pancreatic lipase. *Org. Lett.* **2000,** *2* (3), 347-350.

[2] Papanikos, A.; Rademann, J.; Meldal, M., α-Ketocarbonyl Peptides: A General Approach to Reactive Resin-Bound Intermediates in the Synthesis of Peptide Isosteres for Protease Inhibitor Screening on Solid Support. *J. Am. Chem. Soc.* **2001,** *123* (10), 2176-2181.

[3] Semple, J.; Owens, T.; Nguyen, K.; Levy, O., New Synthetic Technology for Efficient Construction of α-Hydroxy-β-amino Amides via the Passerini Reaction1. *Org. Lett.* **2000,** *2* (18), 2769-2772.

[4] Zhang, L.; Lin, D.; Kusov, Y.; Nian, Y.; Ma, Q.; Wang, J.; Brunn, A.; Leyssen, P.; Lanko, K.; Neyts, J.; Wilde, A.; Snijder, E.; Liu, H.; Hilgenfeld, R., α-Ketoamides as Broad-Spectrum Inhibitors of Coronavirus and Enterovirus Replication: Structure-Based Design, Synthesis, and Activity Assessment. *J. Med. Chem.* **2020,** *63* (9), 4562–4578.

[5] Xu, X. L.; Xu, W. T.; Wu, J. W.; He, J. B.; Xu, H. T., Silver-Promoted Decarboxylative Amidation of α-Keto Acids with Amines. *Org. Biomol. Chem*. **2016**, *42* (14), 9970-9973.

[6] Liu, J.; Liu, Q.; Yi, H.; Qin, C.; Bai, R. P.; Qi, X. T.; Lan, Y.; Lei, A. W., Visible-Light-Mediated Decarboxylation/Oxidative Amidation of α-Keto Acids with Amines under Mild Reaction Conditions Using O^2. *Angew. Chem. Int. Ed.* **2014,** *53* (2), 502-506.

[7] Sperry, J., The Oxidation of Amides to Imides: A Powerful Synthetic Transformation. *Synthesis.* **2011,** *2011* (22), 3569-3580.

[8] Guin, S.; Rout, S.; Gogoi, A.; Ali, W.; Patel, B., A Palladium(II)-Catalyzed Synthesis of α-Ketoamides via Chemoselective Aroyl Addition to Cyanamides. *Adv. Syn. Catal.* **2014,** *356* (11-12), 2559-2565.

[9] Weng, S.; Shen, M.; Kao, J.; Munot, Y.; Chen, C., Chiral N-salicylidene Vanadyl Carboxylate-Catalyzed Enantioselective Aerobic Oxidation of α-hydroxy Esters and Amides. *PNAS America* **2006,** *103* (10), 3522-3527.

[10] Mossetti, R.; Pirali, T.; Tron, G. C.; Zhu, J., Efficient Synthesis of α-Ketoamides via 2-acyl-5-aminooxazoles by Reacting Acyl Chlorides and α-Isocyanoacetamides. *Org. Lett.* **2010,** *12* (4), 820-823.

[11] Murphy, E.; Martinelli, J.; Zaborenko, N.; Buchwald, S.; Jensen, K., Accelerating Reactions with Microreactors at Elevated Temperatures and Pressures: Profiling Aminocarbonylation Reactions. *Angew. Chem. Int. Ed.* **2007,** *46* (10), 1734-1737.

[12] Liu, J.; Zhang, R.; Wang, S.; Sun, W.; Xia, C., A general and Efficient Copper Catalyst for the Double Carbonylation Reaction. *Org. Lett.* **2009,** *11* (6), 1321-1324.

[13] Sumino, S. H.; Fusano, A.; Fukuyama, T.; Ryu, I., Carbonylation Reactions of Alkyl Iodides through the Interplay of Carbon Radicals and Pd Catalysts. *Acc. Chem. Res*. **2014**, *47*(5), 1563–1574.

[14] Kataoka, K.; Wachi, K.; Jin, X.; Suzuki, K.; Sasano, Y.; Iwabuchi, Y.; Hasegawa, J.-y.; Mizuno, N.; Yamaguchi, K., CuCl/TMEDA/nor-AZADO-Catalyzed Aerobic Oxidative Acylation of Amides with Alcohols to Produce Imides. *Chem. Sci.* **2018,** *9* (21), 4756-4768.

[15] Sagadevan, A.; Ragupathi, A.; Lin, C.; Hwu, J.; Hwang, K., Visible-Light Initiated Copper(i)-catalysed Oxidative C–N Coupling of Anilines with Terminal Alkynes: One-Step Synthesis of α-Ketoamides. *Green Chem.* **2015,** *17* (2), 1113-1119.

[16] Shao, J.; Huang, X.; Wang, S.; Liu, B.; Xu, B., A Straightforward Synthesis of N-monosubstituted α-Keto Amides via Aerobic Benzylic Oxidation of Amides. *Tetrahedron* **2012,** *68* (2), 573-579.

[17] Zhang, C.; Jiao, N., Dioxygen Activation under Ambient Conditions: Cu-Catalyzed Oxidative Amidation−Diketonization of Terminal Alkynes Leading to α-Ketoamides. *J. Am. Chem. Soc.* **2010**, *132* (1), 28-29.

[18] a) Jin, H.; Huang, L.; Xie, J.; Rudolph, M.; Rominger, F.; Hashmi, A. S. K., Gold-Catalyzed C-H Annulation of Anthranils with Alkynes: A Facile, Flexible, and Atom-

Economical Synthesis of Unprotected 7-Acylindoles. *Angew. Chem. Int. Ed.* **2016**, *55* (2), 794-797. b) Jin, H.; Tian, B.; Song, X.; Xie, J.; Rudolph, M.; Rominger, F.; Hashmi, A. S. K., Gold-Catalyzed Synthesis of Quinolines from Propargyl Silyl Ethers and Anthranils through the Umpolung of a Gold Carbene Carbon. *Angew. Chem. Int. Ed.* **2016**, *55* (41), 12688-12692. c) Zeng, Z.; Jin, H.; Rudolph, M.; Rominger, F.; Hashmi, A. S. K., Gold(III)-Catalyzed Site-Selective and Divergent Synthesis of 2-Aminopyrroles and Quinoline-Based Polyazaheterocycles. *Angew. Chem. Int. Ed.* **2018**, *57* (50), 16549-16553.

[19] a) Li, P. G.; Zhu, H.; Fan, M.; Yan, C.; Shi, K.; Chi, X. W.; Zou, L. H., Copper-Catalyzed Coupling of Anthranils and α-Keto Acids: Direct Synthesis of α-Ketoamides. *Org. Biomol. Chem.* **2019**, *24* (17), 5902-5907. b) Zhuang, S. Y.; Tang, Y. X.; Chen, X. L.; Wu, Y. D.; Wu, A. X., I^2-DMSO Mediated Oxidative Amidation of Methyl Ketones with Anthranils for the Synthesis of α-Ketoamides. *Org. Biomol. Chem.* **2021**,*19* (19), 4258-4262.

[20] Adak, T.; Schulmeister, J.; Dietl, M. C.; Rudolph, M.; Rominger, F.; Hashmi, A. S. K., Gold-Catalyzed Highly Chemo- and Regioselective C-H Bond Functionalization of Phenols with Haloalkynes. *Eur. J. Org. Chem.* **2019,** *2019* (24), 3867-3876.

[21] Jin, H.; Huang, L.; Xie, J.; Rudolph, M.; Rominger, F.; Hashmi, A. S. K., Gold-Catalyzed C-H Annulation of Anthranils with Alkynes: A Facile, Flexible, and Atom-Economical Synthesis of Unprotected 7-Acylindoles. *Angew. Chem. Int. Ed.* **2016,** *55* (2), 794-797.

[22] Zeng, Z.; Jin, H.; Sekine, K.; Rudolph, M.; Rominger, F.; Hashmi, A. S. K., Gold-Catalyzed Regiospecific C-H Annulation of o-Ethynylbiaryls with Anthranils: π-Extension by Ring-Expansion En Route to N-Doped PAHs. *Angew. Chem. Int. Ed.* **2018,** *57* (23), 6935-6939.

[23] Zeng, Z.; Jin, H.; Rudolph, M.; Rominger, F.; Hashmi, A. S. K., Gold (III)-Catalyzed Site-Selective and Divergent Synthesis of 2-Aminopyrroles and Quinoline-Based Polyazaheterocycles. *Angew. Chem. Int. Ed.* **2018,** *57* (50), 16549-16553.

[24] Jin, H.; Tian, B.; Song, X.; Xie, J.; Rudolph, M.; Rominger, F.; Hashmi, A. S. K., Gold-Catalyzed Synthesis of Quinolines from Propargyl Silyl Ethers and Anthranils through the Umpolung of a Gold Carbene Carbon. *Angew. Chem. Int. Ed.* **2016,** *55* (41), 12688-12692.

[25] Zeng, X.; Liu, S.; Hammond, G. B.; Xu, B., Hydrogen-Bonding-Assisted Brønsted Acid and Gold Catalysis: Access to Both (E)- and (Z)-1,2-Haloalkenes via Hydrochlorination of Haloalkynes. *ACS Catal.* **2018,** *8* (2), 904-909.

[26] Wang, J.; Zhang, S.; Xu, C.; Wojtas, L.; Akhmedov, N. G.; Chen, H.; Shi, X., Highly Efficient and Stereoselective Thioallylation of Alkynes: Possible Gold Redox Catalysis with No Need for a Strong Oxidant. *Angew. Chem. Int. Ed.* **2018,** *57* (23), 6915-6920.

[27] Claus, V.; Molinari, L.; Büllmann, S.; Thusek, J.; Rudolph M.; Rominger, F.; Hashmi, A. S. K., Gold-Catalyzed Cyclisationby 1,4-Dioxidation. *Chem. Eur. J.* **2019**, *25* (40), 9385-9389.

[28] Ye, L. W.; Zhu, X. Q.; Sahani, R. L.; Xu, Y.; Qian, P. C.; Liu, R. S., Nitrene Transfer and Carbene Transfer in Gold Catalysis. C*hem. Rev.* 2020, *121* (14), 9039-9112.

[29] Dhote, P. S.; Ramana, C. V., Interrupting the [Au]-Catalyzed Nitroalkyne Cycloisomerization: Trapping the Putative α-Oxo Gold Carbene with Benzo [c] isoxazole. *Org. Lett.* **2021**, *23* (7), 2632-2637.

[30] Wu, W. Q.; Jiang, H. F.; Haloalkynes: A Powerful and Versatile Building Block in Organic Synthesis, *Acc. Chem. Res*. **2014**, *47* (8), 2483-2504.

[31] Owston, P. G.; Leylâ S. S.; Peter A. T., "The Self-Condensation of o-Aminobenzaldehyde: the Polycyclic Structure of the Picrate Salt of the Diprotonated Tetra-anhydro Tetramer, 4b, 5, 15b, 16-Tetrahydrodibenzo [3, 4: 7, 8] [1, 5] Diazocino-[2, 1-b: 6, 5-b] Diquinazoline-11, 22-di-ium picrate: X-ray Crystal Structure. *J. Chem. Soc., Chem. Commun.*, **1982**, (1), 17-19.

[32] Neese, F.; Wennmohs, F.; Becker, U.; Riplinger, C. The ORCA Quantum Chemistry Program Package. *J. Chem. Phys.* **2020**, *152* (22), 224108.

[33] Perdew, J. P.; Ernzerhof, M.; Burke, K. Rationale for Mixing Exact Exchange with Density Functional Approximations. *J. Chem. Phys.* **1996**, *105* (22), 9982-9985.

[34] Adamo, C.; Barone, V. Toward Reliable Density Functional Methods without Adjustable Parameters: The PBE0 Model. *J. Chem. Phys.* **1999**, *110* (13), 6158-6170.

[35] Weigend, F.; Ahlrichs, R. Balanced Basis Sets of Split Valence, Triple Zeta Valence and Quadruple Zeta Valence Quality for H to Rn: Design and Assessment of Accuracy. *Phys. Chem. Chem. Phys.* **2005**, *7* (18), 3297-3305.

[36] Barone, V.; Cossi, M. Quantum Calculation of Molecular Energies and Energy Gradients in Solution by a Conductor Solvent Model. *J. Phys. Chem. A* **1998**, *102* (11), 1995-2001.

[37] Turgis, T.; Billault, I.; Acherar, S.; Augé, J.; Scherrmann, M. C., Total Synthesis of High Loading Capacity PEG-based Supports: Evaluation and Improvement of the Process by Use of Ultrafiltration and PEG as a Solvent. *Green Chem*. **2013**, *15* (4), 1016-1029.

2.5 Experimental section

2.5.1 General remarks

All commercially available chemicals were purchased from suppliers (ABCR, Acros, Alfa Aesar, Chempur, Merck, Sigma Aldrich) and were used without further purifications. Dry solvents were dispensed from the solvent purification system MB SPS-800-Benchtop. Deuterated solvents were supplied from Euriso-Top or Sigma Aldrich. The NMR spectra, if not noted otherwise, were recorded at room temperature on the following spectrometers: Bruker Avance III 300 (300 MHz), Bruker Avance DRX 300 (300 MHz), Bruker Avance III 400 (400 MHz), Bruker Avance III 500 (500 MHz), Bruker Avance III 600 (600 MHz) or Fourier 300 (300 MHz). Chemical shifts δ are quoted in parts per million (ppm) and coupling constants J in Hertz (Hz). ^{1}H and ^{13}C spectra are calibrated with the deuterated solvents, namely $CDCl_3$ (7.26 ppm; 77.16

ppm). The following abbreviations were used to indicate the signal multiplicity: for the ^{1}H NMR spectra: s (singlet), d (doublet), t (triplet), q (quartet), quint (quartet), sext (sextet), sept (septet), m (multiplet), as well as their combinations; for the ^{13}C NMR spectra: s (quaternary carbon), d (tertiary carbon (CH)), t (secondary carbon (CH_2)) and q (primary carbon (CH_3)). All the ^{13}C NMR spectra were measured with ^{1}H-decoupling and were interpreted with the help of DEPT-135. Mass spectra (MS and HRMS) were determined in the chemistry department of the University Heidelberg under the direction of Dr. J. Gross. EI^{+}-spectra were measured on a JOEL JMS-700 spectrometer [mass analyzer type: Time-of-flight (TOF)]. For ESI^{+}-spectra a Bruker ApexQu FT-ICR-MS spectrometer was applied [mass analyzer type: Fourier transform ion cyclotron resonance (FT-ICR)]. Gas chromatography / Mass Spectroscopy (GC MS) was carried out on two different systems: (i) HP 5972 Mass Selective Detector, coupled with a HP 5890 SERIES II plus Gas Chromatograph, (ii) Agilent 5975C Mass Selective Detector, coupled with an Agilent 7890A Gas Chromatograph. In both cases, as a capillary column, an OPTIMA 5 cross-linked Methyl Silicone column (30 m x, 0.32 mm, 0.25 mm) was employed, and helium was used as the carrier gas. Flash Column Chromatography was accomplished using Silica gel 60 (0.04 – 0.063 mm / 230 – 400 mesh ASTM) purchased from Macherey-Nagel as the stationary phase. As eluents, the mixture of petroleum ether (PE) and ethyl acetate (EA) were used for all products. Analytical Thin Layer Chromatography (TLC) was carried out on precoated Macherey-Nagel POLYGRAM® SIL G/UV254 or Merck TLC Silica Gel 60 F254 aluminum sheets. All geometry optimizations, subsequent frequency analyses, and calculations concerning transition states were performed with the CPCM model for 1,2-dichlorobenzene using Orca 4.0.1.2 on the bwForCluster Justus 2. The PBE0 functional and the def2-SVP basis set was employed. Furthermore, for Au def2-TZVP basis set was used. The heat source is oil bath.

2.5.2 Experiment procedures

General experiment procedure:

A reaction vail was charged with a magnetic stirrer, anthranil (0.4 mmol, 2 equiv), bromoalkyne (0.2 mmol, 1 equiv), PPh_3AuNTf_2 (5 mol%), H_2O (0.4 mmol, 2 equiv), MsOH (10 mol%) in DCB at 60°C temperature for 24 hours. Then the reaction mixture was quenched and washed with brine (10 mL) and dried with Na_2SO_4. The crude product was purified by petroleum ether and ethyl acetate used as eluent. The mixture of petroleum ether (PE) and ethyl acetate (EA) (PE:EA=10:1) were used as eluent for all products if it not mentioned by other eluent.

Procedure of synthesis N-(2-formylphenyl)-2-oxo-2-phenylacetamide (**3a**):

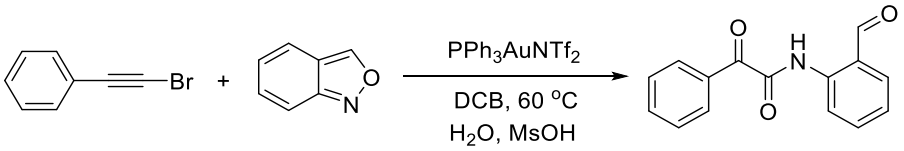

1 mL of DCB was added to a flask by syringe, then 7.39 mg of PPh_3AuNTf_2 (0.01 mmol), 47.612 mg of anthranil (0.4 mmol) and 36.206 mg of bromoalkyne (0.2 mmol) was added into the flask one by one. Following, 7.2 μL of H_2O (0.4 mmol) and 1.28 μL of MsOH (0.02 mmol) was slowly added when the mixture is stirring. After adding of all needed materials, the mixture was stirred for 24 h under an oil bath with 60°C temperature. The reaction mixture was quenched and washed with brine (10 mL) and dried with Na_2SO_4. The crude product was purified by petroleum ether and ethyl acetate (PE:EA=10:1) used as eluent. Then we obtained 38 mg of pale-yellow solid (75% yield). The spectroscopic data of 3a and 3b are in agreement with the previously report, HRMS and elemental analysis data were reported in reference 1.

mmol scale synthesis of **3a**:

10 mL of DCB was added to a flask by big-size syringe, then 73.9 mg of PPh_3AuNTf_2 (0.1 mmol, 5 mol%), 476.14 mg of anthranil (4 mmol) and 362.06 mg of bromoalkyne (2 mmol) was added into the flask one by one. Following, 72 μL of H_2O (2 mmol) and 12.8 μL of MsOH (0.2 mmol) was slowly added when the mixture is stirring. After adding of all needed materials, the mixture was stirred for 24 h under an

oil bath with 60°C temperature. The reaction mixture was quenched and washed with brine (100 mL) and dried with Na_2SO_4. The crude product was purified by petroleum ether and ethyl acetate (PE:EA=10:1) used as eluent. Then we obtained 310 mg of pale-yellow solid (1.22 mmol, 61% yield).

Procedure of synthesis product **1**:

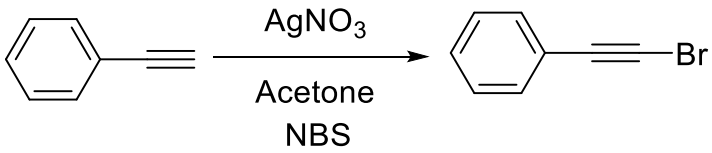

All the starting materials were synthesized by the same method. We purchased the corresponding terminal alkynes to make the starting materials by the reported synthesis way.[5] A reaction vail was charged with a magnetic stirrer, 0.5 g phenylacetylene (5 mmol, 1 equiv), 1g NBS (6 mmol, 1.2 equiv), 85 mg $AgNO_3$ (0.5 mmol, 10 mol%) and 20 mL acetone were added in this reaction vail. Stirring at room temperature for 3 hours. The reaction mixture was purified carefully by petroleum ether used as eluent, and then we got 0.9 g product **1**, all alkyne conversion to the bromoalkyne. All data information is agreed with the before reports.[2]

We purchased product 2.

2.5.3 Mechanistic experiment

We ran the reaction of bromoalkyne **1a** (1 equiv, 0.2 mmol), water (2 equiv, 0.4 mmol), PPh_3AuNTf_2 (5 mol%) and MsOH (10 mol%) in DCB at 60°C temperature for 24 hours. The reaction mixture was quenched and washed with brine (10 mL) and dried with Na_2SO_4. Crude product was purified with petroleum ether and ethyl acetate used as eluent. ω-Bromoacetophenone **4** was formed with a weight of 36.9 mg and a yield of 93%. This experiment result was also confirmed by literatures.[3-5]

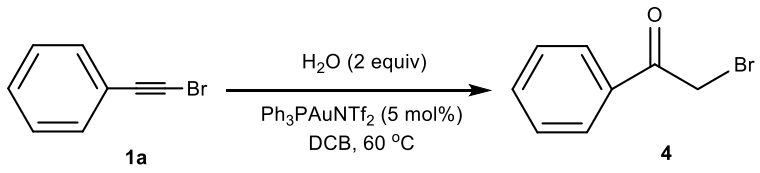

For the further understanding of mechanism, the kinetic study of bromoalkyne hydroation at room temperature is also checked. In our reaction condition, we choose p-dinitrobenzene as the internal standard, d_2-TCE (1,1,2,2-Tetrachloroethane-d_2) as deuterated reagents and keep it stirring for 24 hours. The NMR were checked every 10 minutes at the beginning and every 1 h later, but unfortunately, we can't find conversion after 24 hours, the detail NMR comparison is shown in Scheme 2.10.

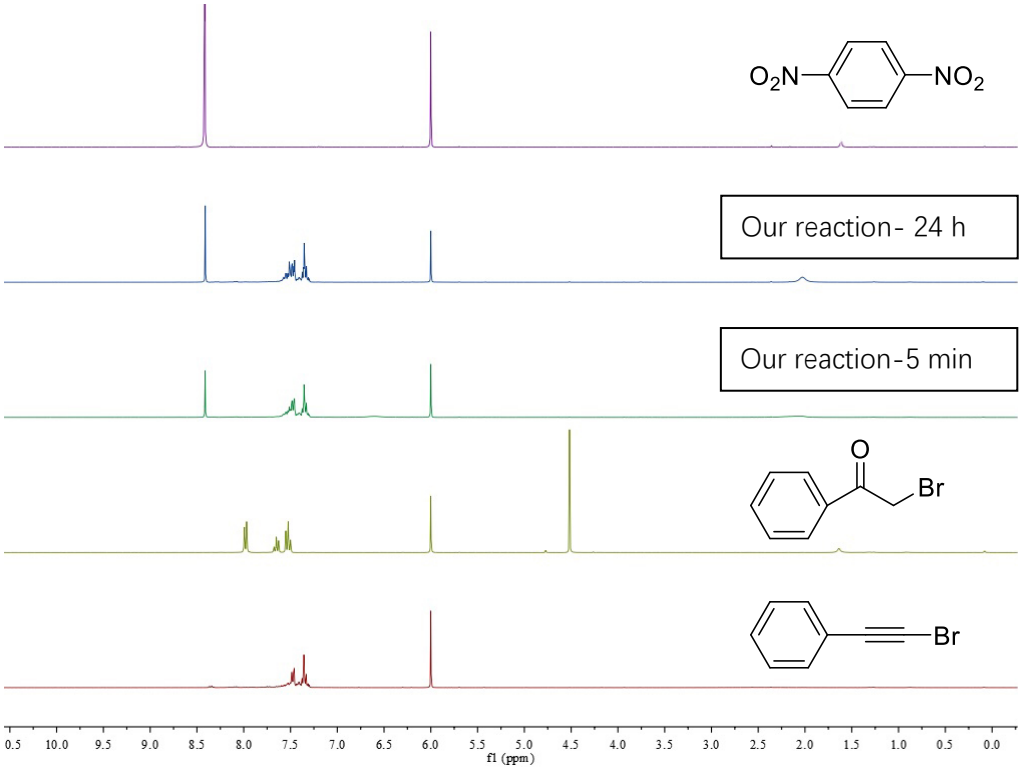

Scheme 2.10 Bromoalkyne hydration at room temperature

To confirm the source of O in **3a**, bromoalkyne **1a** (1 equiv, 0.2 mmol), anthranil (2 equiv, 0.4 mmol), $H_2{}^{18}O$ (2 equiv, 0.4 mmol), PPh_3AuNTf_2 (5 mol%) and MsOH (10 mol%) were added in DCB at 60°C temperature under N_2 for 24 hours. The reaction mixture was quenched and washed with brine (10 mL) and dried with Na_2SO_4. Crude product was purified with petroleum ether and ethyl acetate used as eluent. The ^{18}O labelling product **3a-^{18}O, ^{18}O** was observed. This result ensured that the oxygen comes

from water.

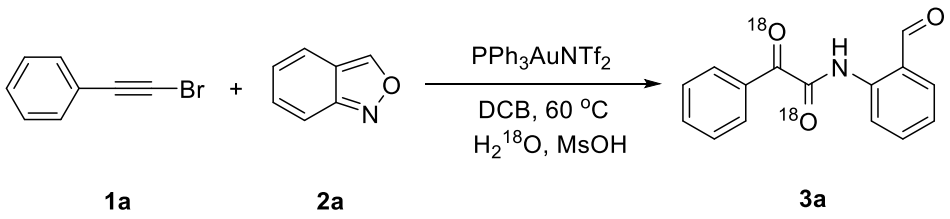

1a **2a** **3a**

2.5.4 Characterization data

(3a) *N*-(2-formylphenyl)-2-oxo-2-phenylacetamide

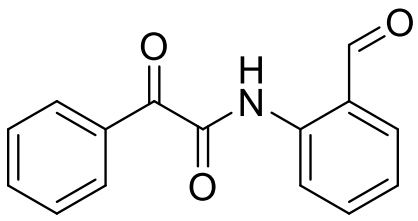

Pale yellow solid, 38 mg, 75%, yield, melting point 107-110 °C.

Purification by column chromatography on silica gel, chromatography eluent: PE to 2% EA in petroleum. R_f = 0.42 (PE/EA=5/1).

^{1}H NMR (300 MHz, $CDCl_3$) δ 12.47 (s, 1H), 10.02 (s, 1H), 8.86 (d, *J* = 8.4 Hz, 1H), 8.42 – 8.36 (d, 2H), 7.78 (dd, *J* = 7.6, 1.5 Hz, 1H), 7.67 (tdd, *J* = 8.7, 5.6, 1.4 Hz, 2H), 7.52 (dd, *J* = 10.6, 4.7 Hz, 2H), 7.35 (td, *J* = 7.6, 0.9 Hz, 1H). ^{13}C NMR (75 MHz, $CDCl_3$) δ 195.1, 186.9, 160.9, 139.4, 136.3, 136.1, 134.8, 133.3, 131.5, 128.7, 124.4, 123.1, 120.3. The spectroscopic data information is agreed with the before reports.[1]

(3b) 2-(2-chlorophenyl)-N-(2-formylphenyl)-2-oxoacetamide

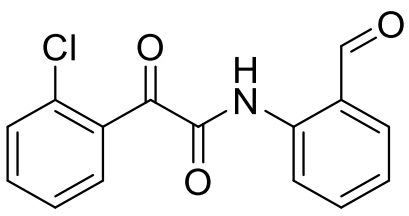

Pale yellow solid, 33 mg, 58% yield, melting point 115.7-117.6 °C.

Purification by column chromatography on silica gel, chromatography eluent: PE to 2% EA in petroleum. R_f = 0.38 (PE/EA=5/1).

^{1}H NMR (300 MHz, $CDCl_3$) δ 12.36 (s, 1H), 9.96 (s, 1H), 8.74 (d, *J* = 8.4 Hz, 1H), 7.71 (dd, *J* = 7.6, 1.5 Hz, 1H), 7.61 (td, *J* = 8.3, 1.4 Hz, 2H), 7.42 (dt, *J* = 8.2, 4.0 Hz, 2H), 7.37 – 7.23 (m, 2H). **^{13}C NMR** (75 MHz, $CDCl_3$) δ 195.2, 189.6, 159.9, 145.7, 139.3, 136.3, 136.2, 134.2, 133.3, 131.3, 130.5, 126.9, 124.6, 123.1, 120.4. The spectroscopic data information is agreed with the before reports.[1]

(3c) *N*-(2-formylphenyl)-2-oxo-2-(4-(trifluoromethyl)phenyl)acetamide

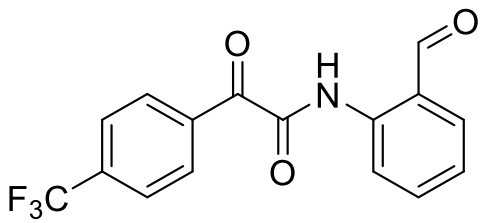

Pale yellow solid, 35 mg, 55% yield, melting point 116.4-118.8 °C.

Purification by column chromatography on silica gel, chromatography eluent: PE to 2% EA in petroleum. R_f = 0.35 (PE/EA=5/1).

^{1}H NMR (300 MHz, $CDCl_3$) δ 12.54 (s, 1H), 10.03 (s, 1H), 8.84 (d, *J* = 8.4 Hz, 1H), 8.52 (d, *J* = 8.2 Hz, 2H), 8.23 (d, *J* = 8.1 Hz, 1H), 7.82 – 7.76 (m, 2H), 7.75 – 7.67 (m, 1H), 7.38 (td, *J* = 7.6, 0.9 Hz, 1H). **^{13}C NMR** (75 MHz, $CDCl_3$) δ 195.2, 186.1, 160.0, 139.0, 136.4, 136.2, 135.9, 131.8, 130.8, 125.7 (q), 124.7, 123.2, 120.4. **HRMS** (ESI-TOF) m/z: $[M+H]^+$ calc'd for $C_{16}H_{10}F_3NO_3$ 321.0613; found 321.0614. **IR**: $\tilde{\nu}$ = 3223, 3176, 3112, 2843, 2751, 1675, 1583, 1521, 1452, 1322, 1275, 1170, 1101, 1064 cm^{-1}

(3d) 2-(3-fluorophenyl)-*N*-(2-formylphenyl)-2-oxoacetamide

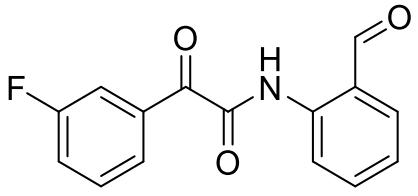

Pale yellow solid, 32 mg, 59% yield, melting point 163.1-165.6 °C.

Purification by column chromatography on silica gel, chromatography eluent: PE to 2% EA in petroleum. R_f = 0.38 (PE/EA=5/1).

^{1}H NMR (300 MHz, $CDCl_3$) δ 12.49 (s, 1H), 10.02 (d, *J* = 0.6 Hz, 1H), 8.84 (d, *J* = 8.4 Hz, 1H), 8.26 – 8.19 (m, 1H), 8.13 (ddd, *J* = 9.5, 2.6, 1.5 Hz, 1H), 7.78 (dd, *J* = 7.6, 1.6 Hz, 1H), 7.70 (ddd, *J* = 9.6, 8.2, 1.7 Hz, 1H), 7.51 (td, *J* = 8.0, 5.5 Hz, 1H), 7.36 (m, 2H). **^{13}C NMR** (75 MHz, $CDCl_3$) δ 207.0, 195.2, 185.6, 164.3, 160.9, 160.3, 150.7, 139.2, 136.2 (d, *J* = 14.6 Hz), 135.1 (d, *J* = 7.1 Hz), 130.4 (d, *J* = 7.5 Hz), 130.0, 127.3 (d, *J* = 3.0 Hz), 125.8, 124.6, 123.2, 121.8 (d, *J* = 21.4 Hz), 120.5 – 120.1 (m), 118.2 (d, *J* = 23.1 Hz). **HRMS** (ESI-TOF) m/z: $[M+H]^+$ calc'd for $C_{15}H_{10}FNO_3$ 271.0645; found 271.0642. **IR**: ṽ = 3223, 2945, 2865, 2492, 2341, 1691, 1590, 1509, 1483, 1443, 1381, 1315, 1260, 1188, 1111, 1020 cm^{-1}

(3e) *N*-(2-formylphenyl)-2-oxo-2-(m-tolyl) acetamide

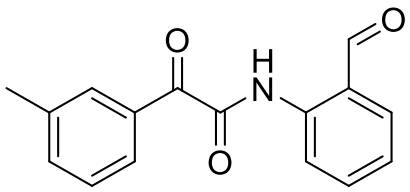

Colorless solid, 27.3 mg, 51% yield, melting point 114.5-116.9 °C.

Purification by column chromatography on silica gel, chromatography eluent: PE to 2% EA in petroleum. R_f = 0.39 (PE/EA=5/1).

^{1}H NMR (400 MHz, $CDCl_3$) δ 12.42 (s, 1H), 10.02 (s, 1H), 8.86 (d, *J* = 8.4 Hz, 1H), 8.18 (d, *J* = 0.7 Hz, 2H), 7.77 (dd, *J* = 7.6, 1.6 Hz, 1H), 7.72 – 7.66 (m, 1H), 7.39 (dtd, *J* = 8.5, 7.7, 4.1 Hz, 3H), 2.45 (s, 3H). **^{13}C NMR** (101 MHz, $CDCl_3$) δ 194.9, 187.0, 160.9, 139.2, 138.4, 136.1, 135.9, 135.3, 133.1, 131.6, 128.5, 128.5, 124.2, 123.0, 120.2, 21.4. **HRMS** (ESI-TOF) m/z: $[M+H]^+$ calc'd for $C_{16}H_{13}NO_3$ 267.0889; found 267.0898. **IR**: ṽ = 3223, 2843, 2760, 2362, 1672, 1600, 1519, 1452, 1399, 1380, 1317, 1279, 1200, 1120, 1033 cm^{-1}

(3f) 2-(4-(tert-butyl)phenyl)-*N*-(2-formylphenyl)-2-oxoacetamide

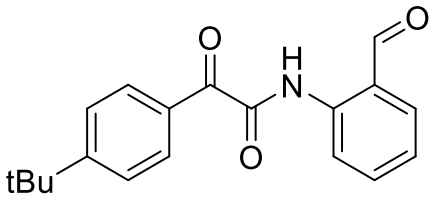

colorless solid, 32.8 mg, 53% yield, melting point 75.9-77.1 °C.

Purification by column chromatography on silica gel, chromatography eulent: PE to 2% EA in petroleum. R_f = 0.36 (PE/EA=5/1).

^{1}H NMR (301 MHz, $CDCl_3$) δ 12.45 (s, 1H), 10.02 (s, 1H), 8.86 (d, *J* = 8.4 Hz, 1H), 8.34 (d, *J* = 8.7 Hz, 2H), 7.77 (dd, *J* = 7.6, 1.5 Hz, 1H), 7.73 – 7.65 (m, 1H), 7.53 (d, *J* = 8.7 Hz, 2H), 7.34 (td, *J* = 7.5, 1.0 Hz, 1H), 1.36 (s, 11H). **^{13}C NMR** (76 MHz, $CDCl_3$) δ 195.1, 158.7, 136.3, 136.1, 131.5, 125.8, 124.3, 123.1, 120.3, 31.1. **HRMS** (ESI-TOF) m/z: $[M+H]^+$ calc'd for $C_{19}H_{19}NO_3$ 309.1438; found 309.1440. **IR**: ṽ =3241, 2966, 2771, 2361, 2329, 1695, 1665, 1602, 1562, 1514, 1476, 1406, 1363, 1312, 1277, 1191, 1164, 1043, 986, 886, 799, 751 cm^{-1}

(3g) *N*-(2-formylphenyl)-2-oxo-2-(4-methoxyphenyl) acetamide

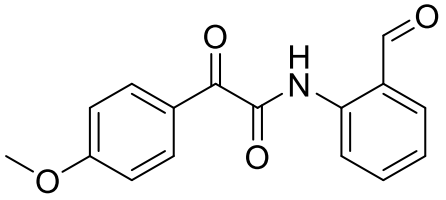

Pale orange solid, 27.2 mg, 48% yield, melting point 155.9-157.1 °C.

Purification by column chromatography on silica gel, chromatography eulent: PE to 2% EA in petroleum. R_f = 0.40 (PE/EA=5/1).

^{1}H NMR (400 MHz, $CDCl_3$) δ 12.46 (s, 1H), 10.01 (s, 1H), 8.85 (d, J = 8.4 Hz, 1H), 8.46 (d, J = 8.9 Hz, 2H), 7.76 (dd, J = 7.6, 1.1 Hz, 1H), 7.68 (t, J = 7.9 Hz, 1H), 7.33 (t, J = 7.5 Hz, 1H), 6.98 (d, J = 8.9 Hz, 2H), 3.90 (s, 3H). **^{13}C NMR** (101 MHz, $CDCl_3$) δ

194.9, 184.7, 164.8, 161.3, 139.3, 136.1, 135.9, 134.0, 126.1, 124.1, 122.9, 120.1, 113.9, 55.6. The spectroscopic data information is agreed with the before reports.[1]

(3h) 2-(4-chlorophenyl)-N-(2-formylphenyl)-2-oxoacetamide

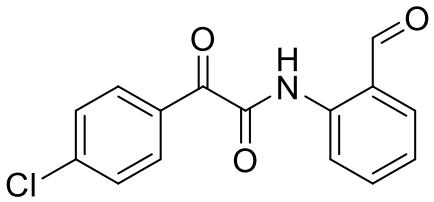

Pale yellow solid, 29 mg, 50% yield, melting point 165.2-169.1 °C.

Purification by column chromatography on silica gel, chromatography eulent: PE to 2% EA in petroleum. R_f = 0.38 (PE/EA=5/1).

^{1}H NMR (400 MHz, $CDCl_3$) δ 12.51 (s, 1H), 10.02 (s, 1H), 8.83 (d, J = 8.3 Hz, 1H), 8.39 (d, J = 8.3 Hz, 2H), 7.78 (d, J = 7.4 Hz, 1H), 7.70 (t, J = 7.7 Hz, 1H), 7.49 (d, J = 8.4 Hz, 2H), 7.36 (t, J = 7.4 Hz, 1H). **^{13}C NMR** (101 MHz, $CDCl_3$) δ 195.0, 160.3, 141.3, 139.0, 136.2, 136.0, 132.8, 131.4, 129.0, 124.4, 122.9, 120.1. The spectroscopic data information is agreed with the before reports.[1]

(3i) *N*-(2-formylphenyl)-2-oxodecanamide

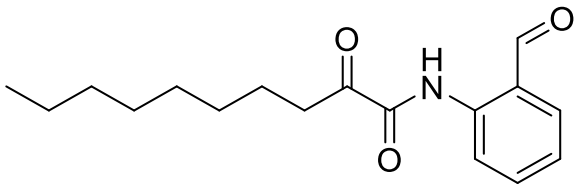

Pale yellow liquid, 30 mg, 52% yield.

Purification by column chromatography on silica gel, chromatography eulent: PE to 2% EA in petroleum. R_f = 0.34 (PE/EA=5/1).

^{1}H NMR (500 MHz, $CDCl_3$) δ 12.26 (s, 1H), 9.93 (s, 1H), 8.71 (d, *J* = 8.4 Hz, 1H), 7.68 (dd, *J* = 7.6, 1.5 Hz, 1H), 7.63 – 7.57 (m, 1H), 7.26 (t, *J* = 7.5 Hz, 1H), 2.92 (t, *J* = 7.3 Hz, 2H), 1.66 – 1.57 (m, 2H), 1.31 – 1.14 (m, 10H), 0.81 (dd, *J* = 9.7, 4.2 Hz,

3H). **^{13}C NMR** (126 MHz, $CDCl_3$) δ 198.4, 194.9, 159.3, 138.9, 136.1 (d, *J* = 32.1 Hz), 124.2, 123.1, 120.1, 36.5, 31.9, 29.6, 29.5, 29.4, 29.3, 29.1, 23.3, 22.7, 14.2. **HRMS** (ESI-TOF) m/z: $[M+H]^+$ calc'd for $C_{17}H_{23}NO_3$ 289.1656; found 289.1664. **IR**: ṽ=3229, 2936, 2848, 2749, 2351, 1682, 1599, 1540, 1447, 1380, 1339, 1268, 1162, 1126, 1054 cm^{-1}

(3j) *N*-(2-formylphenyl)-2-oxooctanamide

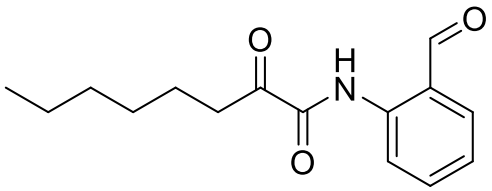

Pale yellow liquid, 28.2 mg, 54% yield.

Purification by column chromatography on silica gel, chromatography eluent: PE to 2% EA in petroleum. R_f = 0.35 (PE/EA=5/1).

^{1}H NMR (400 MHz, $CDCl_3$) δ 12.31 (s, 1H), 10.00 (d, *J* = 0.5 Hz, 1H), 8.77 (d, *J* = 8.4 Hz, 1H), 7.74 (dd, *J* = 7.6, 1.6 Hz, 1H), 7.70 – 7.63 (m, 1H), 7.32 (td, *J* = 7.5, 1.0 Hz, 1H), 2.99 (t, *J* = 7.3 Hz, 2H), 1.68 (dd, *J* = 14.8, 7.4 Hz, 2H), 1.41 – 1.25 (m, 6H), 0.89 (t, *J* = 6.9 Hz, 3H). **^{13}C NMR** (101 MHz, $CDCl_3$) δ 198.3 (s), 194.8 (s), 159.3 (s), 138.9 (s), 135.9 (d, *J* = 24.1 Hz), 124.2 (s), 123.1 (s), 120.1 (s), 36.4 (s), 31.5 (s), 28.7 (s), 22.9 (d, *J* = 83.2 Hz), 14.0 (s). **HRMS** (ESI-TOF) m/z: $[M+H]^+$ calc'd for $C_{15}H_{19}NO_3$ 261.1360; found 261.1374. **IR**: ṽ=3230, 2927, 2860, 2754, 2361, 1694, 1605, 1582, 1520, 1451, 1398, 1353, 1311, 1276, 1195, 1128, 1060, 962 cm^{-1}

(3k) *N*-(2-formylphenyl)-2-oxoheptanamide

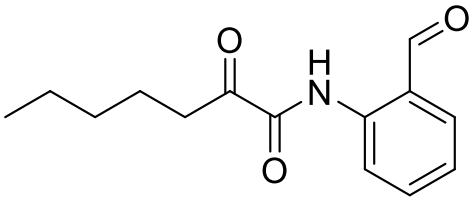

Pale yellow liquid, 25.7 mg, 52% yield.

Purification by column chromatography on silica gel, chromatography eluent: PE to 2% EA in petroleum. R_f = 0.35 (PE/EA=5/1).

^{1}H NMR (500 MHz, $CDCl_3$) δ 12.33 (s, 1H), 10.00 (s, 1H), 8.77 (d, *J* = 8.4 Hz, 1H), 7.75 (dd, *J* = 7.6, 1.5 Hz, 1H), 7.69 – 7.64 (m, 1H), 7.33 (td, *J* = 7.5, 0.9 Hz, 1H), 2.99 (t, *J* = 7.3 Hz, 2H), 1.69 (dd, *J* = 9.2, 5.5 Hz, 2H), 1.41 – 1.32 (m, 4H), 0.91 (t, *J* = 7.1 Hz, 3H). **^{13}C NMR** (126 MHz, $CDCl_3$) δ 198.5, 195.0, 159.5, 139.0, 136.3, 136.0, 124.3, 123.2, 120.2, 36.5, 31.4, 23.1, 22.6, 14.0. **HRMS** (ESI-TOF) m/z: $[M+H]^+$ calc'd for $C_{14}H_{17}NO_3$ 247.1203; found 247.1223. **IR**: ṽ = 3232, 2957, 2928, 2858, 1694, 1675, 1582, 1521, 1452, 1290, 1194, 1125, 1055 cm^{-1}

(3l) *N*-(2-formylphenyl)-2-oxohexanamide

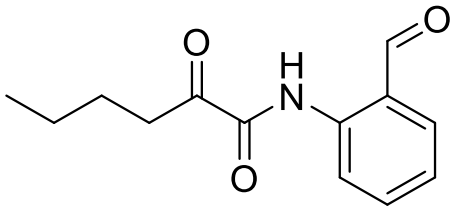

Pale yellow solid, 26 mg, 56% yield, melting point 83.9-94.7 °C.

Purification by column chromatography on silica gel, chromatography eluent: PE to 2% EA in petroleum. R_f = 0.36 (PE/EA=5/1).

^{1}H NMR (500 MHz, $CDCl_3$) δ 12.33 (s, 1H), 10.00 (s, 1H), 8.77 (d, *J* = 8.4 Hz, 1H), 7.75 (dd, *J* = 7.6, 1.5 Hz, 1H), 7.67 (t, *J* = 11.5, 4.3 Hz, 1H), 7.33 (t, *J* = 0.8 Hz, 1H), 3.00 (t, *J* = 7.3 Hz, 2H), 1.72 – 1.63 (m, 2H), 1.41 (dd, *J* = 15.0, 7.5 Hz, 2H), 0.95 (t, *J* = 7.4 Hz, 3H). **^{13}C NMR** (126 MHz, $CDCl_3$) δ 198.5, 195.0, 159.5, 139.0, 136.3, 136.0, 124.3, 123.2, 120.2, 36.3, 25.5, 22.4, 13.9. **HRMS** (ESI-TOF) m/z: $[M+H]^+$ calc'd for $C_{13}H_{15}NO_3$ 233.1046; found 233.1055. **IR**: ṽ = 3235, 2953, 2929, 2869, 1691, 1675, 1581, 1518, 1451, 1399, 1380, 1290, 1275, 1195, 1162, 1126, 1048 cm^{-1}

(3m) *N*-(2-formylphenyl)-2-oxopentanamide

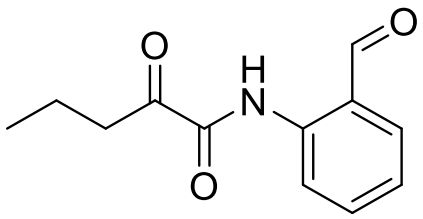

Pale yellow liquid, 26.7 mg, 61% yield.

Purification by column chromatography on silica gel, chromatography eluent: PE to 2% EA in petroleum. R_f = 0.36 (PE/EA=5/1).

^{1}H NMR (400 MHz, $CDCl_3$) δ 12.21 (s, 1H), 9.90 (d, *J* = 0.4 Hz, 1H), 8.67 (d, *J* = 8.4 Hz, 1H), 7.65 (dd, *J* = 7.6, 1.6 Hz, 1H), 7.56 (td, *J* = 8.3, 1.6 Hz, 2H), 7.23 (td, *J* = 7.5, 1.0 Hz, 1H), 2.88 (t, *J* = 7.2 Hz, 2H), 1.67 – 1.56 (m, *J* = 14.7, 7.3 Hz, 3H), 0.91 (t, *J* = 7.4 Hz, 5H). **^{13}C NMR** (101 MHz, $CDCl_3$) δ 198.4, 195.0, 159.5, 136.3, 136.0, 124.3, 124.3, 120.3, 38.5, 38.5, 16.9, 13.8, 13.8. **HRMS** (ESI-TOF) m/z: $[M+H]^+$ calc'd for $C_{12}H_{13}NO_3$ 219.0889; found 219.0886. **IR**: ṽ = 3232, 2960, 2917, 2849, 1695, 1604, 1582, 1521, 1449, 1397, 1288, 1193, 1158, 1046 cm^{-1}

(3n) *N*-(2-formylphenyl)-4-methyl-2-oxopentanamide

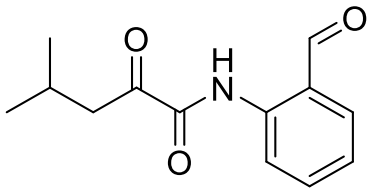

Pale yellow solid, 28 mg, 60% yield, melting point 68.6-70.7.

Purification by column chromatography on silica gel, chromatography eluent: PE to 2% EA in petroleum. R_f = 0.37 (PE/EA=5/1).

^{1}H NMR (400 MHz, $CDCl_3$) δ 12.24 (s, 1H), 9.93 (s, 1H), 8.70 (d, *J* = 8.4 Hz, 1H), 7.68 (dd, *J* = 7.6, 1.6 Hz, 1H), 7.59 (dt, *J* = 11.3, 2.1 Hz, 2H), 7.28 – 7.22 (m, 1H), 2.81 (d, *J* = 6.8 Hz, 2H), 2.18 (td, *J* = 13.4, 6.7 Hz, 1H), 0.93 (d, *J* = 6.7 Hz, 6H). **^{13}C NMR** (101 MHz, $CDCl_3$) δ 198.1, 195.0, 159.6, 136.2, 136.0, 124.3, 124.3, 120.2, 45.1, 24.7,

22.7, 22.7. **HRMS** (ESI-TOF) m/z: $[M+H]^+$ calc'd for $C_{13}H_{15}NO_3$ 233.1046; found 233.1050. **IR**: $\tilde{\nu}$ = 3237, 2958, 2916, 2873, 2849, 1671, 1579, 1510, 1449, 1372, 1277, 1190, 1136, 1116, 1046 cm^{-1}

(3o) 3-Cyclohexyl-*N*-(2-formylphenyl)-2-oxopropanamide

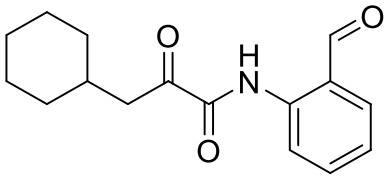

Pale yellow solid, 30 mg, 55% yield, melting point 122-124.1 °C.

Purification by column chromatography on silica gel, chromatography eluent: PE to 2% EA in petroleum. R_f = 0.40 (PE/EA=5/1).

^{1}H NMR (400 MHz, $CDCl_3$) δ 12.24 (s, 1H), 9.93 (s, 1H), 8.70 (d, *J* = 8.4 Hz, 1H), 7.67 (dd, *J* = 7.6, 1.6 Hz, 1H), 7.64 – 7.52 (m, 1H), 7.25 (td, *J* = 7.5, 1.0 Hz, 1H), 2.80 (d, *J* = 6.8 Hz, 2H), 1.62 (dddd, *J* = 10.1, 6.8, 4.0, 2.8 Hz, 7H), 1.30 – 1.06 (m, 6H), 0.97 (dd, *J* = 11.7, 2.5 Hz, 3H). **^{13}C NMR** (101 MHz, $CDCl_3$) δ 198.1, 195.0, 159.6, 139.1, 136.2, 136.0, 124.3, 124.3, 123.2, 120.2, 43.8, 34.0, 33.3, 26.3, 26.2. **HRMS** (ESI-TOF) m/z: $[M+H]^+$ calc'd for $C_{16}H_{19}NO_3$ 273.1359; found 273.1348. **IR**: $\tilde{\nu}$ = 3232, 2950, 2915, 2849, 2758, 2361, 1715, 1673, 1605, 1585, 1524, 1448, 1396, 1361, 1311, 1285, 1199, 1162, 1034 cm^{-1}

(3p) 2-cyclopentyl-N-(2-formylphenyl)-2-oxoacetamide

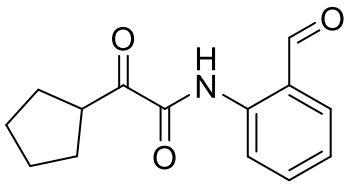

Pale yellow solid, 17 mg, 35% yield, melting point 78-79 °C.

Purification by column chromatography on silica gel, chromatography eluent: PE to 2% EA in petroleum. R_f = 0.39 (PE/EA=5/1).

^{1}H NMR (400 MHz, $CDCl_3$) δ 12.35 (s, 1H), 10.00 (s, 1H), 8.79 (d, *J* = 8.4 Hz, 1H), 7.75 (dd, *J* = 7.6, 1.4 Hz, 1H), 7.70 – 7.63 (m, 1H), 7.32 (t, *J* = 7.5 Hz, 1H), 2.04 – 1.62 (m, 9H). **^{13}C NMR** (75 MHz, $CDCl_3$) δ 194.8, 136.1, 135.8, 124.1, 120.0, 44.3, 29.0, 26.2. **HRMS** (ESI-TOF) m/z: $[M+H]^+$ calc'd for $C_{14}H_{15}NO_3$ 245.0946; found 245.0944. **IR**: ṽ = 3207, 2961, 2920, 2865, 1718, 1666, 1582, 1522, 1448, 1357, 1313, 1260, 1192, 1155, 1087, 1026 cm^{-1}

(3q) 2-cyclohexyl-N-(2-formylphenyl)-2-oxoacetamide

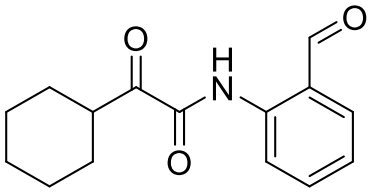

Pale yellow solid, 17 mg, 32% yield, melting point 80-81 °C.

Purification by column chromatography on silica gel, chromatography eluent: PE to 2% EA in petroleum. R_f = 0.40 (PE/EA=5/1).

^{1}H NMR (300 MHz, CDCl3) δ 12.32 (s, 1H), 9.99 (s, 1H), 8.79 (d, J = 8.4 Hz, 1H), 7.71 (ddd, J = 15.8, 11.1, 4.3 Hz, 2H), 7.32 (t, J = 7.5 Hz, 1H), 2.05 – 1.60 (m, 5H), 1.50 – 1.18 (m, 6H). **^{13}C NMR** (75 MHz, CDCl3) δ 194.8, 147.6, 136.1, 135.8, 124.1, 120.0, 43.3, 28.2, 25.4. **HRMS** (ESI-TOF) m/z: $[M+H]^+$ calc'd for $C_{15}H_{17}NO_3$ 259.1101; found 259.1098. **IR**: ṽ = 3206, 2929, 2841, 2754, 1715, 1680, 1603, 1522, 1448, 1371, 1290, 1249, 1231, 1188, 1155, 1100, 1030 cm^{-1}

(3r) *N*-(4-chloro-2-formylphenyl)-2-oxoheptanamide

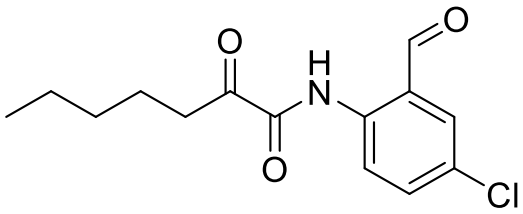

yellow solid, 23.7 mg, 42% yield, melting point 69-73 °C.

Purification by column chromatography on silica gel, chromatography eluent: PE to 2% EA in petroleum. R_f = 0.38 (PE/EA=5/1).

^{1}H NMR (600 MHz, $CDCl_3$) δ 12.23 (s, 1H), 9.93 (s, 1H), 8.76 (d, *J* = 9.0 Hz, 1H), 7.71 (d, *J* = 2.5 Hz, 1H), 7.65 – 7.58 (m, 1H), 2.98 (t, *J* = 7.3 Hz, 2H), 1.71 – 1.66 (m, 2H), 1.40 – 1.32 (m, 4H), 0.94 – 0.87 (m, 3H). **^{13}C NMR** (151 MHz, $CDCl_3$) δ 198.2, 193.7, 159.3, 152.9, 137.5, 135.8, 129.5, 124.1, 121.7, 36.5, 31.3, 23.1, 22.5, 14.0. **HRMS** (ESI-TOF) m/z: $[M+H]^+$ calc'd for $C_{14}H_{16}NO_3Cl$ 281.0813; found 281.0821. **IR**: ṽ=3223, 2954, 2929, 2867, 1696, 1576, 1510, 1466, 1413, 1378, 1304, 1261, 1181, 1129, 893, 847, 798, 765, 750, 727 cm^{-1}

(3s) *N*-(4-bromo-2-formylphenyl)-2-oxoheptanamide

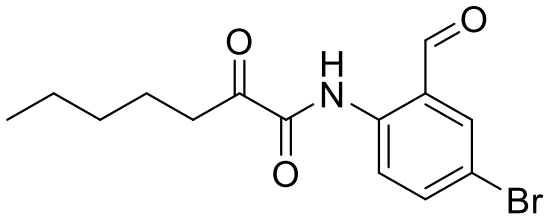

yellow solid, 29.4 mg, 45% yield, melting point 68.6-69.4 °C.

Purification by column chromatography on silica gel, chromatography eluent: PE to 2% EA in petroleum. R_f = 0.38 (PE/EA=5/1).

^{1}H NMR (400 MHz, $CDCl_3$) δ 12.21 (s, 1H), 9.92 (d, *J* = 0.5 Hz, 1H), 8.70 (d, *J* = 8.9 Hz, 1H), 7.85 (d, *J* = 2.4 Hz, 1H), 7.75 (dd, *J* = 8.9, 2.3 Hz, 1H), 2.98 (t, *J* = 7.3 Hz, 2H), 1.73 – 1.65 (m, 2H), 1.40 – 1.33 (m, 4H), 0.94 – 0.86 (m, 3H). **^{13}C NMR** (101 MHz, $CDCl_3$) δ 198.0, 193.5, 152.8, 138.6, 138.3, 137.9, 124.4, 121.9, 36.4, 31.2, 25.8, 22.4, 13.9. **HRMS** (ESI-TOF) m/z: $[M+H]^+$ calc'd for $C_{14}H_{16}NO_3Br$ 325.0308; found 325.0321. **IR**: ṽ = 3343, 3224, 2926, 2853, 2360, 1696, 1576, 1508, 1463, 1409, 1376, 1279, 1179, 1130, 1099, 1028, 878, 844, 797, 765 cm^{-1}

(4) 2-Bromoacetophenone

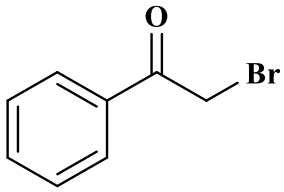

Colorless liquid, 36.9 mg, 93% yield.

Purification by column chromatography on silica gel, chromatography eluent: PE to 2% EA in petroleum. R_f = 0.48 (PE/EA=10/1).

^{1}H NMR (301 MHz, $CDCl_3$) δ 8.03 – 7.95 (m, 1H), 7.61 (d, *J* = 7.4 Hz, 1H), 7.55 – 7.45 (m, 1H), 4.46 (s, 1H). **^{13}C NMR** (76 MHz, CDCl3) δ 133.95 (s), 128.89 (d, J = 4.9 Hz), 30.87 (s).

(1) Bromoalkyne

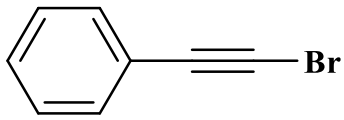

Pale green liquid, 0.9 g, ≥99% yield.

Purification by column chromatography on silica gel, chromatography eluent: petroleum. R_f = 0.88 (PE).

^{1}H NMR (301 MHz, $CDCl_3$) δ 7.49 – 7.42 (m, 1H), 7.42 – 7.36 (m, 1H), 7.36 – 7.29 (m, 1H).

2.5.5 Solid state molecular structure

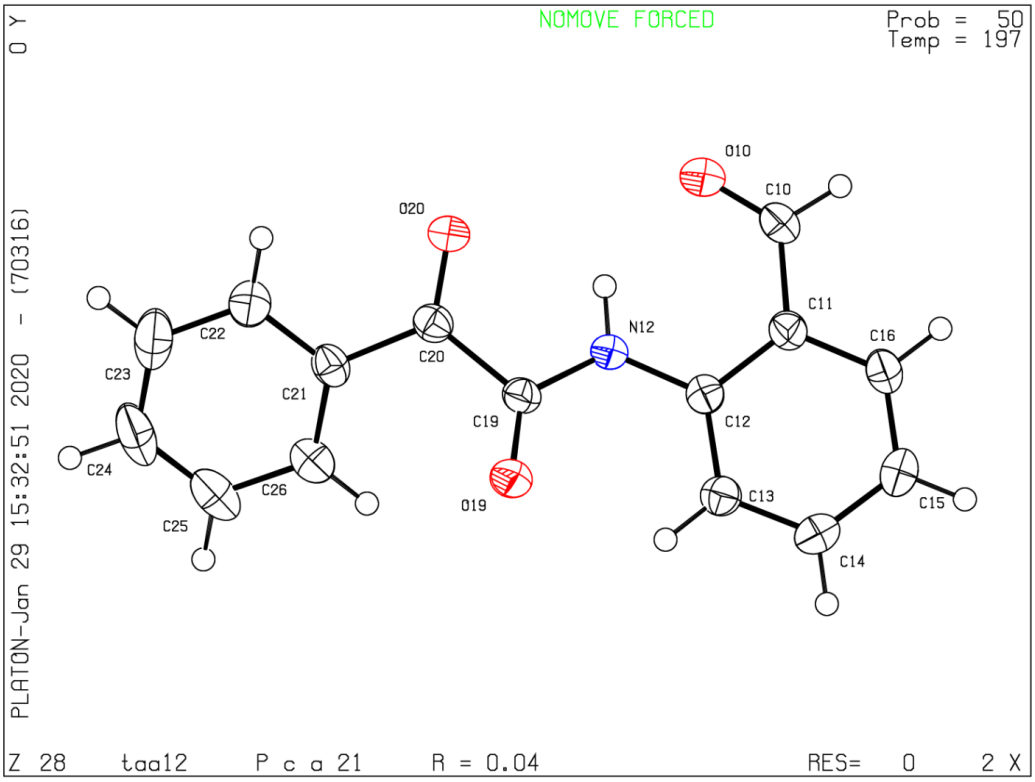

Scheme 2.11 Solid state molecular structure of **3a**

Empirical formula	$C_{15}H_{11}NO_3$
Formula weight	253.25
Temperature	197(2) K
Wavelength	0.71073 Å
Crystal system	orthorhombic
Space group	$Pca2_1$
Z	4
Unit cell dimensions	a = 12.8763(12) Å □ =90 deg.
	b = 14.1314(12) Å □ =90 deg.
	c = 6.7411(6) Å □ =90 deg.

Volume	1226.61(19) $Å^3$
Density (calculated)	1.37 g/cm^3
Absorption coefficient	0.10 mm^{-1}
Crystal shape	needle
Crystal size	0.245 x 0.036 x 0.032 mm^3
Crystal colour	yellow
Theta range for data collection	2.1 to 26.7 deg.
Index ranges	-16□h□16, -17□k□17, -8□l□8
Reflections collected	12048
Independent reflections	2603 (R(int) = 0.0559)
Observed reflections	2084 (I > 2□(I))
Absorption correction	Semi-empirical from equivalents
Max. and min. transmission	0.96 and 0.88
Refinement method	Full-matrix least-squares on F^2
Data/restraints/parameters	2603 / 1 / 176
Goodness-of-fit on F^2	1.07
Final R indices (I>2sigma(I))	R1 = 0.043, wR2 = 0.109
Absolute structure parameter	0.1(9)
Largest diff. peak and hole	0.18 and -0.19 $eÅ^{-3}$

Product 3a: yellow crystal (needle), dimensions 0.245 x 0.036 x 0.032 mm^3, crystal system orthorhombic, space group $Pca2_1$, Z=4, a=12.8763(12) Å, b=14.1314(12) Å, c=6.7411(6) Å, alpha=90 deg, beta=90 deg, gamma=90 deg, V=1226.61(19) $Å^3$, rho=1.371 g/cm^3, T=197(2) K, $Theta_{max}$= 26.723 deg, radiation MoK□, lambda=0.71073 Å, 0.5 deg omega-scans with CCD area detector, covering the asymmetric unit in reciprocal space with a mean redundancy of 8.17and a completeness of 99.9% to a resolution of 0.79 Å, 12048 reflections measured, 2603 unique (R(int)=0.0559), 2084 observed (I > 2□(I)), intensities were corrected for Lorentz and

polarization effects, an empirical scaling and absorption correction was applied using SADABS[1] based on the Laue symmetry of the reciprocal space, mu=0.10mm^{-1}, T_{min}=0.88, T_{max}=0.96, structure solved with SHELXT-2018/2 (Sheldrick 2015)[2] and refined against F^2 with a Full-matrix least-squares algorithm using the SHELXL-2018/3 (Sheldrick, 2018) software[3], 176 parameters refined, hydrogen atoms were treated using appropriate riding models, except H12 at N12, which was refined isotropically, Flack absolute structure parameter 0.1(9), goodness of fit 1.07 for observed reflections, final residual values R1(F)=0.043, wR(F^2)=0.109 for observed reflections, residual electron density -0.19 to 0.18 eÅ^{-3}. CCDC ..... contains the supplementary crystallographic data for this paper. The data can be obtained free of charge from The Cambridge Crystallographic Data Centre via www.ccdc.cam.ac.uk/structures.

Lit. 1: (SADABS-2016/2 - Bruker AXS area detector scaling and absorption correction) Krause, L., Herbst-Irmer, R., Sheldrick G.M. & Stalke D., J. Appl. Cryst. 48 (2015) 3-10.

Lit. 2: (SHELXT - Integrated space-group and crystal structure determination) Sheldrick G. M., Acta Cryst. A71 (2015) 3-8.

Lit. 3: (program SHELXL-2018/3 (Sheldrick, 2018) for structure refinement) Sheldrick G. M., Acta Cryst. (2015). C71, 3-8

Lit. APEX, APEX2, SMART, SAINT, SAINT-Plus:
Bruker (2007). "Program name(s)". Bruker AXS Inc., Madison, Wisconsin, USA.

2.5.6 References

[1] Li, P. G.; Zhu, H.; Fan, M.; Yan, C.; Shi, K.; Chi, X. W.; Zou, L. H., Copper-Catalyzed Coupling of Anthranils and α-Keto Acids: Direct Synthesis of α-Ketoamides. *Org. Biomol. Chem*. **2019**, *24* (17), 5902-5907.

[2] Wu, W. Q.; Jiang, H. F., Haloalkynes: A Powerful and Versatile Building Block in Organic Synthesis. *Acc. Chem. Res.* **2014**, *47* (8), 2483−2504.

[3] Zou, H. X.; Jiang, J.; Yi, N. N.; Fu, W. Q.; Deng, W.; Xiang, J. N., Highly Efficient Synthesis of α-Halomethylketones via Ce(SO4)2/Acid Co-Catalyzed Hydration of Alkynes. *Chin. J. Chem*. **2016**, *34* (12), 1251-1254.

[4] Ye, M.; Wen, Y. L.; Li, H. F.; Fu, Y. J.; Wang, Q. H., Metal-Free Hydration of Aromatic Haloalkynes to α-Halomethyl Ketones. *Tetrahedron Lett*. **2016**, *57* (45), 4983-4986.

[5] Zeng, M.; Huang, R. X.; Li, W. Y.; Liu, X. W.; He, F. L.; Zhang, Y. Y.; Xiao, F., In(OTf)3/Acid Co-catalyzed Hydration of 1-Haloalkynes to α-Halomethyl Ketones. *Tetrahedron*, **2016**, *72* (27-28), 3818-3822.

Chapter 3. Gold-Catalyzed Hydroamination of Terminal Alkynes as One-Pot Access to Oximes

3.1 Introduction

Oximes are one of the most versatile scaffolds in chemistry, which not only have biological activity against microorganisms,[1-4] but also show great benefit for the synthesis of Nylon 6 and the resulting caprolactam in industry.[5] Thus, It's of importance to research the synthesis process of oxime. Some common oxime scaffolds are exhibited in Scheme 3.1. A typical synthesis of aromatic oximes is easily feasible starting from aldehydes/ketones, which usually utilize hydroxylamine hydrochloride as the "N-OH" source (Scheme 3.2a).[6-8] Aliphatic oximes can be accessible from nucleophilic carbon precursors in combination with nitrites.[9-10]Another way to address the synthesis of oxime is the hydroamination of alkynes in a single step.[11-12]

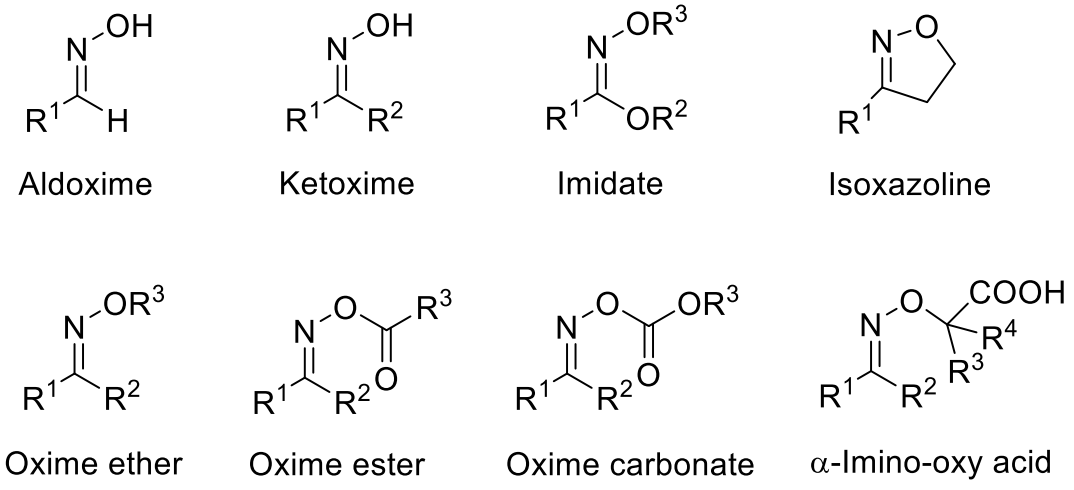

Scheme 3.1 Common oxime scaffolds

Alkynes are widely studied in gold chemistry, mainly for nucleophilic additions such as hydroamination, cyclization, etc. In particular, the nucleophilic addition of water to alkynes to produce ketones proves that alkynes can be used as precursors of carbonyl compounds in some cases.[13-18] Accordingly, alkynes can be converted to oximes with a single step in some particular conditions. In 2008, Beauchemin's group reported an

intermolecular Cope-type hydroamination of alkynes to deliver oximes in good yields, even though high temperature and sealed flask which are the drawback of the direct access to oximes from alkynes were needed (Scheme 3.2b).[19] Recently, TBN (tert-butyl nitrite)-mediated oximosulfonylation of alkynes with sulfonyl hydrazines was presented by the Wang group, the reaction process via a radical pathway under N_2 atmosphere and giving α-sulfonylethanone oximes in good yields (Scheme 3.2c).[20] Although extensive research has been carried out to synthesize oximes directly from alkynes, these transformations rely on complex reaction conditions, which are inevitably accompanied by waste of energy and are not economical. Thus here, a gold-catalyzed hydroamination of terminal alkynes with hydroxylamine-*O*-sulfonic acid (HOSA) in a mild single-pot reaction process was developed, which delivering oximes with good yields (Scheme 3.2d).

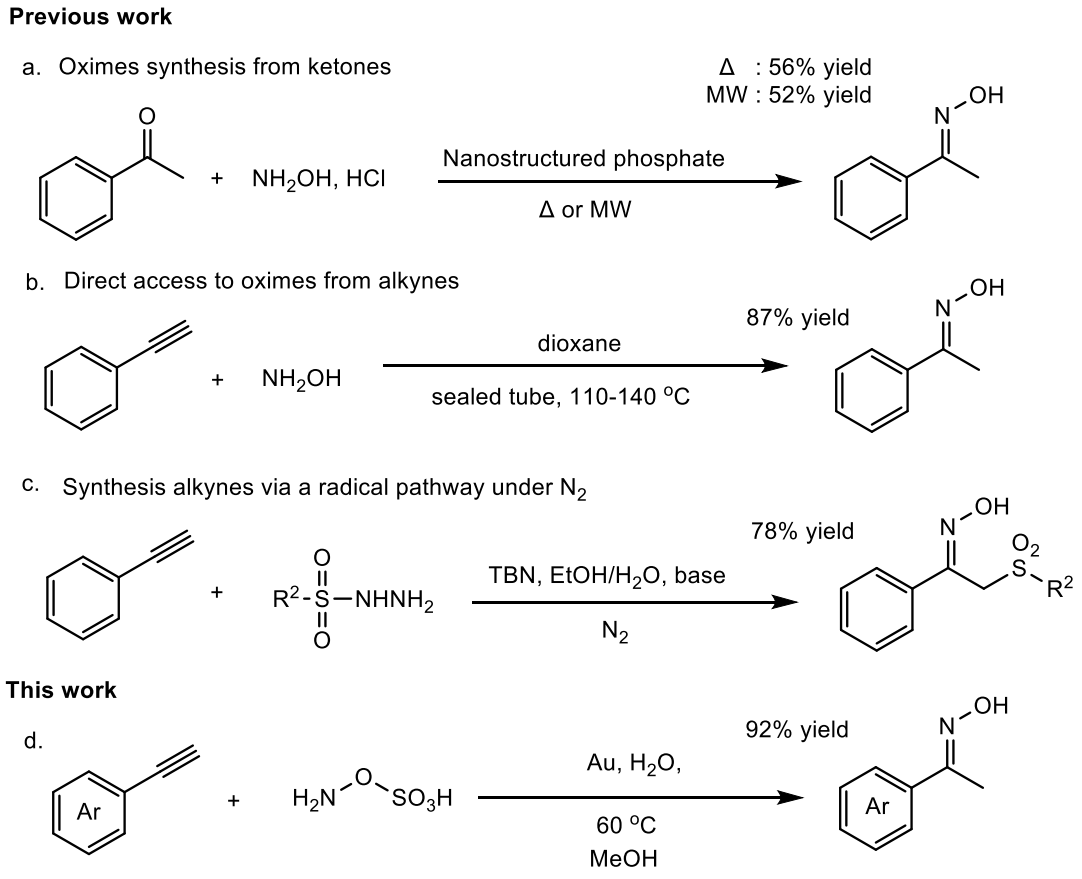

Scheme 3.2 Previous reports and our work for oxime synthesis

3.2 Result and discussion

3.2.1 Optimization of the reaction conditions

The initial investigation was conducted with 1.0 equivalent of phenylacetylene (**2a**), 1.0 equiv of hydroxylamine-*O*-sulfonic acid (HOSA) (**1a**), 1.0 equivalent of H_2O with $AgNTf_2$ (5 mol%) in MeOH at 60 °C. The aromatic oxime (**3a**) was obtained in 36% yield. Interestingly, the variation of silver catalysts did not effect the reaction yield strongly (entries 1-4). To improve the reaction efficiency, gold complexes were systematically investigated as catalysts. The exchange of ligands from DMS to PPh_3 ligands (entries 5-11) at the Au complexes enhanced the reaction yields (40-74% yields). To achieve the best catalytic efficiency, other commonly used catalysts $Pd(PPh_3)_2Cl_2$, $CuBr_2$, $Fe_2SO_4 \cdot 7H_2O$ and $Rh_2(esp)_2$ (entries 12-15) were investigated, too. But the yield showed that the PPh_3NTf_2Au (entry 16) gave the optimal yield (92%). Next, solvent and temperature screening showed that MeOH as solvent given better yields in the presence of PPh_3AuNTf_2 at 60 °C temperature (entries 17-19). Of course, the control experiment without catalyst was conducted, no reaction was observed (entry 20). The reaction optimization is attached in Table 3.1.

Table 3.1 Reaction optimization

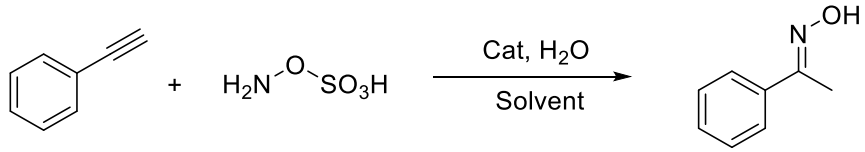

1a 2a 3a

Entry	Catalyst	Solvent	Yield (%)[a]
1	$AgNTf_2$ (5 mol%)	MeOH	36
2	AgOTf (5 mol%)	MeOH	33
3	AgOTs (5 mol%)	MeOH	30
4	$AgSbF_6$ (5 mol%)	MeOH	29
5	PPh_3AuCl (5 mol%)	MeOH	74
6	DMSAuCl (5 mol%)	MeOH	40

7	JohnPhosAuCl (5 mol%)	MeOH	67
8	$(PhO)_3PAuCl$ (5 mol%)	MeOH	53
9	$(cy)_3PAuCl$(5 mol%)	MeOH	62
10	IPrAuCl (5 mol%)	MeOH	65
11	DppmAuCl(5 mol%)	MeOH	48
12	$Pd(PPh_3)_2Cl_2$	MeOH	22
13	$CuBr_2$	MeOH	70
14	$Fe_2SO_4·7H_2O$	MeOH	43
15	$Rh_2(esp)_2$	MeOH	26
16	PPh_3NTf_2Au	MeOH	92
17	PPh_3NTf_2Au	C_2H_5OH	14
18	PPh_3NTf_2Au	MeOH,rt	28
19	PPh_3NTf_2Au	MeOH,100℃	10
20	----	MeOH	0

3.2.2 Substrate scope

Having optimized reaction conditions in hand, next we seek to explore the reaction scope. Numerous terminal alkynes were employed as shown in Scheme 3.3. Alkyne groups bearing *p*-Br (product **3b**), *p*-OMe (product **3c**), *p*-tBu (product **3d**) and *m*-isopropyl (product **3e**) were well tolerated to give the expected products in 42%-88% yield. Especially, phenylacetylene (product **3a**) showed the best efficiency for the production of oxime, with the yields up to 92% yield. To continue, substituted *o*-Me (product **3f**), *m*-Me (product **3g**), *p*-Cl (product **3h**), *m*-NO_2 (product **3i**) and *p*-NO_2 (product **3j**) were tested, these provided the product in an increasing tendency, from 47%-83% yield. Later, we prolonged the reaction scope with other differently substituted groups. *m-, o-, p*-F substituted arene systems (product **3k**, **3l**, **3m**) in yields of 55%, 82% and 71%. Two methyl groups on the *o*- and *p*- position derived the yield of (product **3n**) of 49% yield. For a *o*-OMe group, the product **3o** was obtained in the yield of 51%. A 1-naphthyl group (product **3p**) delivered a normal oxime yield of 64%

yield. Alkynes bearing the groups of diphenyl (product **3q**), *p*-F_3C (product **3r**) and *p*-alkenyl (product **3s**) all gave a good oxime yield of 72%, 73% and 68% respectively. For the *o*-phenylethynyl substituent (product **3t**), *o*-Cl (product **3u**), *o*-Br (product **3v)** and a three-fold substituted (*o*-F, *o*-F, *p*-F) group (product **3w**), the yields showed a little decrease with 46%, 44%, 42% and 39% respectively. Alkynes with an amino group (*o*-NH_2, *m*-F) (product **3x**) or an *o*- carbonyl group (product **3y**) unfortunately were not tolerated under our reaction condition. We can conclude according to the above scope that the reaction of terminal alkynes with hydroxylamine-*O*-sulfonic acid (HOSA) to directly fabricate oxime tolerates a wide range of substituents.

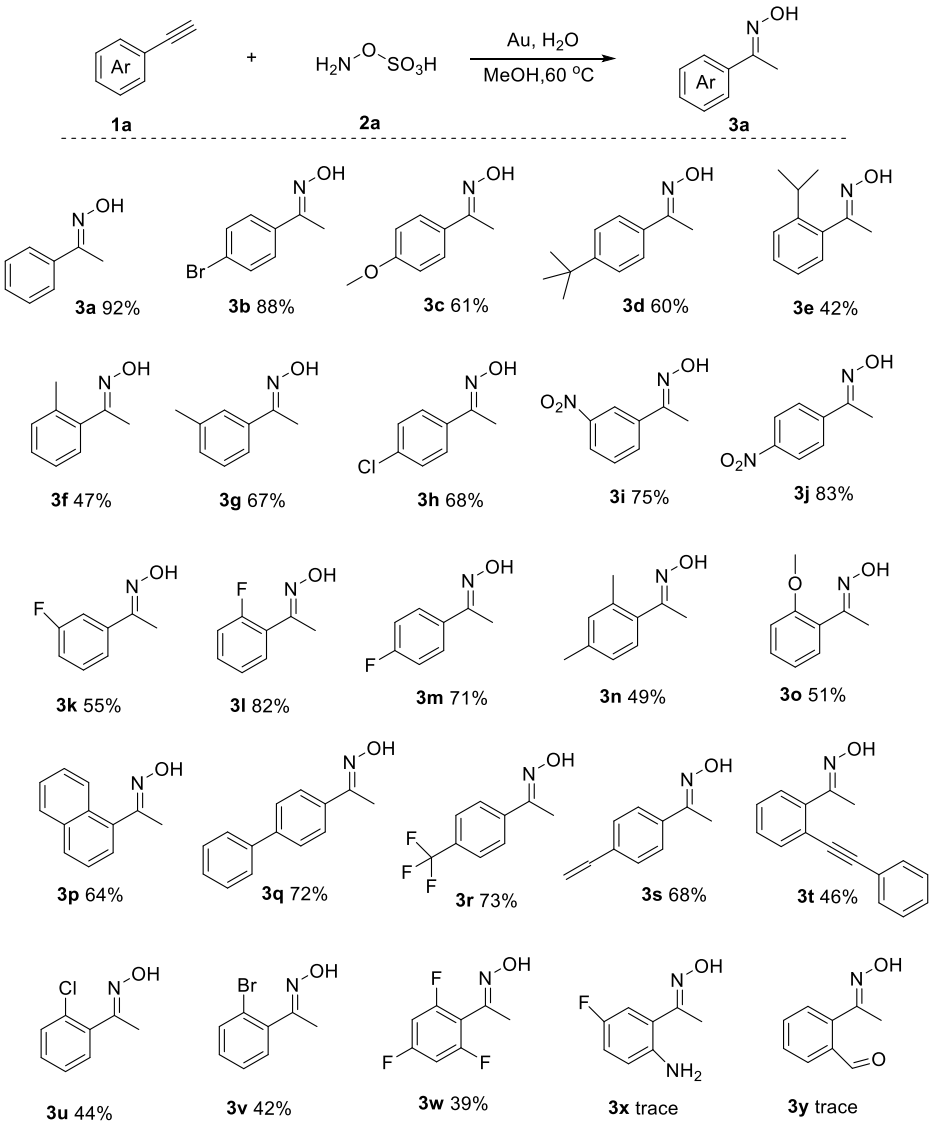

Scheme 3.3 Reaction scope. Reaction conditions: **1a** (0.2 mmol), **2a** (0.2 mmol), H_2O (0.2 mmol) and PPh_3AuNTf_2 (5 mol%) in MeOH (1 mL) at 60 °C temperature for 24 h.

To explore the scope of hydroxylamine-*O*-sulfonic acid (HOSA) part, we choose two substrates with a -Ts and -OTs group as exhibited in Scheme 3.4 to run the reaction, unfortunately, we only got the ketone, and no oxime. This means that in our set, the hydroxylamine-*O*-sulfonic acid (HOSA) is necessary.

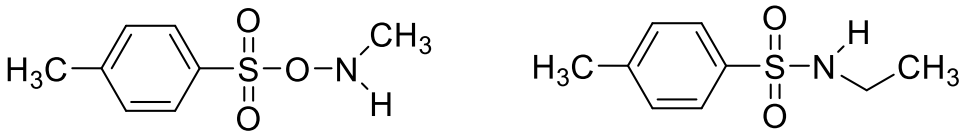

Scheme 3.4 Substrates with -Ts and -OTs group

3.2.3 Mechanistic study

To explore the reaction mechanism, the comparative experiment was carried out under the same reaction condition without hydroxylamine-O-sulfonic acid (HOSA), we only obtained the acetophenone as product with a yield of 90% (Scheme 3.5a). This result is also confirmed by various previous reports. [21-25] Then we run the reaction with acetophenone and hydroxylamine-O-sulfonic acid (HOSA) under the normal conditions, we harvested the expected oximes as product (Scheme 3.5b). In our particular reaction set, we can get supposed oxime directly (shown in Scheme 3.5c). These above results explain that hydroxylamine-*O*-sulfonic acid (HOSA) is the more reactive nucleophile and reacting directly.

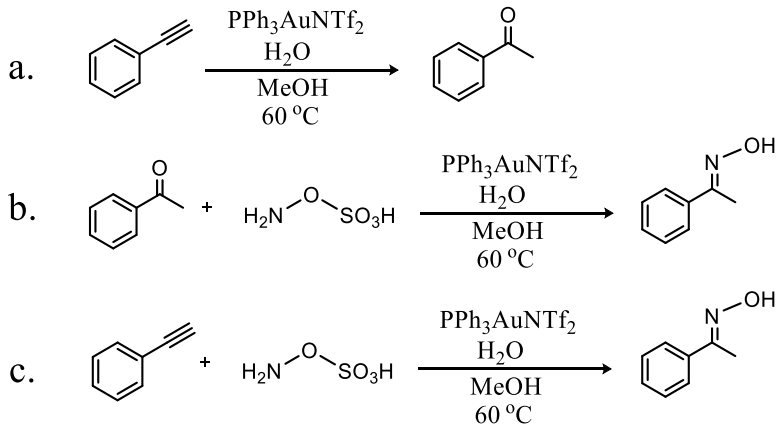

Scheme 3.5 Mechanistic elucidation

For the further investigation of the reaction mechanism and the reaction kinetics, the

kinetic study of phenylacetylene hydroamination at room temperature and 50 °C were checked by an automatically NMR testing. In our reaction condition, we choose MeOD (Methanol-d_4) as deuterated reagents and keep the reaction solution in NMR tube. The NMR data were automatically checked for 12 h. The kinetic study data at 50 °C temperature is shown in Scheme 3.6 and the kinetic study at room temperature is shown in Scheme 3.7. Obviously, in our reaction set, the phenylacetylene hydroamination can't be achieved at room temperature.

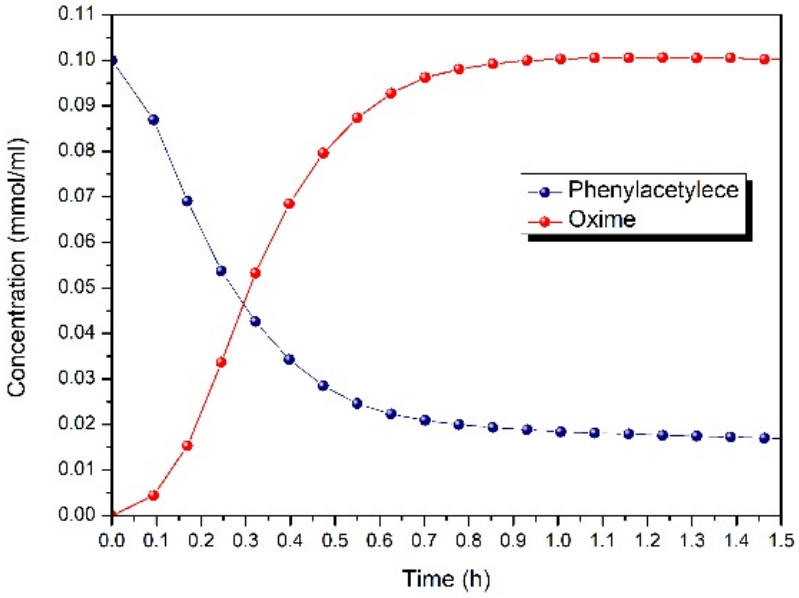

Scheme 3.6 Kinetic study of Phenylacetylene hydroamination at 50 °C.

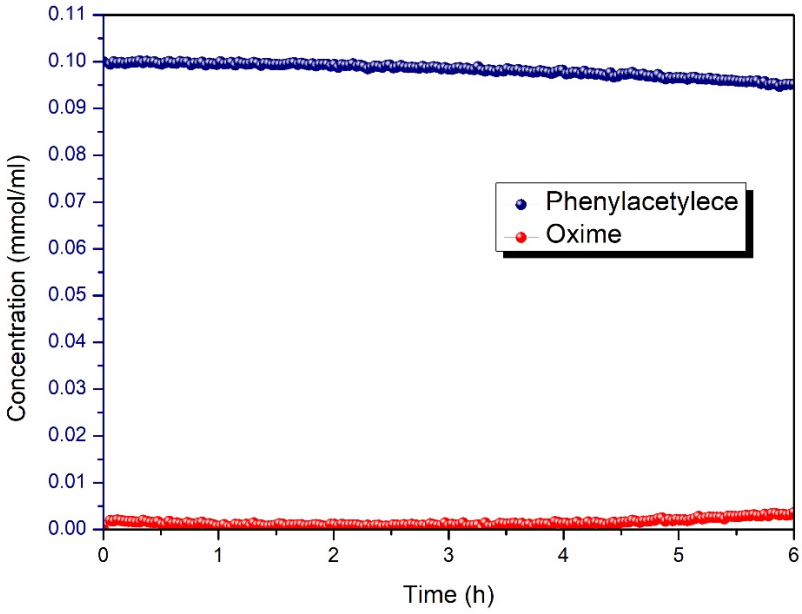

Scheme 3.7 Kinetic study of Phenylacetylene hydroamination at room temperature.

Based on the above mechanistic elucidation, we postulate a reasonable mechanism for our one-step oxime synthesis from terminal alkynes and hydroxylamine-O-sulfonic acid (HOSA). As shown in Scheme 3.8, the terminal alkyne is converted to intermediate **I** with Au(I) catalyst and hydroxylamine-O-sulfonic acid (HOSA) firstly, then the oxime formed under steps of intermediate **I** after hydrolysis of the O-S bond.

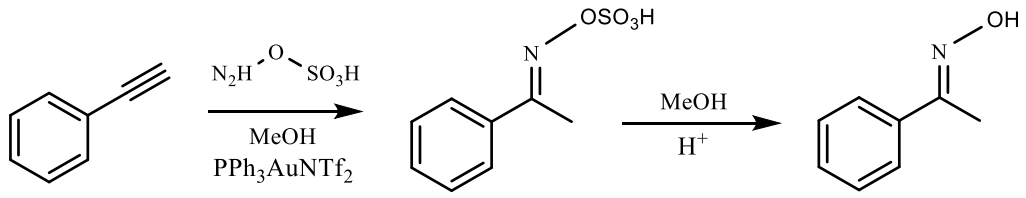

I

Scheme 3.8 Reaction mechanism

The possible reaction mechanism is in line with the thermodynamic data obtained by DFT calculations (Scheme 3.9). My colleague Martin C. Dietl conducted this calculation. The geometries of all possible intermediates were first optimized, followed by frequency analyses on a B3LYP[26-29]/def2-SVP[30] level of theory. For gold, additionally the basis set def2-TZVP[30] was applied. Upon coordination of the gold catalyst to phenylacetylene, HOSA attacks the activates triple bond of **I** to form transition state **TS** in an endergonic reaction step (ΔG = 12.2 kcal/mol). Afterwards, the transition state collapses to form **II** in an exergonic step (ΔG = - 6.05 kcal/mol), which directly undergoes protodemetallation to yield enamine **III** (ΔG = - 0.29 kcal/mol). **III** then tautomerizes in an exergonic reaction step (ΔG = - 0.29 kcal/mol) to the imine **IV**, whose formation was confirmed by mass spectrometry. Hydrolysis of IV by one equivalent of water leads to the oxime **V** in an exergonic reaction step (ΔG = -1.76 kcal/mol). Indeed, this species was detected after purification by flash column chromatography. Therefore, it is assumed that **IV** undergoes hydrolysis in the course of workup.

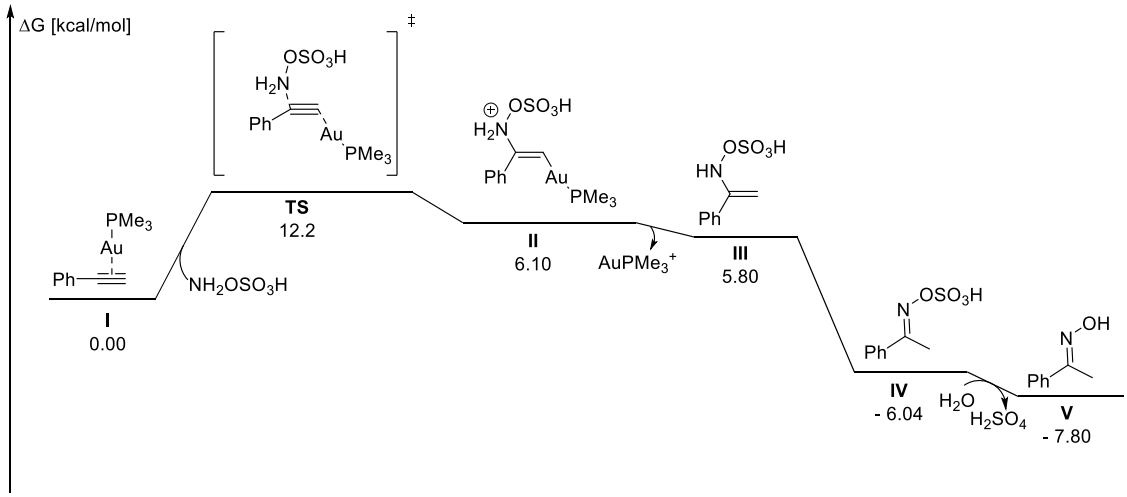

Scheme 3.9 Computational study of the mechanism.

3.2.4 Green chemistry metrics

Generally, chemical syntheses should be built upon green chemistry principles.[31-35] Therefore, we have calculated the green chemistry metrics for the synthesis of oxime (3b) on a preparative scale (Table 3.2). As given in equation (1) and equation (2), atom economy (AE) is "how much of the reactants remain in the final desired product", reaction mass efficiency (RME) is "the percentage of the mass of the reactants that remain in the product. Overall, our green process can enable the synthesis of oxime (3b) with an E-factor of 32.5, 58% atom economy, 53.4% atom efficiency, 100% carbon efficiency and 53.6% reaction mass efficiency.

$$\text{Atom economy}(\%) = \frac{\text{Molecular mass of desired product}}{\text{Molecular mass of all reactants}} \times 100\% \qquad \text{Equation (1)}$$

$$\text{Reaction mass efficiency}\ (\%) = \frac{\text{Mass of desired product}}{\text{Mass of all reactants}} \times 100\% \qquad \text{Equation (2)}$$

Table 3.2 green chemistry principles of the synthesis of oxime

Reactant (1b)	phenylacetylene	0.020g	0.0002 mol	FW 102.14
Reactant (2)	HOSA	0.023g	0.0002 mol	FW 113.01
Auxiliary	H_2O	0.0036g	0.0002 mol	FW 18.01
Solvent	MeOH	0.792g		
Product (3b)	Oxime	0.025g	0.00018mol	FW 135.17

Product yield= 92%

E-factor= $\frac{0.020+0.023+0.0036+0.792-0.025}{0.025}$ =32.5 Kg waste per Kg product

Atom economy=$\frac{135.17}{233.16}$=58%

Atom efficiency=92% x 58%/100 = 53.4%

Carbon efficiency=$\frac{8}{8+0}$=100%

Reaction mass efficiency=$\frac{0.025}{0.020+0.023+0.0036}$=53.6%

3.3 Conclusions

In summary, we found a facial and convenient one-step route to generate oximes from terminal alkynes and hydroxylamine-O-sulfonic acid (HOSA) by Au(I) catalysis. The DFT calculation and kinetics study were conducted to research the reaction mechanism. The green chemistry metric calculation shows the whole reaction process tolerate the wasting and economy good. This one-pot green process to fabricate oximes should not only play a role in biological and industry, but also has a positive response to carbon neutralization faced on the energy crisis. We believe that our reaction design would be valuable for the future economy chemistry.

3.4 References

[1]. Meyer, V.; Janny, A., Ueber Stickstoffhaltige Acetonderivate. *Ber. Dtsch. Chem. Ges.* **1882**, *15* (1), 1164-1167.

[2]. Worek, F.; Thiermann, H.; Wille, T., Oximes in Organophosphate Poisoning: 60 Years of Hope and Despair. *Chem. Biol. Interact*. **2016**, 259, 93-98.

[3]. Sukhorukov, A. Y.; Ioffe, S. L., Chemistry of Six-Membered Cyclic Oxime Ethers. Application in the Synthesis of Bioactive Compounds. *Chem. Rev.* **2011**, *111* (8), 5004-

5041.

[4]. Kölmel, D. K.; Kool, E. T., Oximes and Hydrazones in Bioconjugation: Mechanism and Catalysis. *Chem. Rev*. **2017**, *117* (15), 10358-10376.

[5] Zong, B. N.; Sun. B.; Cheng, S. B.; Mu, X. H.; Yang, K. Y.; Zhao, J. Q.; Zhang, X. X.; Wu, W., Green Production Technology of the Monomer of Nylon-6: Caprolactam. *Engineering*. **2017**, *3* (3), 379-384.

[6] Rosenberg, S.; Silver, S. M.; Sayer, J. M.; Jencks, W. P., Evidence for Two Concurrent Mechanisms and a Kinetically Significant Proton Transfer Process in Acid-Catalyzed Omethyloxime Formation, *J. Am. Chem. Soc.* **1974**, *96* (26), 7986-7998.

[7] Elmakssoudi, A.; Abdelouahdi, K.; Zahouily, M.; Clark, J.; Solhy, A., Efficient Conversion of Aldehydes and Ketones into Oximes using a Nanostructured Pyrophosphate Catalyst in a Solvent-free Process. *Catal. Commun.* **2012**, 29, 53-57.

[8] Cortés, I.; Kaufman, T. S.; Bracca, A. B., A Convenient and Eco-friendly Cerium (III) Chloride-Catalysed Synthesis of Methoxime Derivatives of Aromatic Aldehydes and Ketones. *R. Soc. Open Sci.* **2018**, *5* (5), 180279.

[9] Fischer, H.; Noller, C. R., "2, 4-Dimethyl-3, 5-dicarbethoxypyrrole." *Org. Synth.* **1935**, *15* (17), 4.

[10] Fischer H., Kryptopyrrole. *Org. Synth.* **1941**, 21, 67-70.

[11] Okamoto, T.; Kobayashi, K.; Oka, S.; Tanimoto, S., A High-Yield Regiospecific Synthesis of Keto Oximes from Aryl-Conjugated Ethylenes and Ethyl Nitrite in the Presence of Cobalt Complex and BH_4^-. *J. Org. Chem.* **1988**, *53* (21), 4897-4901.

[12] Moran, J.; Gorelsky, S. I.; Dimitrijevic, E.; Lebrun, M. E.; Bedard, A. C.; Seguin, C.; Beauchemin, A. M., Intermolecular Cope-Type Hydroamination of Alkenes and Alkynes using Hydroxylamines. *J. Am. Chem. Soc.* **2008**, *130* (52), 17893-17906.

[13] Muller, T. E.; Hultzsch, K. C.; Yus, M.; Foubelo, F.; Tada, M., Hydroamination: Direct Addition of Amines to Alkenes and Alkynes. *Chem. Rev.* **2008**, *108* (9), 3795-3892.

[14] Alonso, F.; Beletskaya, I. P.; Yus, M., Transition-Metal-Catalyzed Addition of Heteroatom-Hydrogen Bonds to Alkynes. *Chem. Rev.* **2004**, *104* (6), 3079-3160.

[15] Dorel, R.; Echavarren, A. M., Gold(I)-Catalyzed Activation of Alkynes for the Construction of Molecular Complexity. *Chem. Rev.* **2015**, *115* (17), 9028-9072.

[16] Pyykkö, P., Theoretical Chemistry of Gold. III. *Chem. Soc. Rev.* **2008**, *37* (9), 1967-1997.

[17] Aguilar, D.; Contel, M.; Urriolabeitia, E. P., Mechanistic Insights into the One-pot Synthesis of Propargylamines from Terminal Alkynes and Amines in Chlorinated Solvents Catalyzed by Gold Compounds and Nanoparticles. *Chem*. **2010**, *16* (30), 9287-9296.

[18] Lavallo, V.; Frey, G. D.; Donnadieu, B.; Soleilhavoup, M.; Bertrand, G., Homogeneous Catalytic Hydroamination of Alkynes and Allenes with Ammonia. *Angew. Chem. Int. Ed.* **2008**, *47* (28), 5224-5228.

[19] Moran, J.; Gorelsky, S. I.; Dimitrijevic, E.; Lebrun, M. E.; Bedard, A. C.; Seguin, C.; Beauchemin, A. M.; Intermolecular Cope-Type Hydroamination of Alkenes and Alkynes using Hydroxylamines. *J. Am. Chem. Soc.* **2008**, *130* (52), 17893-17906.

[20] Wang, B.; Yan, Z.; Liu, L.; Wang, J.; Zha, Z.; Wang, Z., TBN-Mediated Regio- and Stereoselective Sulfonylation & Oximation (Oximosulfonylation) of Alkynes with Sulfonyl Hydrazines in EtOH/H_2O. *Green Chem.* **2019**, *21* (2), 205-212.

[21] Taşdemir, V.; Menges, N., Gold-Catalyzed Cyclization of Non-conjugated Ynone-oxime Derivatives: Incorporation of Solvent Molecule. *Asian J. Org. Chem.* **2020**, *9* (12), 2108-2111.

[22] Zhu, F. X.; Wang, W.; Li, H. X., Water-Medium and Solvent-Free Organic Reactions over a Bifunctional Catalyst with Au Nanoparticles Covalently Bonded to HS/SO3H Functionalized Periodic Mesoporous Organosilica. *J. Am. Chem. Soc.* **2011**, *133* (30), 11632-11640.

[23] Oss, G.; Ho, J.; Nguyen, T. V., Tropylium Ion Catalyzes Hydration Reactions of Alkynes. *Eur. J. Org. Chem.* **2018**, *2018* (29), 3974-3981.

[24] Nairoukh, Z.; Avnir, D.; Blum, J., Acid-Catalyzed Hydration of Alkynes in Aqueous Microemulsions. *ChemSusChem*. **2013**, *6* (3), 430-432.

[25] Gonzalez-de-Castro, A.; Xiao, J., Green and Efficient: Iron-Catalyzed Selective

Oxidation of Olefins to Carbonyls with O_2. *J. Am. Chem. Soc.* **2015**, *137* (25), 8206-8218.

[26] Becke, A. D., Density-Functional Thermochemistry. I. The Effect of The Exchange-Only Gradient Correction. *Chem. Phys.* **1992**, *96* (3), 2155-2160.

[27] Lee, C.; Yang, W.; Parr, R. G., Development of The Colle-Salvetti Correlation-Energy Formula into a Functional of The Electron Density. *Phys. Rev. B*. **1988**, *37* (2), 785-789.

[28] Vosko, S. H.; Wilk, L.; Nusair, M., Accurate Spin-Dependent Electron Liquid Correlation Energies for Local Spin Density Calculations: A Critical Analysis. *Can. J. Phys.* **1980***, 58* (8), 1200-1211.

[29] Stephens, P. J.; Devlin, F. J.; Chabalowski, C. F.; Frisch, M. J., Ab Initio Calculation of Vibrational Absorption and Circular Dichroism Spectra Using Density Functional Force Fields. *J. Phys. Chem*. **1994**, *98* (45), 11623-11627.

[30] Weigend, F.; Ahlrichs, R., Balanced Basis Sets of Split Valence, Triple Zeta Valence and Quadruple Zeta Valence Quality for H to Rn: Design and Assessment of Accuracy. *Phys. Chem. Chem. Phys.* **2005**, *7* (18), 3297-3305.

[31] Kataoka, K.; Wachi, K.; Jin, X.; Suzuki, K.; Sasano, Y.; Iwabuchi, Y.; Hasegawa, J. Y.; Mizuno, N.; Yamaguchi, K., CuCl/TMEDA/nor-AZADO-Catalyzed Aerobic Oxidative Acylation of Amides with Alcohols to Produce Imides. *Chem. Sci.* **2018**, *9* (21), 4756-4768.

[32] Turgis, R.; Billault, I.; Acherar, S.; Augé, J.; Scherrmann, M. C., Total Synthesis of High Loading Capacity PEG-Based Supports: Evaluation and Improvement of the Process by use of Ultrafiltration and PEG as a Solvent. *Green Chem.* **2013**, *15* (4), 1016-1029.

[33] Augé, J.; Scherrmann, M. C., Determination of the Global Material Economy (GME) of Synthesis Sequences—A Green Chemistry Metric to Evaluate the Greenness of Products. *New J. Chem.* **2012**, *36* (4), 1091-1098.

[34] Curzons, A. D.; Constable, D. J.; Mortimer, D. N.; Cunningham, V. L., So You Think Your Process Is Green, How do You Know?—Using Principles of Sustainability

to Determine What Is Green–a Corporate Perspective. *Green Chem.* **2001**, *3* (1), 1-6.
[35] Trost, B. M., The Atom Economy—A Search for Synthetic Efficiency. *Science.* **1991**, *254* (5037), 1471-1477.

3.5 Experimental section

3.5.1 General remarks

All commercially available chemicals were purchased from suppliers (ABCR, Acros, Alfa Aesar, Chempur, Merck, Sigma Aldrich) and were used without further purifications. Dry solvents were obtained from the solvent purification system MB SPS-800-Benchtop. Deuterated solvents were supplied from Euriso-Top or Sigma Aldrich. The NMR spectra, if not noted otherwise, were tested at room temperature with the following spectrometers: Bruker Avance III 300 (300 MHz), Bruker Avance DRX 300 (300 MHz), Bruker Avance III 400 (400 MHz), Bruker Avance III 500 (500 MHz), Bruker Avance III 600 (600 MHz) or Fourier 300 (300 MHz). Chemical shifts δ are quoted in parts per million (ppm) and coupling constants J in hertz (Hz). ^{1}H and ^{13}C spectra are calibrated with the deuterated solvents, namely $CDCl_3$ (7.26 ppm; 77.16 ppm). The following abbreviations were used to explain the signal multiplicity: for the ^{1}H NMR spectra: s (singlet), d (doublet), t (triplet), q (quartet), quint (quartet), sext (sextet), sept (septet), m (multiplet), as well as their combinations; for the ^{13}C NMR spectra: s (quaternary carbon), d (tertiary carbon (CH)), t (secondary carbon (CH_2)) and q (primary carbon (CH_3)). All the ^{13}C NMR spectra were measured with ^{1}H-decoupling and were interpreted with the help of DEPT-135. Mass spectra (MS and HRMS) were measured in the chemistry department of the University Heidelberg. EI^+-spectra were determined on a JOEL JMS-700 spectrometer [mass analyzer type: Time-of-flight (TOF)]. Bruker ApexQu FT-ICR-MS spectrometer was used [mass analyzer type: Fourier transform ion cyclotron resonance (FT-ICR)] for ESI^+-spectra. Gas chromatography / Mass Spectroscopy (GC MS) was carried out on two different systems: (i) HP 5972 Mass Selective Detector, coupled with a HP 5890 SERIES II plus

Gas Chromatograph, (ii) Agilent 5975C Mass Selective Detector, coupled with an Agilent 7890A Gas Chromatograph. In both cases, as a capillary column, an OPTIMA 5 cross-linked Methyl Silicone column (30 m x, 0.32 mm, 0.25 mm) was employed, and helium was used as the carrier gas. Flash Column Chromatography was accomplished by using Silica gel 60 (0.04 – 0.063 mm / 230 – 400 mesh ASTM) purchased from Macherey-Nagel as the stationary phase. As eluents, the mixture of petroleum ether (PE) and ethyl acetate (EA) were used for all products. Analytical Thin Layer Chromatography (TLC) was carried out on precoated Macherey-Nagel POLYGRAM® SIL G/UV254 or Merck TLC Silica Gel 60 F254 aluminum sheets. All geometry optimizations, subsequent frequency analyses, and calculations concerning transition states were performed with the CPCM model for 1,2-dichlorobenzene using Orca 4.0.1.2 on the bwForCluster Justus 2. The PBE0 functional and the def2-SVP basis set was employed. Furthermore, for Au def2-TZVP basis set was used. The heat source is oil bath.

3.5.2 Experiment procedures

General procedure:

A reaction vail was charged with a magnetic stirrer, alkynes (0.2 mmol, 1 equiv), hydroxylamine-*O*-sulfonic acid (HOSA) (0.2 mmol, 1 equiv), H_2O (0.2 mmol, 1 equiv), PPh_3AuNTf_2 (0.01 mmol, 5% equiv) in MeOH at 60 °C temperature for 24 hours. Then the reaction mixture was quenched and washed with brine (10 mL) and dried with Na_2SO_4. Crude product was purified by petroleum ether and ethyl acetate used as eluent. The mixture of petroleum ether (PE) and ethyl acetate (EA) (PE:EA=10:1) were used as eluent for all products if it not mentioned by other eluent.

Procedure of synthesis (E)-1-phenylethan-1-one oxime (**3a**):

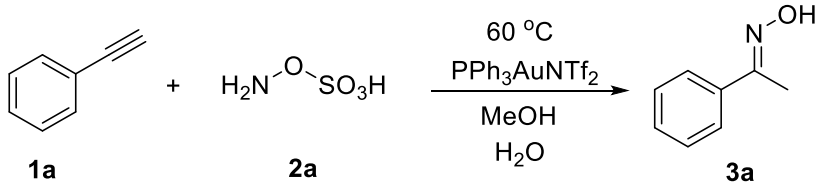

1a **2a** **3a**

1 mL of MeOH was added to a flask by syringe, then 7.39 mg of PPh_3AuNTf_2 (0.01 mmol), 20.4 mg of alkynes (0.2 mmol), 22.6 mg of hydroxylamine-*O*-sulfonic acid (HOSA) (0.2 mmol) and 3.6 uL H_2O (0.2 mmol) was added into the flask one by one. After adding of all needed materials, the mixture was stirred for 24 h under an oil bath with 60°C temperature. Then the reaction mixture was quenched and washed with brine (10 mL) and dried with Na_2SO_4. Crude product was purified by petroleum ether and ethyl acetate (PE:EA=10:1) used as eluent. Then we obtained 24.8 mg of yellow liquid (92% yield).

mmol scale synthesis of **3a**:

10 mL of MeOH was added to a flask by big-size syringe, then 73.9 mg of PPh_3AuNTf_2 (0.1 mmol), 204 mg of alkynes (2 mmol), 226 mg of hydroxylamine-*O*-sulfonic acid (HOSA) (2 mmol) and 36 uL H_2O (2 mmol)was added into the flask one by one. After adding of all needed materials, the mixture was stirred for 24 h under an oil bath with 60°C temperature. Then the reaction mixture was quenched and washed with brine (100 mL) and dried with Na_2SO_4. Crude product was purified by petroleum ether and ethyl acetate (PE:EA=10:1) used as eluent. Then we obtained 229 mg of pale-yellow solid (1.69 mmol, 84% yield).

We purchased product **1** and **2**.

3.5.3 Mechanistic experiment

Reaction without hydroxylamine-O-sulfonic acid (HOSA):

We carried out the reaction of 20.4 mg of Phenylacetylene **1a** (1 equiv, 0.2 mmol), 3.6 μL of H_2O (1 equiv, 0.2 mmol), 7.39 mg of PPh_3AuNTf_2 (5 mol%, 0.01 mmol), in 1 mL of MeOH at 60°C temperature for 24 hours. Then the crude product was purified by petroleum ether and ethyl acetate used as eluent. The expected product acetophenone **4** was obtained with a weight of 21.8 mg and a yield of 90%. This experiment result was also confirmed by literatures.[1-8]

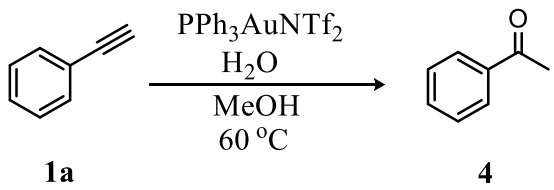

1a **4**

Reaction without Phenylacetylene:

We carried out the reaction of hydroxylamine-*O*-sulfonic acid (HOSA) **2a** (1 equiv, 0.2 mmol), PPh_3AuNTf_2 (5 mol%), H_2O (1 equiv, 0.2 mmol) in MeOH at 60°C temperature for 24 hours. No new product formed.

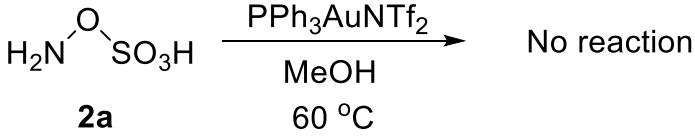

2a

Reaction with $H_2{}^{18}O$:

We carried out the reaction of Phenylacetylene **1a** (1 equiv, 0.2 mmol), hydroxylamine-*O*-sulfonic acid (HOSA) **2a** (1 equiv, 0.2 mmol), PPh_3AuNTf_2 (5 mol%) in MeOH at 60°C temperature for stirring, then the $H_2{}^{18}O$ (1 equiv, 0.2 mmol) was added into the mixture and keep stirring for 24 h. Following, the crude reaction mixture was tested by HRMS, and we find the intermediate and $H_2S^{18}OO_3$ in the system. Following, Crude mixture was quenched, washed with brine (10 mL), dried with Na_2SO_4 and purified by petroleum ether and ethyl acetate used as eluent. The product **3a** was obtained.

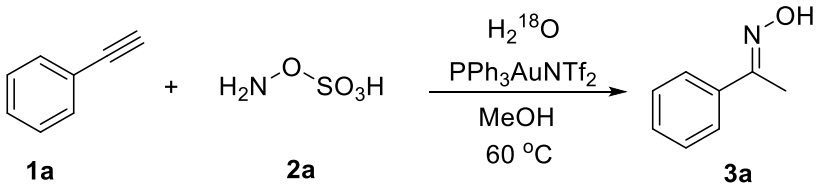

1a **2a** **3a**

Kinetic study at 50 °C:

In our reaction condition, we choose MeOD (Methanol-d_4) as deuterated reagents, 5.11 mg of Phenylacetylene **1a** (1 equiv, 0.05 mmol), 5.65 mg of hydroxylamine-*O*-sulfonic acid (HOSA) **2a** (1 equiv, 0.05 mmol), 0.9 μL of H_2O (1 equiv, 0.05 mmol)

and 1.85 mg of PPh_3AuNTf_2 (5 mol%, 0.0025 mmol) were added in 0.5 mL of MeOD (Methanol-d_4) in NMR tube. The NMR data were automatically checked at 50 ^oC temperature for 12 h.

Kinetic study at room temperature:

For the further understanding of mechanism, the kinetic study of Phenylacetylene hydroamination at room temperature is checked. In our reaction condition, we choose MeOD (Methanol-d_4) as deuterated reagents, 5.11 mg of Phenylacetylene **1a** (1 equiv, 0.05 mmol), 5.65 mg of hydroxylamine-*O*-sulfonic acid (HOSA) **2a** (1 equiv, 0.05 mmol), 0.9 μL of H_2O (1 equiv, 0.05 mmol) and 1.85 mg of PPh_3AuNTf_2 (5 mol%, 0.0025 mmol) were added in 0.5 mL of MeOD (Methanol-d_4) in NMR tube. The NMR data were automatically checked at room temperature for 12 h.

3.5.4 Characterization data

(3a) (E)-1-phenylethan-1-one oxime

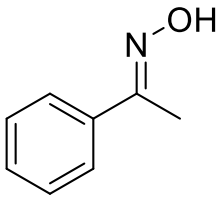

Yellow liquid, 24.8 mg, 92% yield.

Purification by column chromatography on silica gel, chromatography eluent: PE to 2% EA in petroleum. R_f = 0.38 (PE/EA=10/1).

^{1}H NMR (300 MHz, $CDCl_3$) δ 8.97 (s, 1H), 7.63 (dd, *J* = 6.7, 3.0 Hz, 1H), 7.52 – 7.30 (m, 1H), 2.31 (s, 1H). **^{13}C NMR** (75 MHz, $CDCl_3$) δ 156.06, 136.51, 129.23, 128.49, 126.03, 12.23. **HRMS** (ESI-TOF) m/z: $[M+H]^+$ calc'd for C_8H_9NO 135.0754; found 135.0749. **IR**: $\tilde{\nu}$ = 3094, 1740, 1685, 1586, 1566, 1486, 1426, 1397, 1354, 1319, 1266, 1176, 1090, 1077, 1010, 958, 866, 824, 751, 711, 681, 608 cm^{-1}

(3b) (E)-1-(4-bromophenyl)ethan-1-one oxime

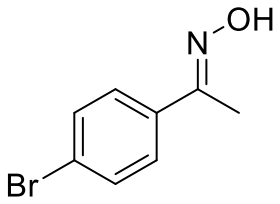

Yellow liquid, 37.6 mg, 88% yield.

Purification by column chromatography on silica gel, chromatography eluent: PE to 2% EA in petroleum. R_f= 0.4 (PE/EA=10/1).

^{1}H NMR (301 MHz, CDCl3) δ 9.02 (s, 1H), 7.50 (d, J = 1.4 Hz, 1H), 2.28 (s, 1H). **^{13}C NMR** (76 MHz, $CDCl_3$) δ 155.21, 135.33, 131.67, 127.56, 123.57, 12.09. **HRMS** (ESI-TOF) m/z: $[M+H]^+$ calc'd for C_8H_8BrNO 214.0648; found 241.0650. **IR**: ṽ = 3351, 3063, 3005, 2965, 2924, 2860, 1969, 1905, 1820, 1692, 1599, 1582, 1491, 1449, 1360, 1303, 1271, 1180, 1160, 1103, 1078, 1024, 1001, 956, 927, 851, 762, 692, 617 cm^{-1}

(3c) (E)-1-(4-methoxyphenyl)ethan-1-one oxime

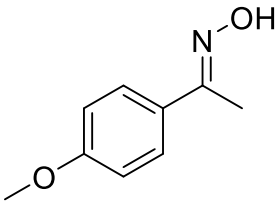

Yellow liquid, 20 mg, 61% yield.

Purification by column chromatography on silica gel, chromatography eluent: PE to 2% EA in petroleum. R_f= 0.36 (PE/EA=10/1).

^{1}H NMR (300 MHz, $CDCl_3$) δ 8.84 (s, 1H), 7.30 (t, *J* = 8.1 Hz, 1H), 7.24 – 7.16 (m, 1H), 7.04 – 6.80 (m, 1H), 3.84 (s, 1H), 2.29 (s, 1H). **^{13}C NMR** (75 MHz, $CDCl_3$) δ 159.62, 155.97, 137.92, 129.47, 118.61, 115.06, 111.34, 55.29, 12.28. **HRMS** (ESI-TOF) m/z: $[M+H]^+$ calc'd for $C_9H_{11}NO_2$ 165.0784; found 165.0797. **IR**: ṽ = 3346, 3003, 2938, 2835, 2072, 1934, 1749, 1682, 1599, 1578, 1488, 1454, 1428, 1368, 1289, 1223, 1181, 1099, 1079, 1038, 1003, 939, 852, 779, 740, 689, 650 cm^{-1}

(3d) (E)-1-(4-(tert-butyl)phenyl)ethan-1-one oxime

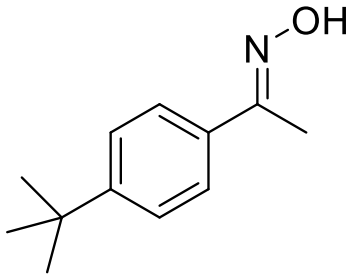

Yellow liquid, 23 mg, 60% yield.

Purification by column chromatography on silica gel, chromatography eluent: PE to 2% EA in petroleum. R_f = 0.35 (PE/EA=10/1).

^{1}H NMR (300 MHz, $CDCl_3$) δ 8.93 (s, 1H), 7.57 (d, *J* = 8.4 Hz, 1H), 7.41 (d, *J* = 8.5 Hz, 1H), 2.30 (s, 1H), 1.34 (s, 1H). **^{13}C NMR** (75 MHz, $CDCl_3$) δ 155.88, 152.42, 133.67, 125.75, 125.43, 34.67, 31.20, 12.14. **HRMS** (ESI-TOF) m/z: $[M+H]^+$ calc'd for $C_{12}H_{17}NO$ 191.1257; found 191.1230. **IR**: $\tilde{\nu}$ = 3348, 2965, 2906, 2870, 1683, 1606, 1563, 1464, 1406, 1357, 1271, 1192, 1113, 1015, 957, 838, 634 cm^{-1}

(3e) (E)-1-(2-isopropylphenyl)ethan-1-one oxime

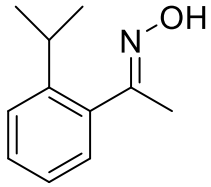

Brown liquid, 14.8 mg, 42% yield.

Purification by column chromatography on silica gel, chromatography eluent: PE to 2% EA in petroleum. R_f = 0.33 (PE/EA=10/1).

^{1}H NMR (300 MHz, $CDCl_3$) δ 7.34 (d, *J* = 3.1 Hz, 1H), 7.23 – 7.12 (m, 1H), 3.25 – 2.89 (m, 1H), 2.21 (s, 1H), 1.23 (d, *J* = 6.9 Hz, 1H). **^{13}C NMR** (75 MHz, $CDCl_3$) δ 158.47, 146.65, 128.14, 125.80, 125.69, 30.07, 24.21, 16.77. **HRMS** (ESI-TOF) m/z: $[M+H]^+$ calc'd for $C_{11}H_{15}NO$ 177.1148; found 177.1110. **IR**: $\tilde{\nu}$ = 3260, 3063, 3024, 2963, 2926, 2869, 1768, 1747, 1647, 1600, 1575, 1490, 1460, 1446, 1364, 1301, 1260, 1205, 1088, 1066, 1017, 916, 798, 757, 648 cm^{-1}

(3f) (E)-1-(o-tolyl)ethan-1-one oxime

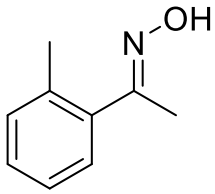

White solid, 14 mg, 47% yield, melting point 57.1-58.2 ℃.

Purification by column chromatography on silica gel, chromatography eluent: PE to 2% EA in petroleum. R_f = 0.36 (PE/EA=10/1).

^{1}H NMR (300 MHz, $CDCl_3$) δ 8.38 (s, 1H), 7.21 (dd, *J* = 9.4, 4.0 Hz, 1H), 2.35 (s, 1H), 2.21 (s, 1H). **^{13}C NMR** (75 MHz, $CDCl_3$) δ 158.19, 130.63, 128.52, 128.12, 125.79, 19.99, 15.77. **HRMS** (ESI-TOF) m/z: $[M+H]^+$ calc'd for $C_9H_{11}NO$ 149.0410; found 149.0403. **IR**: ṽ = 3235, 3058, 2950, 2924, 1966, 1898, 1856, 1601, 1492, 1433, 1378, 1364, 1310, 1272, 1159, 1125, 1079, 1042, 1031, 1011, 952, 925, 872, 810, 753, 728, 649 cm^{-1}

(3g) (E)-1-(m-tolyl)ethan-1-one oxime

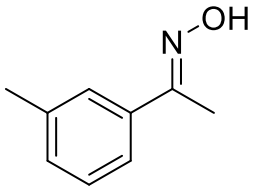

Yellow liquid, 20 mg, 67% yield.

Purification by column chromatography on silica gel, chromatography eluent: PE to 2% EA in petroleum. R_f = 0.35 (PE/EA=10/1).

^{1}H NMR (301 MHz, $CDCl_3$) δ 8.89 (s, 1H), 7.35 (dd, *J* = 5.5, 4.7 Hz, 1H), 7.19 (dd, *J* = 10.7, 4.3 Hz, 1H), 7.12 (d, *J* = 7.6 Hz, 1H), 2.31 (s, 1H), 2.22 (s, 1H). **^{13}C NMR** (76 MHz, $CDCl_3$) δ 156.23, 138.12, 136.51, 129.99, 128.39, 126.69, 123.21, 21.45, 12.33. **HRMS** (ESI-TOF) m/z: $[M+H]^+$ calc'd for $C_9H_{11}NO$ 149.0816; found 149.0831. **IR**: ṽ = 2962, 2922, 2864, 1683, 1604, 1586, 1426, 1357, 1275, 1193, 1083, 1019, 959, 856, 790, 748, 691 cm^{-1}

(3h) (E)-1-(4-chlorophenyl)ethan-1-one oxime

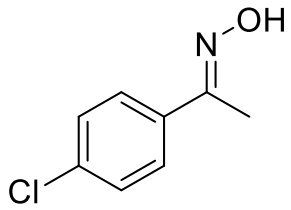

Yellow liquid, 23 mg, 68% yield.

Purification by column chromatography on silica gel, chromatography eluent: PE to 2% EA in petroleum. R_f = 0.38 (PE/EA=10/1).

^{1}H NMR (301 MHz, $CDCl_3$) δ 7.57 (d, *J* = 8.6 Hz, 1H), 7.35 (d, *J* = 8.6 Hz, 1H), 2.27 (s, 1H). **^{13}C NMR** (75 MHz, $CDCl_3$) δ 155.14, 135.25, 134.93, 128.69, 127.30, 26.55, 12.00. **HRMS** (ESI-TOF) m/z: $[M+H]^+$ calc'd for C_8H_8ClNO 169.0286; found 169.0217. **IR**: ṽ = 3005, 2963, 2922, 1685, 1588, 1571, 1488, 1428, 1397, 1358, 1261, 1176, 1094, 1013, 958, 827, 761, 622 cm^{-1}

(3i) (E)-1-(3-nitrophenyl)ethan-1-one oxime

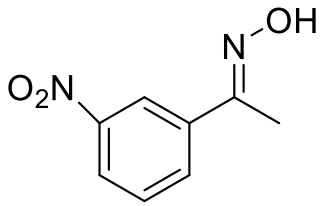

Yellow solid, 27 mg, 75% yield, melting point 71.4-72.2 ℃.

Purification by column chromatography on silica gel, chromatography eluent: PE to 2% EA in petroleum. R_f = 0.39 (PE/EA=10/1).

^{1}H NMR (301 MHz, $CDCl_3$) δ 8.48 (s, 1H), 8.23 (ddd, *J* = 8.2, 2.2, 1.0 Hz, 1H), 8.03 – 7.96 (m, 1H), 7.56 (t, *J* = 8.0 Hz, 1H), 2.34 (s, 1H). **^{13}C NMR** (76 MHz, $CDCl_3$) δ 154.21, 138.13, 129.45, 123.81, 121.05, 11.97. **HRMS** (ESI-TOF) m/z: $[M+H]^+$ calc'd for $C_8H_8N_2O_3$ 180.0599; found 180.0541. **IR**: ṽ = 3364, 3106, 3090, 2926, 2008, 1947, 1818, 1733, 1691, 1615, 1574, 1526, 1472, 1432, 1391, 1348, 1318, 1278, 1252, 1168, 1110, 1079, 1062, 1021, 1000, 972, 911, 873, 820, 764, 739, 723, 674, 663 cm^{-1}

(3j) (E)-1-(4-nitrophenyl)ethan-1-one oxime

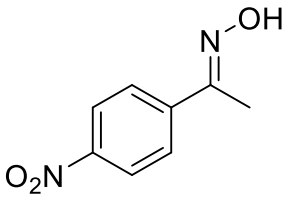

Yellow solid, 30 mg, 83% yield, melting point 58.3-59 ℃.

Purification by column chromatography on silica gel, chromatography eluent: PE to 2% EA in petroleum. R_f = 0.38 (PE/EA=10/1).

^{1}H NMR (301 MHz, $CDCl_3$) δ 8.17 (d, *J* = 9.1 Hz, 1H), 7.75 (d, *J* = 9.0 Hz, 1H), 2.25 (s, 1H). **^{13}C NMR** (75 MHz, $CDCl_3$) δ 196.28, 147.52, 129.30, 123.86, 30.91, 26.97, 23.61. **HRMS** (ESI-TOF) m/z: $[M+H]^+$ calc'd for $C_8H_8N_2O_3$ 180.0529; found 180.0490. **IR**: ṽ = 3111, 3085, 2962, 2852, 2247, 1687, 1601, 1566, 1510, 1409, 1342, 1316, 1258, 1107, 1011, 922, 874, 854, 819, 732, 689 cm^{-1}

(3k) (E)-1-(3-fluorophenyl)ethan-1-one oxime

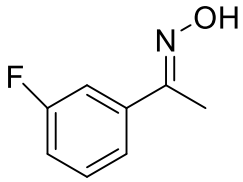

Yellow liquid, 16.8 mg, 55% yield.

Purification by column chromatography on silica gel, chromatography eluent: PE to 2% EA in petroleum. R_f = 0.33 (PE/EA=10/1).

^{1}H NMR (301 MHz, $CDCl_3$) δ 9.36 (s, 1H), 7.50 – 7.27 (m, 1H), 7.18 – 6.97 (m, 1H), 2.29 (s, 1H). **^{13}C NMR** (76 MHz, $CDCl_3$) δ 164.46, 155.12, 138.69, 138.59, 130.08, 129.97, 121.75, 121.71, 116.28, 116.00, 113.20, 112.90, 12.27. **HRMS** (ESI-TOF) m/z: $[M+H]^+$ calc'd for C_8H_8FNO 153.0584; found 153.0562. **IR**: ṽ = 3078, 2917, 2849, 1689, 1587, 1486, 1443, 1391, 1358, 1320, 1270, 1197, 1069, 1003, 878, 791, 753, 701, 683 cm^{-1}

(3l) (E)-1-(2-fluorophenyl)ethan-1-one oxime

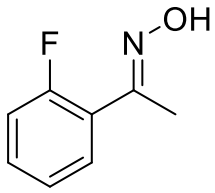

Yellow liquid, 25 mg, 82% yield.

Purification by column chromatography on silica gel, chromatography eluent: PE to 2% EA in petroleum. R_f = 0.34 (PE/EA=10/1).

^{1}H NMR (500 MHz, $CDCl_3$) δ 9.32 (s, 1H), 7.46 (td, *J* = 7.6, 1.7 Hz, 1H), 7.39 – 7.32 (m, 1H), 7.16 (td, *J* = 7.6, 0.7 Hz, 1H), 7.11 (dd, *J* = 11.0, 8.4 Hz, 1H), 2.30 (d, *J* = 2.3 Hz, 1H). **^{13}C NMR** (126 MHz, $CDCl_3$) δ 161.44, 159.44, 154.09, 154.08, 130.71, 130.64, 129.35, 129.32, 124.23, 124.20, 116.33, 116.16, 14.69, 14.65. **HRMS** (ESI-TOF) m/z: $[M+H]^+$ calc'd for C_8H_8FNO 153.0584; found 153.0565. **IR**: ṽ = 3081, 3010, 2930, 1686, 1610, 1575, 1481, 1454, 1362, 1288, 1232, 1212, 1156, 1114, 1024, 966, 899, 876, 829, 762, 647 cm^{-1}

(3m) (E)-1-(4-fluorophenyl)ethan-1-one oxime

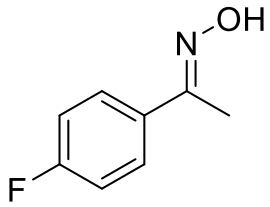

Yellow liquid, 21.7 mg, 71% yield.

Purification by column chromatography on silica gel, chromatography eluent: PE to 2% EA in petroleum. R_f = 0.33 (PE/EA=10/1).

^{1}H NMR (500 MHz, $CDCl_3$) δ 8.36 (s, 1H), 7.61 (dd, *J* = 8.9, 5.4 Hz, 1H), 7.07 (t, *J* = 8.7 Hz, 1H), 2.28 (s, 1H). **^{13}C NMR** (126 MHz, $CDCl_3$) δ 164.39, 162.41, 155.18, 132.61, 132.58, 127.88, 127.81, 115.54, 115.37, 12.15. **HRMS** (ESI-TOF) m/z: $[M+H]^+$ calc'd for C_8H_8FNO 153.0584; found 153.0561. **IR**: ṽ = 3121, 3083, 3021, 2959, 2928, 1908, 1687, 1599, 1563, 1512, 1471, 1449, 1414, 1390, 1351, 1322, 1288,

1265, 1241, 1171, 1159, 1104, 1086, 1014, 998, 926, 898, 867, 841, 785, 759, 694, 636, 610 cm^{-1}

(3n) (E)-1-(4-fluorophenyl)ethan-1-one oxime

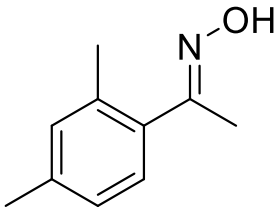

Yellow liquid, 16 mg, 49% yield.

Purification by column chromatography on silica gel, chromatography eluent: PE to 2% EA in petroleum. R_f = 0.31 (PE/EA=10/1).

^{1}H NMR (300 MHz, $CDCl_3$) δ 8.19 (s, 1H), 7.12 (d, *J* = 7.6 Hz, 1H), 7.08 – 6.97 (m, 1H), 2.32 (s, 2H), 2.20 (s, 1H). **^{13}C NMR** (75 MHz, $CDCl_3$) δ 158.19, 138.31, 135.52, 134.55, 131.43, 128.09, 126.45, 21.09, 19.99, 15.79. **HRMS** (ESI-TOF) m/z: $[M+H]^+$ calc'd for $C_{10}H_{13}NO$ 163.0992; found 163.0976. **IR**: ṽ = 3256, 2921, 2857, 1733, 1647, 1614, 1505, 1447, 1364, 1304, 1275, 1233, 1137, 1067, 1010, 936, 906,817, 757, 722, 621 cm^{-1}

(3o) (E)-1-(2-methoxyphenyl)ethan-1-one oxime

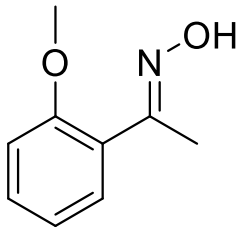

Orange liquid, 16.8 mg, 51% yield.

Purification by column chromatography on silica gel, chromatography eluent: PE to 2% EA in petroleum. R_f = 0.33 (PE/EA=10/1).

^{1}H NMR (300 MHz, $CDCl_3$) δ 8.72 (s, 1H), 7.30 (t, *J* = 8.1 Hz, 1H), 7.24 – 7.17 (m, 2H), 6.99 – 6.84 (m, 1H), 3.84 (s, 3H), 2.29 (s, 3H). **^{13}C NMR** (75 MHz, $CDCl_3$) δ 159.63, 155.98, 137.92, 129.47, 118.61, 115.07, 111.33, 55.29, 12.25. **HRMS** (ESI-TOF) m/z: $[M+H]^+$ calc'd for $C_9H_{11}NO_2$ 165.0784; found 165.0603. **IR**: ṽ = 3350, 3076,

3004, 2942, 2837, 2071, 1686, 1597, 1585, 1486, 1452, 1430, 1357, 1333, 1277, 1223, 1181, 1092, 1043, 994, 970, 875, 861, 789, 688 cm^{-1}

(3p) (E)-1-(naphthalen-1-yl)ethan-1-one oxime

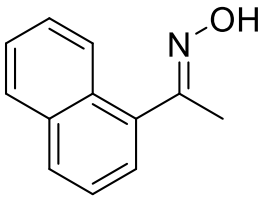

Brown liquid, 23.7 mg, 64% yield.

Purification by column chromatography on silica gel, chromatography eluent: PE to 2% EA in petroleum. R_f = 0.33 (PE/EA=10/1).

^{1}H NMR (301 MHz, $CDCl_3$) δ 8.67 (d, *J* = 8.6 Hz, 1H), 8.04 – 7.68 (m, 1H), 7.62 – 7.33 (m, 1H), 2.67 (s, 1H). **^{13}C NMR** (76 MHz, $CDCl_3$) δ 201.85, 133.96, 133.02, 130.12, 128.65, 128.38, 128.04, 126.42, 125.98, 124.30, 29.97. **HRMS** (ESI-TOF) m/z: $[M+H]^+$ calc'd for $C_{12}H_{11}NO$ 185.0726; found 185.0717. **IR**: ṽ = 3338, 3049, 3003, 2922, 1942, 1828, 1681, 1620, 1593, 1573, 1508, 1461, 1433, 1396, 1355, 1279, 1241, 1214, 1194, 1144, 1128, 1077, 1023, 941, 866, 803, 776, 738, 682, 651 cm^{-1}

(3q) (E)-1-([1,1'-biphenyl]-4-yl)ethan-1-one oxime

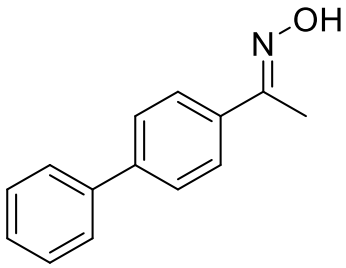

Yellow solid, 30 mg, 72% yield, melting point 123.9-124.5 ℃.

Purification by column chromatography on silica gel, chromatography eluent: PE to 2% EA in petroleum. R_f = 0.3 (PE/EA=10/1).

^{1}H NMR (300 MHz, $CDCl_3$) δ 8.04 (d, *J* = 8.3 Hz, 1H), 7.73 – 7.60 (m, 1H), 7.43 (ddd, *J* = 10.9, 9.7, 5.7 Hz, 1H), 2.64 (s, 1H). ^{13}C NMR (75 MHz, $CDCl_3$) δ 197.75, 145.79, 135.85, 128.94, 128.90, 128.22, 127.26, 127.22, 26.65. **HRMS** (ESI-TOF) m/z: $[M+H]^+$ calc'd for $C_{14}H_{13}NO$ 211.0992; found 211.0962. **IR**: ṽ = 2999, 2918, 1679,

1602, 1560, 1486, 1451, 1432, 1404, 1359, 1343, 1313, 1283, 1263, 1209, 1180, 1121, 1078, 1020, 1007, 961, 841, 764, 721, 691 cm^{-1}

(3r) (E)-1-(4-(trifluoromethyl)phenyl)ethan-1-one oxime

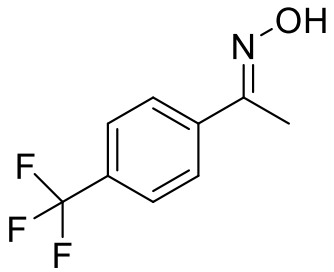

Yellow liquid, 29.6 mg, 73% yield.

Purification by column chromatography on silica gel, chromatography eluent: PE to 2% EA in petroleum. R_f= 0.32 (PE/EA=10/1).

^{1}H NMR (400 MHz, $CDCl_3$) δ 8.06 (d, *J* = 8.1 Hz, 1H), 7.74 (d, *J* = 8.2 Hz, 1H), 2.65 (s, 1H). **^{13}C NMR** (101 MHz, $CDCl_3$) δ 196.97, 128.62, 125.70, 125.66, 26.76. **HRMS** (ESI-TOF) m/z: $[M+H]^+$ calc'd for $C_9H_8F_3NO$ 203.0553; found 203.0573. **IR**: $\tilde{\nu}$ = 3360, 3069, 2929, 1935, 1800, 1692, 1614, 1568, 1511, 1410, 1361, 1320, 1288, 1263, 1166, 1121, 1092, 1081, 1063, 1015, 961, 926, 896, 843, 763, 718, 669, 606 cm^{-1}

(3s) (E)-1-(4-vinylphenyl)ethan-1-one oxime

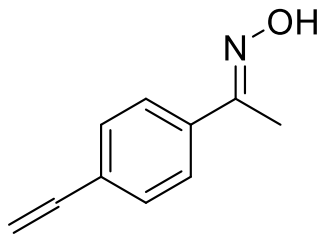

White solid, 22 mg, 68% yield, melting point 116.6-117.8 ℃.

Purification by column chromatography on silica gel, chromatography eluent: PE to 2% EA in petroleum. R_f= 0.33 (PE/EA=10/1).

^{1}H NMR (301 MHz, $CDCl_3$) δ 8.46 (s, 1H), 7.66 – 7.54 (m, 1H), 7.42 (d, *J* = 8.3 Hz, 1H), 6.70 (d, *J* = 10.9 Hz, 1H), 5.79 (dd, *J* = 17.6, 0.7 Hz, 1H), 5.29 (dd, *J* = 10.9, 0.7 Hz, 1H), 2.29 (s, 1H). **^{13}C NMR** (75 MHz, $CDCl_3$) δ 155.77, 147.51, 138.43, 136.22, 126.28, 126.17, 114.67, 11.95. **HRMS** (ESI-TOF) m/z: $[M+H]^+$ calc'd for $C_{10}H_{11}NO$

161.0835; found 161.0826. **IR**: ṽ = 3292, 3234, 3122, 3086, 3063, 2985, 2922, 1922, 1835, 1627, 1557, 1513, 1402, 1366, 1312, 1209, 1187, 1124, 1084, 997, 923, 845, 802, 743 cm^{-1}

(3t) (E)-1-(2-(phenylethynyl)phenyl)ethan-1-one oxime

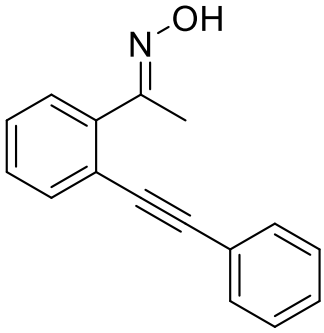

Brown solid, 21.6 mg, 46% yield, melting point 167.1-167.9 ℃.

Purification by column chromatography on silica gel, chromatography eluent: PE to 2% EA in petroleum. R_f = 0.31 (PE/EA=10/1).

^{1}H NMR (301 MHz, $CDCl_3$) δ 8.18 (d, *J* = 7.3 Hz, 1H), 7.51 – 7.33 (m, 2H), 7.27 (ddd, *J* = 7.1, 5.4, 1.0 Hz, 1H), 2.19 (s, 1H). **^{13}C NMR** (101 MHz, $CDCl_3$) δ 134.25, 133.22, 130.44, 130.25, 129.55, 128.27, 128.08, 127.81, 127.55, 127.38, 127.35, 118.92, 11.51. **HRMS** (ESI-TOF) m/z: $[M+H]^+$ calc'd for $C_{16}H_{13}NO$ 235.0992; found 235.0977. **IR**: ṽ = 3346, 3057, 3028, 2929, 2851, 1955, 1716, 1598, 1492, 1455, 1446, 1380, 1261, 1217, 1179, 1083, 1020, 972, 915, 886, 853, 803, 755, 698, 659 cm^{-1}

(3u) (E)-1-(2-chlorophenyl)ethan-1-one oxime

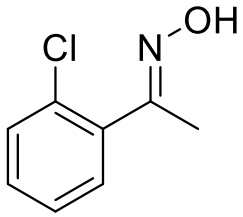

Yellow liquid, 15 mg, 44% yield.

Purification by column chromatography on silica gel, chromatography eluent: PE to 2% EA in petroleum. R_f = 0.35 (PE/EA=10/1).

^{1}H NMR (301 MHz, $CDCl_3$) δ 8.95 (s, 1H), 7.47 – 7.36 (m, 1H), 7.38 – 7.22 (m, 1H), 2.27 (s, 1H). **^{13}C NMR** (76 MHz, $CDCl_3$) δ 156.93, 136.68, 132.57, 130.00, 129.95,

126.85, 15.71. **HRMS** (ESI-TOF) m/z: $[M+H]^+$ calc'd for C_8H_8ClNO 169.0321; found 169.0309. **IR**: $\tilde{\nu}$ = 3070, 2922, 1684, 1572, 1473, 1432, 1385, 1356, 1297, 1242, 1130, 1096, 1042, 915, 867, 813, 755, 672, 664 cm^{-1}

(3v) (E)-1-(2-bromophenyl)ethan-1-one oxime

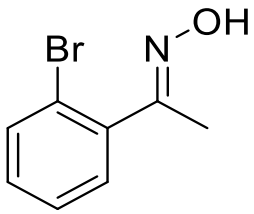

White solid, 18 mg, 42% yield, melting point 128.4-129.3 ℃.

Purification by column chromatography on silica gel, chromatography eluent: PE to 2% EA in petroleum. R_f = 0.34 (PE/EA=10/1).

^{1}H NMR (300 MHz, $CDCl_3$) δ 8.19 (s, 1H), 7.60 (dd, *J* = 7.9, 0.6 Hz, 1H), 7.38 – 7.27 (m, 1H), 7.25 – 7.18 (m, 1H), 2.26 (s, 1H). **^{13}C NMR** (75 MHz, $CDCl_3$) δ 158.16, 138.77, 133.13, 130.11, 130.07, 127.40, 15.85. **HRMS** (ESI-TOF) m/z: $[M+H]^+$ calc'd for C_8H_8BrNO 212.9784; found 212.9773. **IR**: $\tilde{\nu}$ = 3222, 2922, 1935, 1823, 1663, 1633, 1591, 1563, 1479, 1426, 1365, 1313, 1254, 1163, 1106, 1026, 1013, 984, 954, 923, 875, 756, 726, 681, 638 cm^{-1}

(3w) (E)-1-(2,4,6-trifluorophenyl)ethan-1-one oxime

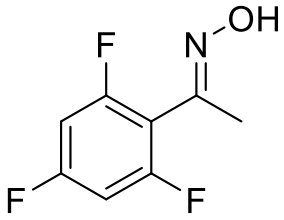

Yellow liquid, 14.7 mg, 39% yield.

Purification by column chromatography on silica gel, chromatography eluent: PE to 2% EA in petroleum. R_f = 0.36 (PE/EA=10/1).

^{1}H NMR (301 MHz, $CDCl_3$) δ 8.31 (s, 1H), 6.49 (s, 1H), 6.46 (s, 1H), 3.80 (s, 1H). **13C NMR** (101 MHz, CDCl3) δ 193.75, 163.44, 163.34, 163.20, 160.91, 160.81, 98.73, 98.71, 98.45, 98.43, 56.02, 32.46, 20.17. **HRMS** (ESI-TOF) m/z: $[M+H]^+$ calc'd for

$C_8H_6F_3NO$ 189.0242; found 189.0267. **IR**: $\tilde{\nu}$ = 3121, 3081, 3020, 2959, 2930, 1908, 1686, 1610, 1575, 1512, 1481, 1454, 1414, 1390, 1362, 1288, 1264, 1232, 1212, 1156, 1114, 1086, 1024, 966, 899, 876, 829, 785, 762, 647, 615 cm^{-1}

(4) Acetophenone

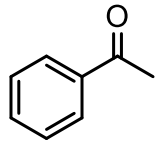

White liquid (21.8 mg, 90% yield)

Purification by column chromatography on silica gel, chromatography eluent: PE to 2% EA in petroleum. R_f = 0.35 (PE/EA=10/1).

^{1}H NMR (301 MHz, $CDCl_3$) δ 7.95, 7.93, 7.93, 7.57, 7.55, 7.54, 7.54, 7.52, 7.47, 7.44, 7.42, 2.58. The ^{1}H NMR data information is agreed with the before reports.[8]

3.5.5 References

[1] Scrivanti, A.; Matteoli, U.; Beghetto, V.; Antonaroli, S.; Scarpelli, R.; Crociani, B., Iminophosphine-Palladium(0) Complexes as Catalysts in the Alkoxycarbonylation of Terminal Alkynes. *J. Mol. Catal. A. Chem*. **2001**, *170* (1-2), 51-56.

[2] Fernandez, Gabriela A.; Chopa, Alicia B.; Silbestri, Gustavo F., A Structure/Catalytic Activity Study of Gold(I)-NHC Complexes, as well as Their Recyclability and Reusability, in the Hydration of Alkynes in Aqueous Medium. *Catal. Sci. Technol*. **2016**, *6* (6), 1921-1929.

[3] Catano, Bryant.; Lee, John.; Kim, Claudia.; Farrell, David.; Petersen, Jeffrey L.; Xing, Yalan., Iron(III) Catalyzed Halo-Functionalization of Alkynes. *Tetrahedron Lett.* **2015**, *56* (27), 4124-4127.

[4] Taşdemir, V.; Menges, N., Gold-Catalyzed Cyclization of Non-conjugated Ynone-oxime Derivatives: Incorporation of Solvent Molecule. *Asian J. Org. Chem.* **2020**, *9* (12), 2108-2111.

[5] Zhu, F. X.; Wang, W.; Li, H. X., Water-Medium and Solvent-Free Organic Reactions over a Bifunctional Catalyst with Au Nanoparticles Covalently Bonded to HS/SO3H Functionalized Periodic Mesoporous Organosilica. *J. Am. Chem. Soc.* **2011**, *133* (30), 11632-11640.

[6] Oss, G.; Ho, J.; Nguyen, T. V., Tropylium Ion Catalyzes Hydration Reactions of Alkynes. *Eur. J. Org. Chem.* **2018**, *2018* (29), 3974-3981.

[7] Nairoukh, Z.; Avnir, D.; Blum, J., Acid-Catalyzed Hydration of Alkynes in Aqueous Microemulsions. *ChemSusChem*. **2013**, *6* (3), 430-432.

[8] Gonzalez-de-Castro, A.; Xiao, J., Green and Efficient: Iron-Catalyzed Selective Oxidation of Olefins to Carbonyls with O_2. *J. Am. Chem. Soc.* **2015**, *137* (25), 8206-8218.